EUROPEAN COMMISSION

Community Research

MATISSE

Materials' Innovations for Safe and Sustainable nuclear in Europe

Support to the development of joint research actions between national programmes on advanced nuclear materials

FP7-Fission-2013
Combination of Collaborative project (CP) and Coordination and Support Actions (CSA)

Grant agreement no: 604862
Start date: 01/11/2013 Duration: 48 Months

D.4.32

Compatibility assessment of surface modified ODS under relevant FNR environment

MatISSE – Contract Number: 604862

Document title	Compatibility assessment of surface modified ODS under relevant FNR environment
Author(s)	Annette Heinzel (KIT), Alfons Weisenburger (KIT), Marta Serrano (CIEMAT), Rebeca Hernandez Pascual (CIEMAT), Enrica Ricci (CNR), D. Ripamonti (CNR), D. Giuranno (CNR), Serguei Gavrilov (SCK•CEN), Erich Stergar (SCK•CEN), Vanackere Tom (University of Gent)
Number of pages	64
Document type	Delivrable
Work Package	4
Document number	D4.32
Issued by	KIT
Date of completion	28/11/2017
Dissemination level	Confidential, only for consortium members (including the Commission Services)

Summary

After longer exposure time at higher temperature (650 and 700°C) both steels 9 and 12Cr ODS with and without GESA treated surface (gepulste Elektronenstrahlanlage) showed a dissolution attack. They can´t be used without additional corrosion protection like Al alloying in the surface for example by GESA. The clear positive effect with Al was also shown.

An overall positive effect of the GESA treatment was not found. Inside the GESA treated layer an increased diffusion was noticed. The formed columnar structure seems to favour diffusion along grain boundary, which leads in the most case to a worse behaviour. This columnar structure was typically formed in the modified layer of 9 and 12Cr ODS steel. A positive effect by GESA was found on the 14Cr ODS steel at 650°C and 10^{-6}wt%O in the liquid Pb where local inner diffusion was prevented. At 450°C and low oxygen concentration ($5.1*10^{-8}$wt% O) in Pb, the improved diffusion leads to a slightly better behaviour. However, all specimens showed a dissolution attack at 650°C and $1.9*10^{-7}$wt% O in the Pb. This situation has to be avoided, especially during the start of the reactor, where a high oxygen consumption can be expected.

12Cr GESA showed a better behaviour than the non-treated steel at 600°C. This could be due to the fact that the corrosion protection seems to be weak during the change of the oxidation mechanism from multil-layered oxide to a single spinel type oxide. This transition in oxidation behaviour seems to be shifted to higher temperatures using GESA treated specimens due to an increased diffusion, which fosters enhanced oxide growth. For 9Cr ODS this change in oxidation is observed between 600 and 650°C and for 12Cr ODS between 550°C and 600°C.

The enhanced diffusion due to the GESA process leads to a slightly better behaviour in the liquid Pb at 450°C having a low oxygen concentration ($5.1*10^{-8}$wt% O). At 650°C all specimens showed a dissolution attack already after 2000h and low oxygen concentrations of $1.9*10^{-7}$wt% . This situation has to be avoided, especially during the start of the reactor, where a high oxygen consumption can be expected.

The temperature transient test 550°C-750°C (24h) -550°C showed no influence on the corrosion behaviour. After an increase to 1000°C, the thick oxide layers spalled off. The thinner oxide layer on the GESA samples seems to be a bit more stable.

Furthermore, no negative effect was observed due to a decreasing oxygen content at 450°C. However, the oxygen content in Pb was after 6700h still in the range of 10^{-6}wt%, which is still high enough to form Fe_3O_4

Concerning the tensile test, 9%Cr-, 12%Cr- and 14%Cr-ODS steels are susceptible to LME in LBE environment. The GESA surface treatment do not prevent appearance of LME in tensile tests, but probably even enhance it. 14%Cr-ODS(CEA) demonstrated least susceptibility to LME, probably due to more effective LME crack arrest in columnar microstructure. 14%Cr chromium content is not the reason for LME retarding effect in 14%Cr ODS steel.

Approval

Rev.	Date	First author	WP leader	Project Coordinator
1	11/2017	A. Heinzel, KIT 22/11/2017	M. Serrano; CIEMAT 27/11/2017	P.F. Giroux, CEA 28/11/2017

Distribution list

Name	Organisation	Comments
All beneficiaries	MatISSE	

Table of contents

1 Foreword

The report is divided in two parts. The first part deals with corrosion test of ODS steels with and without surface treatment in liquid Pb. In the second part the susceptibility of ODS to liquid metal embrittlement in LBE environment is presented.

2 Material and exposure condition

Within previous EU projects like GETMAT and MATTER, ODS fabrication processes and the mechanical behavior in relation to the ODS microstructure were investigated. The ODS steels related work concerns the behavior in liquid lead under both transient and off-normal conditions with respect to high temperatures as well as low oxygen contents. Furthermore, it should be tested if a surface treatment can reduce the inhomogeneity's on the ODS steel surface, which were most probably responsible for local attack as observed in tests of the GETMAT project.

2.1 Material

Samples used for investigations are taken from 9Cr (T91) and 12Cr ODS bars which were produced within the GETMAT project (Deliverable D1.3 and D1.13b). The chemical composition is shown in Tab. 1. The 9Cr ODS steel has additionally Si, Mn and Mo, the 12Cr ODS instead has W and Ti.

	Si	Mn	Cr	Mo	V	W	Ti	Y	O	Ni
9Cr ODS	0.4	0.47	8.9	0.76	0.2	--	--	0.28	0.15	--
12 Cr ODS	0.02-0.03	<0.01	12.2	<0.01	--	1.94	0.25	0.17	0.12	--
14Cr ODS	0.32	0,27	13.5	--	--	0.9		0.2		0.16

Tab. 1: chemical composition of 9Cr ODS, 12Cr ODS and 14Cr ODS

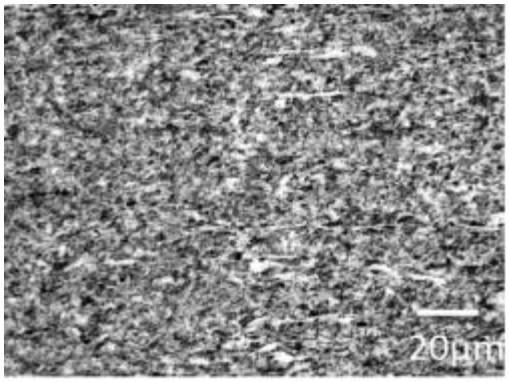

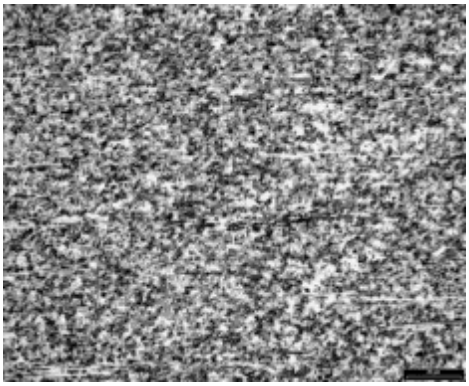

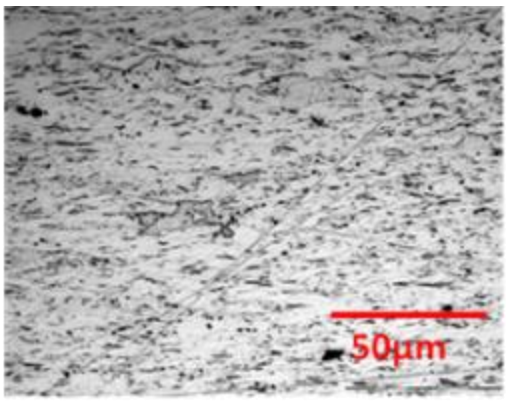

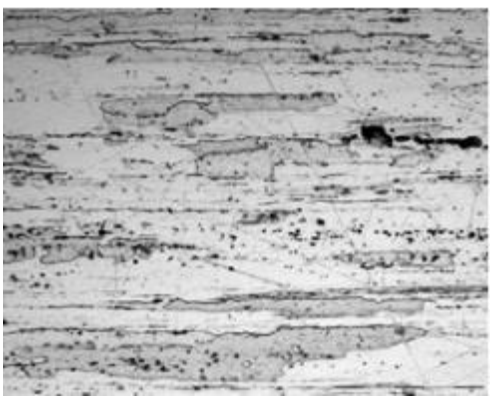

Fig. 1: Cross section of 9Cr ODS (top), 12 Cr ODS (bottom) steel; Left: cut perpendicular to the rolling direction Right: cut in rolling direction

Grains of both materials are elongated in rolling direction. In addition, pores and precipitations like TiO (in the 9Cr ODS steel) are aligned in rolling direction. In the case of 12 Cr ODS steel Mo enrichment occurs. Additional to the 9 and 12Cr ODS in some experiments also a 14Cr ODS steel was tested. This steel was produced within the GETMAT project, too. Its chemical composition is depicted as well in Tab. 1.

Previous corrosion tests of ODS steels showed localized attack, most probably due to inhomogeneities in the steel. Therefore, part of the steel samples were additionally treated using the pulsed electron facility GESA (gepulste Elektronenstrahlanlage) [1]. Under the influence of the electron beam, the material surface is melted rapidly, followed by rapid quenching due to heat conduction into the bulk material. For the ODS treatment three pulses were used with an energy input of: 52 J/cm² in the first pulse, 76 J/cm² in the second and 78 J/cm² in the third pulse. Such melting and re-solidifying should clean the surface area and reduce inhomogeneities and therefore improve the corrosion behavior. Fig. 2 shows a cross section of the materials in pristine state and after GESA treatment.

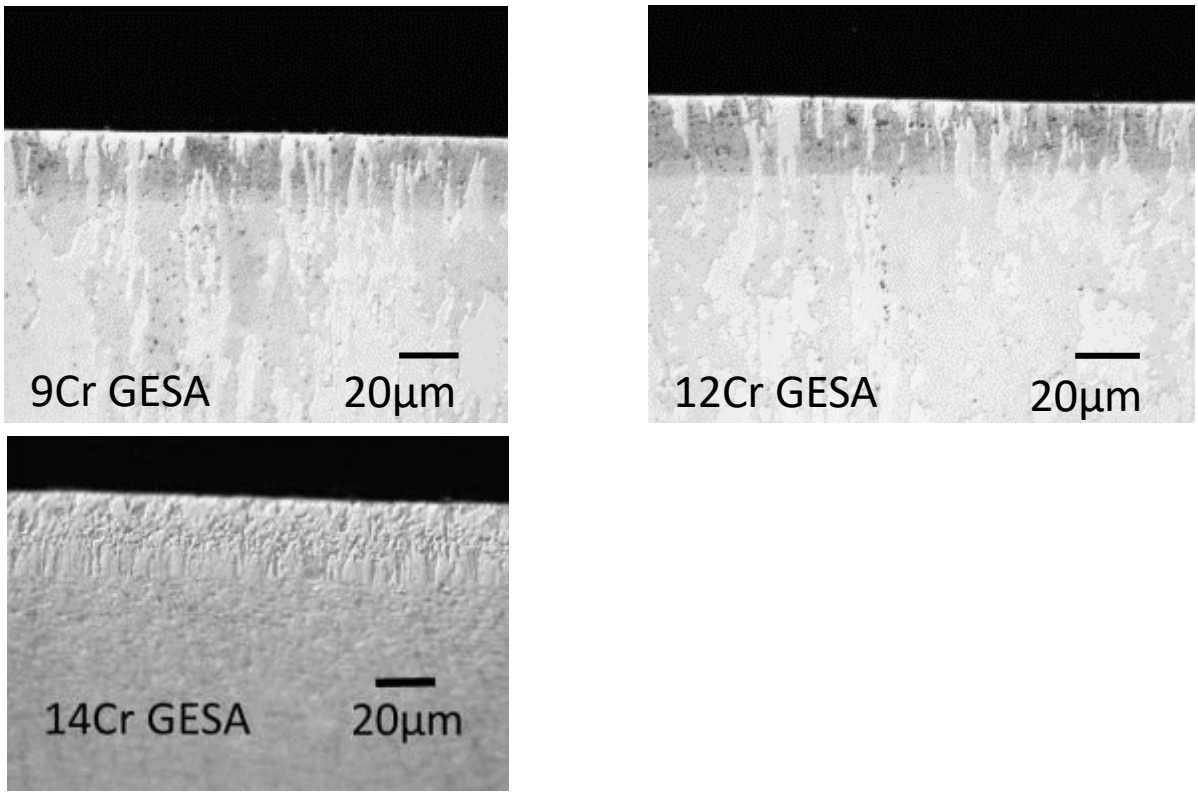

Fig. 2: Cross section of 9Cr ODS (top left), 12 Cr ODS (top right) and 14Cr ODS (bottom left) steel after GESA treatment showing a restructured surface layer.

The GESA treated materials have a restructured surface layer. In the case of the 9Cr ODS it is around 23.5µm thick. The 12Cr ODS steel was melted up to a depth of around 21µm and the 14Cr ODS up to 30µm. The columnar structure of the affected layer of the 9 and 12Cr ODS steel seems to be quite similar to that of the original steel, but at the edges the grain axes are aligned in cooling direction. The GESA treatment of the 9 and 12Cr ODS was performed in direction of the elongated grains structure due to the manufacturing process. The structure of the 14Cr ODS after GESA treatment steel is slightly different. At the transition to the bulk material a columnar structure is visible and above a little bit coarser grains like in the bulk were formed. Here, the GESA treatment was perpendicular to the elongated grains.

Al alloying in the surface can have a positive effect on corrosion, therefore, in some specimens Al was alloyed into the surface using the GESA process. First, Al was sputtered by EBPVB (electron beam physical vapor deposition) on the surface of the ODS steels and than the Al-coated steel was re-melted using GESA. During the GESA treatment, a great part of the Al evaporates, but the remainder, about 25%, is alloyed into the steel. It mixes with the molten steel

surface layer. Fig. 3 shows a cross section of a 12Cr ODS sample with surface Al alloying. Close to the surface, an Al content of around 6wt% was measured by EDS (Energy-dispersive X-ray spectroscopy).

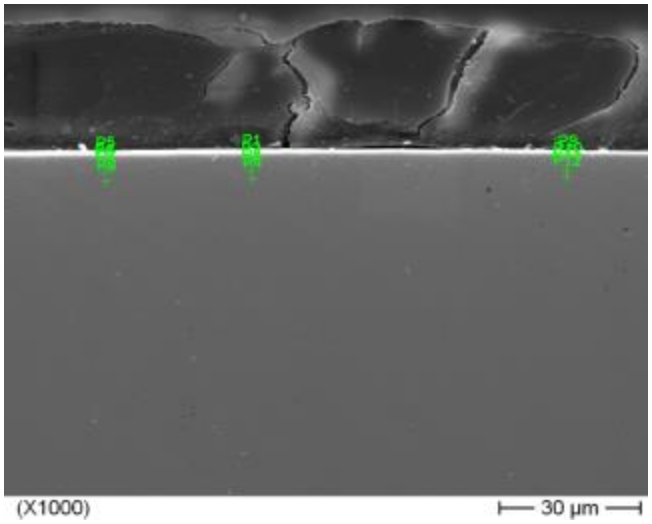

Point Nr.	Al wt%
1	6.45
2	4.24
3	4.25
4	3.95
5	6.17
6	4.77
7	4.75
8	3.69
9	6.44
10	4.18
11	4.06
12	3.68

Fig. 3: left-cross section of 12Cr ODS sample with Al alloying and marked points of the EDS measurement; right-measured Al content at the marked points

2.2 Exposure condition

In the first experiment, steels were tested at constant temperatures between 550°C and 700°C up to 10.000h in lead with an oxygen concentration of 10^{-6}wt% and with lower oxygen concentration at 450°C / $5.1*10^{-8}$wt% O and at 600°C / $1.9*10^{-7}$wt% O. Temperature, exposure time, materials as well as location of test equipment are listed in Tab. 2 and Tab. 3.

	550°C		600°C			650°C		700°C		
	2000	5000	2000	5000	10000	2000	5000	2000	5000	10000
9Cr		X	X	X	X	X	X	X	X	X
9Cr GESA		X	X	X	X	X	X	X	X	X
9Cr Al		X				X	X			
12Cr	X	X	X	X	X	X	X	X	X	X
12Cr GESA	X		X	X	X	X	X	X	X	X
12Cr Al	X	X				X	X			
	KIT		CIEMAT			KIT		CIEMAT		

Tab. 2: Test condition at constant temperature and an oxygen content of 10^{-6}wt% in lead: temperature, exposure time, materials and test location

	450°C		650°C	
	2000	5000	2000	5000
9Cr	X	X	X	X
9Cr GESA	X	X	X	X
12Cr	X	X	X	X
12Cr GESA	X	X	X	X
	CNR			

Tab. 3: Test condition at constant temperature and an oxygen content in lead of $5.1*10^{-8}$wt% O at 450°C and $1.9*10^{-7}$wt% O at 600°C: temperature, exposure time, materials and test location

In a second experimental campaign, accidental conditions were targeted. The selection of the temperature transient experiments based on the results of EU FP7 project LEADER WP5 Task 5.5: Analyses of representative DEC events of the ETDR (Alfred). The main interest was on two events:

a) T-DEC 4: ULOHS + ULOF, no reactor trip, DHR-1: loss of all primary pumps and main heat exchangers (MHXs) feed water which cases a cladding temperature increasing to 800°C for some seconds and an elevated temperature of around 750°C for around 3h.
b) T-DEC 3: ULOHS, PPs operating, no reactor trip, DHR-1 : loss of MHXs feed water, which causes a cladding temperature increase from 500°C to 700°C for about 3h.

In both cases, the temperatures increase up to 700°C or 750°C, respectively, for around 3 hours. To address the scenarios in one experiment the temperature was raised after being controlled at 550°C for 2000h to 750°C and kept there for 24h followed by a cooling down phase to 550°C where it was kept until a total exposure time of 5000h was reached. In a second experiment, the temperature is increased to 1000°C to explore even more sever conditions. After such an event, a reactor scram would happen. Therefore, the test was stopped after 2072h after the 24h hold at 1000h. . Chosen test conditions are depicted in Tab. 4.

Material	Temperature [°C]	Oxygen content [wt%]	time	Organization
9Cr and 12Cr ODS; 9Cr and 12Cr ODS GESA	550 -750 -550	10^{-6}	5000h (after 2000h to 750°C for 24h)	KIT
9Cr and 12Cr ODS; 9Cr and 12Cr ODS GESA	550-1000-550	10^{-6}	2072h (after 2000h to 1000°C for 24h)	CIEMAT

Tab. 4: Test conditions of temperature transient experiments: materials, temperature, oxygen content, exposure time and test location

A loss of the oxygen control system was simulated in the last experiments. Therefore, samples (9Cr and 12Cr ODS with and without treatment GESA) were exposed 2000h in lead at 450°C under a constant Ar flow and then in a Ar-5%H2 mixture for additional 4700h,

Material	Temperature [°C]	Oxygen content [wt%]	time	Organization
9Cr and 12Cr ODS; 9Cr and 12Cr ODS GESA	450	Ar (first 2000h) / $10^{-3,6}$ Ar-5%H2 (4700h) / 10^{-4}–10^{-6}	5000h	CNR

Tab. 5: Test conditions of loss of oxygen control system experiments: materials, temperature, oxygen content, time, test location

No gas bubbling into the Pb baths was provided. The oxygen content was measured by two Pt-air electrodes, which were immersed in each bath. The signals of the two electrodes were congruous.

The mean value of the voltage measured at the start of the test under Ar (Air-liquide Ar-N60) was 0.72013 V after the first 48 h. Afterward, an average value of U = 0.713 ± 0.06 V was measured for 2000 h until the transition from Ar to Ar 5% H_2.

After the change of the gas, the voltage increased very slowly and after approximately 1700 h from the switching, it has reached the mean value of 0.886 ± 0.03 V. This mean value was maintained for about 3000 h until the end of the test (total time = 6700 h).

Based on the measured values of the sensors signals and in agreement with C. Schroer et al [2], the corresponding oxygen content during the experiment can be calculated:

Gas	T[K]	Time [h]	[V] (mean value)	Co [wt%]
Argon	723	48	0,720	$10^{-3,6}$
	723	48-2000	0,713	$10^{-3,5}$
Ar –H2(5%at)	723	2000 ÷ ~3700	~0,74 ÷ ~0,88	~$10^{-3,9}$ ÷ ~$10^{-5,8}$

	723	~3700 ÷ ~6700	0,886	$10^{-5,92}$

Tab. 6: calculated oxygen contents during the loss of oxygen test

Test were performed in three different laboratories: KIT - COSTA test facilities [3], CIEMAT test facility and CNR-CorAl_Twin apparatus. The COSTA facility at KIT and the test facility form CIEMAT are quite similar, Fig. 4. They consist of a furnace with a quartz tube in which several alumina crucibles containing the lead can be placed. Each crucible contained only one specimen with following dimensions 27x7x2mm.

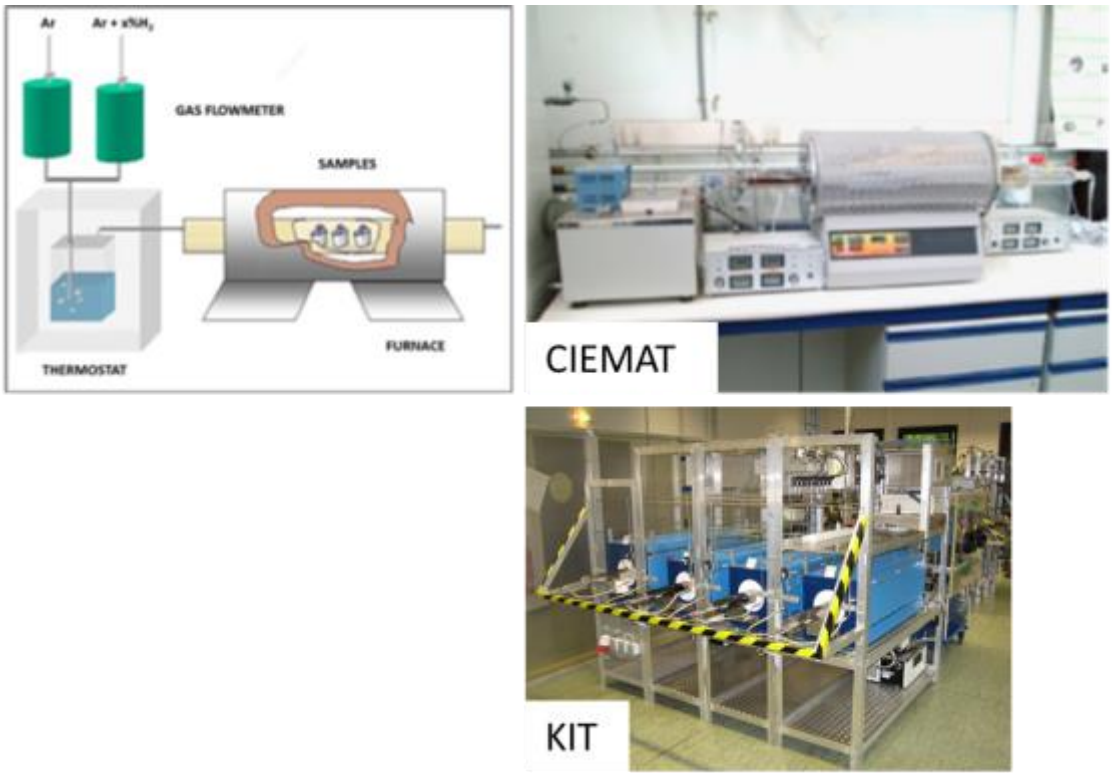

Fig. 4: scheme of the experimental setup (top left); test facility at CIEMAT (top right); COSTA test facilities at KIT (bottom right)

The oxygen concentration in the liquid metal was controlled via the gas atmosphere by establishing a defined H_2/H_2O ratio, which determines the chemical potential of oxygen in the liquid metal [4]. H_2/H_2O ratio is established by mixing Ar (carrier gas) and Ar-H_2 together to reach the desired hydrogen concentration, Fig. 4 top left. This gas mixture bubbles though a water bath with a defined temperature to get the right water vapour pressure. Afterwards the gas is purged during the whole test though the furnace. The oxygen content and the moisture of the gas leaving the furnace were controlled and monitored over the entire exposure time to guarantee constant conditions.

The CorAl Twin facility at CNR consists of two furnaces that operate independently at different temperatures, Fig. 5. Both furnaces have the same atmosphere. The liquid metal inside the furnace is filled in alumina crucibles which contain beside the samples a gas feeding tube and Pt-air oxygen sensors to monitor the oxygen content directly in the liquid lead. During the experiments, Ar or a mixture of Ar-5%H_2 is purged through the liquid metal.

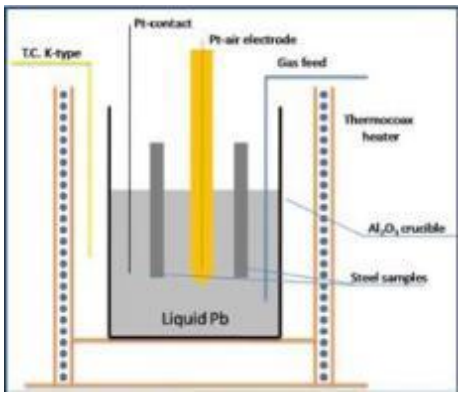

Fig. 5: scheme of the experimental setup (left); test facility at CNR (right);

3 Experimental results at constant temperature and 10^{-6}wt%

3.1 550°C - KIT

3.1.1 9Cr and 12 Cr ODS

The behaviour of 9 and 12Cr ODS after exposure to oxygen containing lead (10^{-6}wt% O) at 550°C is shown in Fig. 6. Both steels form a thick multi-layered oxide, which consists of magnetite, Fe-Cr spinel and an inner diffusion zone in the case of 12Cr ODS.

9Cr ODS

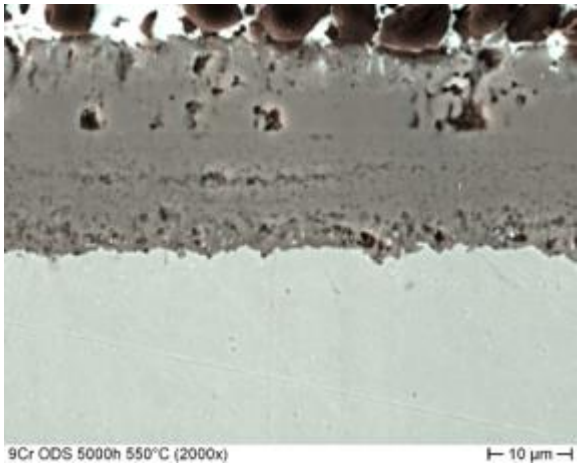

12Cr ODS

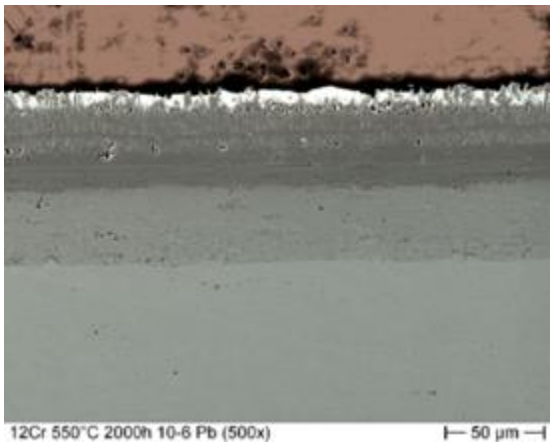

2000h

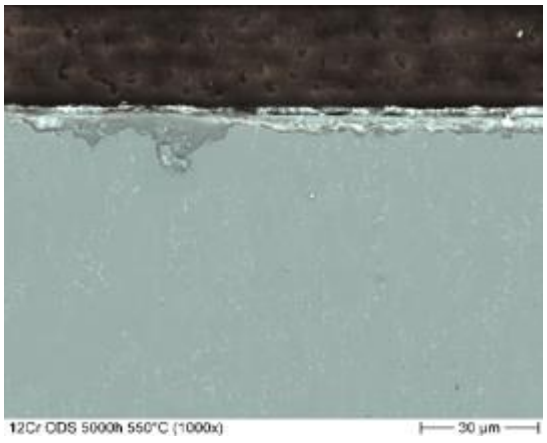

5000h

Fig. 6: 9CrODS (top) after 5000h and 12CrODS (bottom) after 2000 and 5000h exposure at 550°C in lead with oxygen contain of 10^{-6} wt. % O

An EDS line scan on the cross section of the 12Cr ODS sample after 2000h exposure is depicted in Fig. 7. In this cross section, the oxygen affected zone (oxide layer + inner oxidation) layer is around 78µm thick. The outer part consists only of Fe and O, which hints to a magnetite layer usually growing outwards. Underneath this layer starts the earlier surface of the steel marked by the appearance of W. Here, the slightly enriched Cr content together with Fe and O hints on a Fe-Cr spinel which a thickness of 14,4 µm in the measured place. The inner diffusion zone (IOZ) starts with the reduction of oxygen to around 10wt%. The observed oxidation of the grain boundary is typical for an IOZ. The 12Cr ODS as well as the 9Cr ODS steel can have lead inclusions in the magnetite layer. After 5000h the 9Cr ODS steel is still covered by the multi-layered oxide, while large parts of the oxide spalled off from the 12Cr ODs steel.

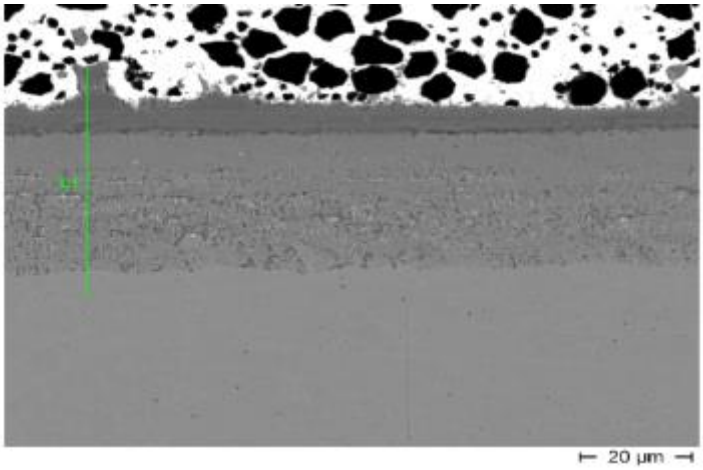

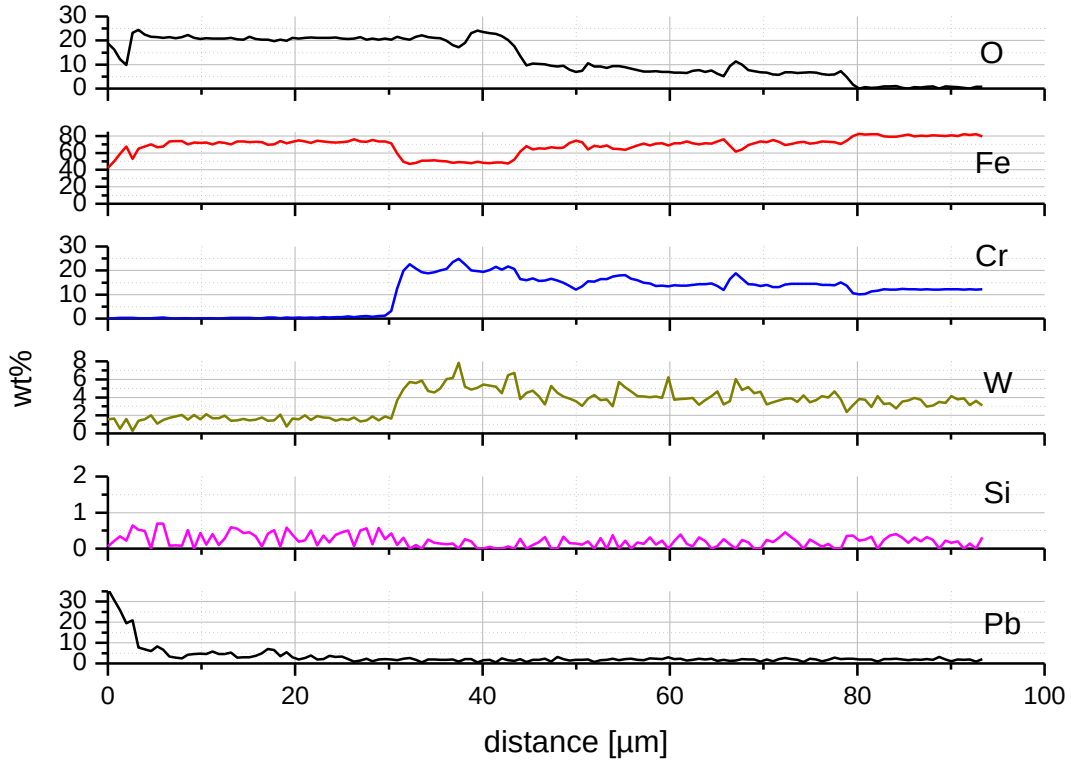

Fig. 7: EDS line scan conducted on 12Cr ODS specimen exposed to 2000h at 550°C in Pb containing 10^{-6}wt% oxygen

3.1.1 9Cr and 12 Cr ODS GESA

The behaviour of 9 and 12Cr ODS steel treated with GESA is depicted in Fig. 8. After 5000h the 9Cr ODS GESA (Fig. 7 left) shows a Fe-Cr spinel layer at the top with an inner diffusion zone underneath. Pb can be included in the spinel layer, while dissolution attack was not observed.

The behaviour of 12Cr ODS steel after 2000h exposure is shown at the right side. A homogenous Fe-Cr spinel oxide layer of around 8.5µm thickness was formed on the surface. In most regions, a border strip is marking the boundary between the bulk and the oxide layer formed by an increase of Cr and Si. Nevertheless, Pb can be included in the oxide layer.

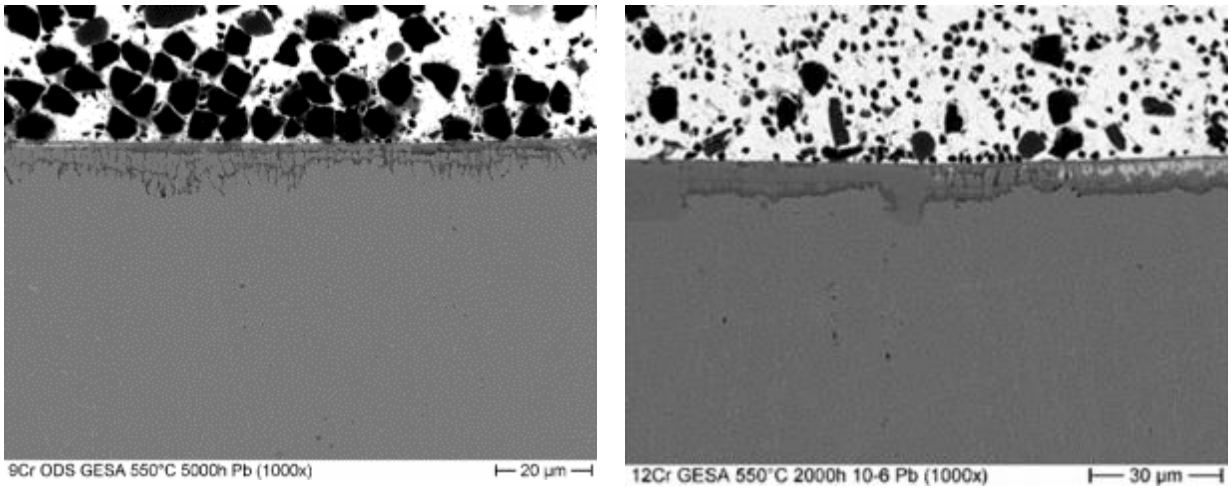

Fig. 8: 9Cr ODS GESA after 5000h (left) and 12Cr ODS GESA after 2000h (right) exposure to liquid Pb with an oxygen content of 10^{-6} wt% at 550°C

3.1.2 14Cr / 2000h

14Cr ODS steel was tested at 550°C up to 2000h in Pb with an oxygen content of 10^{-6}wt%. After the exposure a thin oxide layer consisting of a Cr rich Cr-Fe spinel was formed, Fig. 9. No dissolution attack was visible, but areas with inner oxidation.

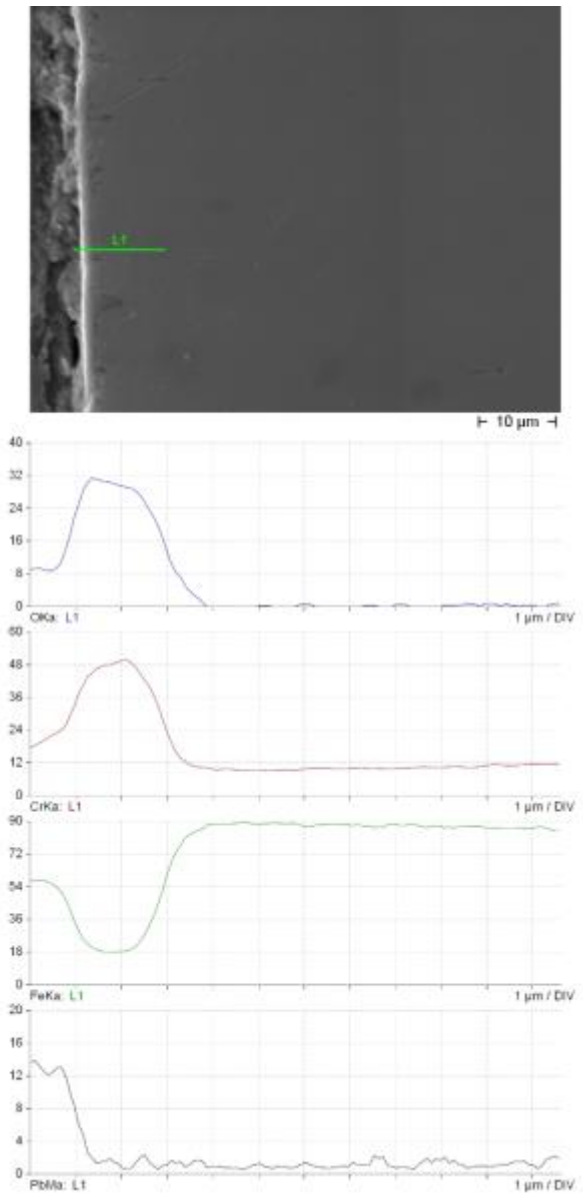

Fig. 9: EDS line scan measurement on 14Cr ODS specimen exposed 2000h at 550°C in Pb containing 10^{-6}wt% oxygen

3.1.1 9Cr Al and 12 Cr ODS Al

If sufficient Al is alloyed into the surface, a thin oxide layer is formed on the ODS steel after 2000h and 5000h, see Fig. 10 bottom. Such oxide layer prevents dissolution attack and is known to be stable and protective for long term use in Pb-Alloys. The 9 Cr ODS steel had nearly no Al in the surface, therefore, it behaves like the 9Cr ODS steel just with GESA treatment. Apart from some Pb inclusions in the upper part of the GESA treated layer no liquid metal attack was visible.

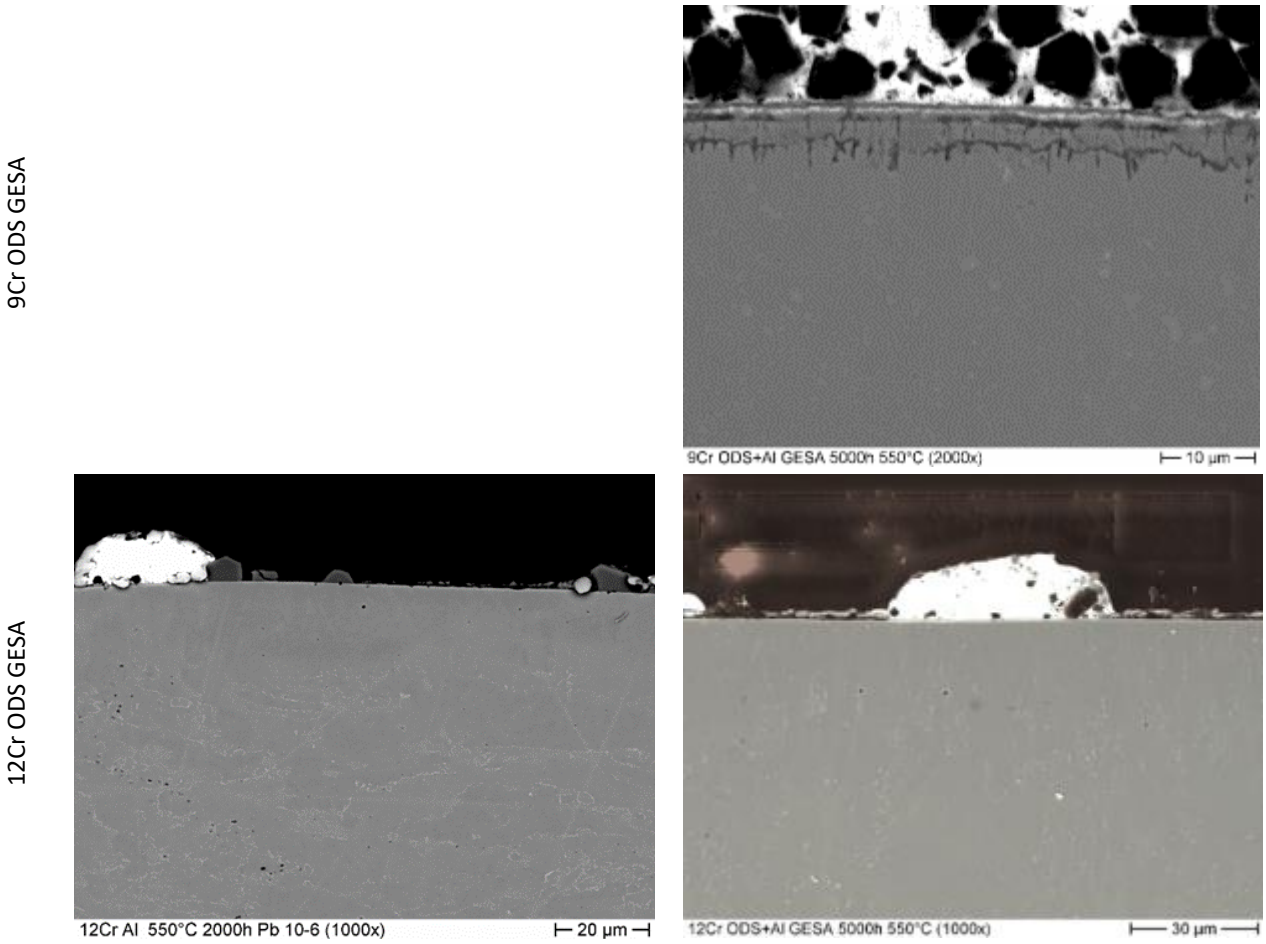

Fig. 10: 9CrODS Al (top) after 5000h and 12CrODS Al (bottom) after 2000 and 5000h exposure at 550°C in lead with oxygen content of 10^{-6} wt. % O

Fig. 11 shows an EDS line scan on the cross section of 12Cr ODS Al alloyed by GESA after 2000h of exposure at 550°C. The oxide layer is very thin. Only at the beginning of the scan oxide is detectable togehter with Al, also Ti is slighty enrichted here. Similar conditions could be observed after 5000h exposure. No liquid metal attack was visible on this specimen.

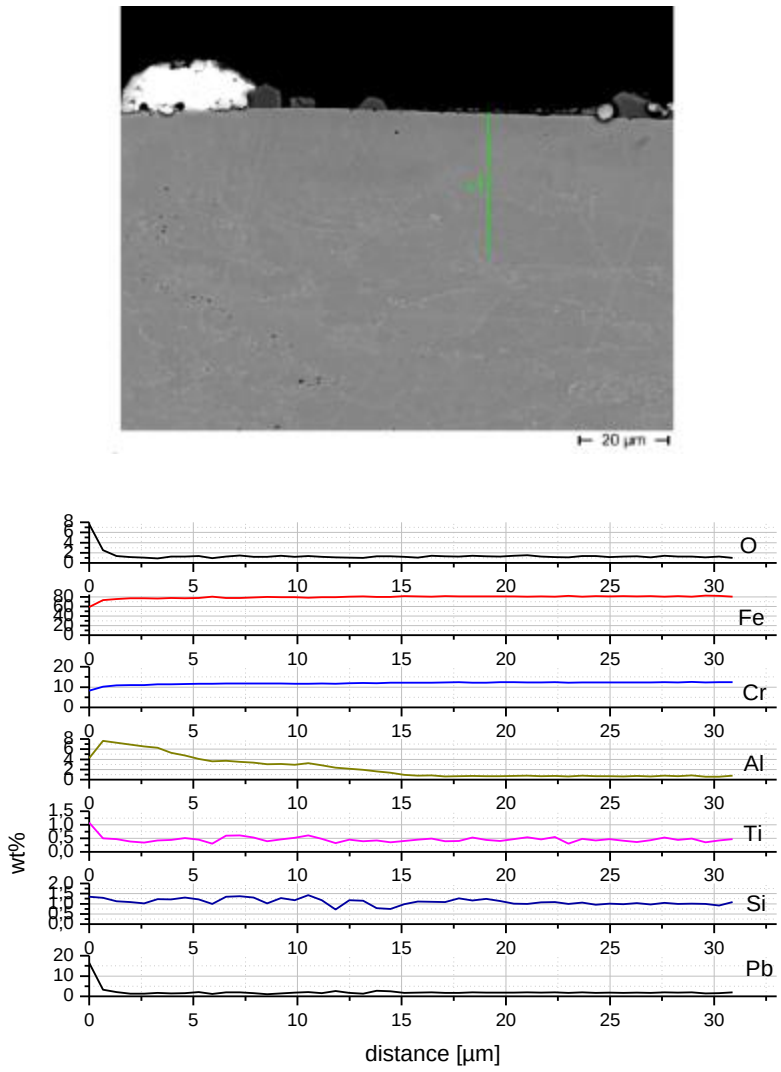

Fig. 11: EDS line scan conducted on 12Cr ODS with Al alloyed by GESA, exposed 2000h at 550°C to Pb containing 10^{-6}wt% oxygen

3.2 600°C - CIEMAT

3.2.1 9Cr and 12Cr ODS

Fig. 12 shows the time evolution of the oxide layers for the two ODS-Cr steels (9Cr ODS top, 12 Cr ODS bottom) in liquid lead at 600°C with 10^{-6} wt% oxygen. Stable oxide layers at almost the entire surface of all specimens are observed at all exposure times even after 10000h. Except a few Pb inclusions in the oxide layer, only in isolated zones and only after 10.000h a dissolution attack up to 32µm was found on the 9Cr ODS. Pb inclusions were also found on the 12 Cr ODS steel but single areas with dissolution attack occurred already after 2000h. At 10.000h dissolution zones of up to 40µm were detected.

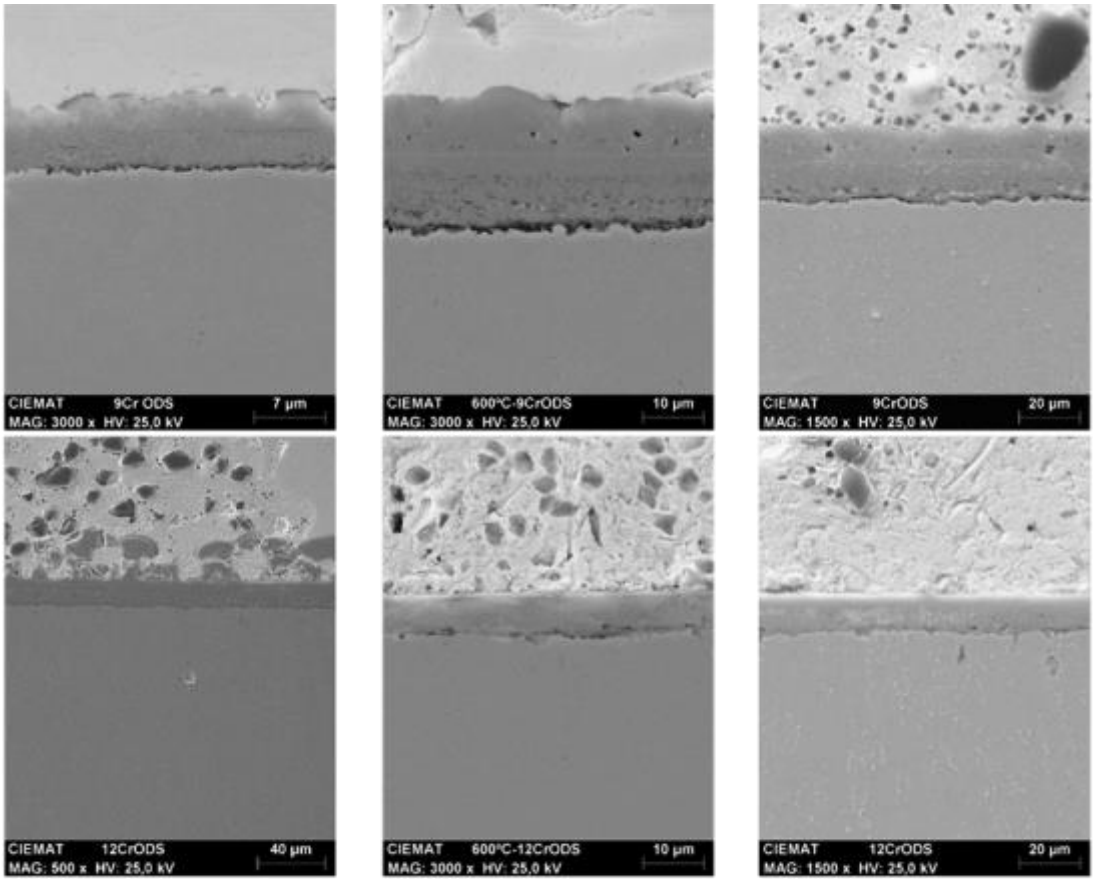

Fig. 12: 9CrODS (top) and 12CrODS (bottom) tested at 600°C in lead with oxygen contain of 10^{-6} wt. % O, at different exposure times

The composition of the oxide scale for each of the specimens was characterized by elemental mapping during EDS analysis. Fig. 13 and Fig. 14 show an example of the elemental mapping obtained for the 9Cr and 12Cr ODS steels after 10.000h of exposure. There is a big difference in the formed oxide layer between these two steels. Whereas 9Cr ODS specimens at 600°C have a Fe-rich outer layer followed by Fe-Cr spinel and Cr oxide at the boarder to the bulk material, the 12Cr ODS specimens have Fe-Cr spinel at the top and Cr oxide underneath. At the 12Cr ODS only at small and isolated points Fe-based oxide is only observed top of the spinel. Typical are also Fe rich areas and nods in the Cr-Fe spinel, Fig. 14. In addition, Ti is detected within the oxide layer and in some areas Pb inclusions are observed.

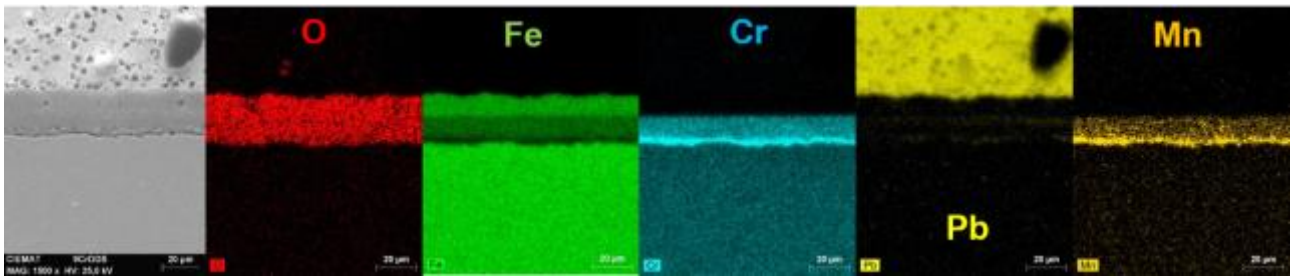

Fig. 13: Elemental mapping of EDX analysis of 9CrODS tested at 600ºC, 10-6 wt. % O and 10000 h.

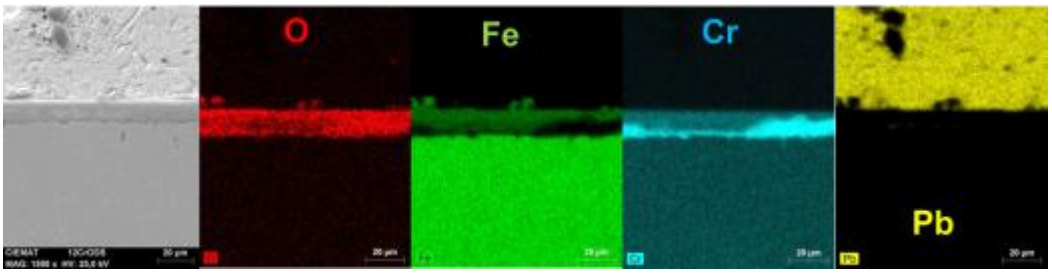

Fig. 14: Elemental mapping of EDS analysis of 12CrODS tested at 600ºC, 10^{-6} wt. % O and 10000 h.

The average thicknesses of the formed oxide layer on the 9Cr ODS and 12Cr ODS steel at the different exposure times are depicted in Tab. 7. For longer exposue times the thickness of the oxide scale is larger for the 9Cr ODS compared to the 12Cr ODS, what can mainly be attributed to the formation of multlayered oxide scales on the 9Cr ODS.

600°C		Average thickness (µm)		
		2000 h	**5000h**	**10000h**
9Cr ODS	**Outer layer (Fe-O)**	~6	~10	~11
	Inner layer (Cr-Mn-O)	~1	~12	~13
	total	~7	~22	~24
12Cr ODS	**Cr-oxide /Cr-Fe spinel**	~17-20	~9-10	~14-15

Tab. 7: Average thickness of the formed oxide layer on the 9Cr ODS and 12Cr ODS steel at 600°C after different exposure times

3.2.1 9Cr and 12 Cr ODS GESA

Fig. 15 shows the time evolution of the oxide layer of the two ODS-Cr steels with the GESA treatment in liquid lead at 600 °C with an oxygen content of 10^{-6} wt%.

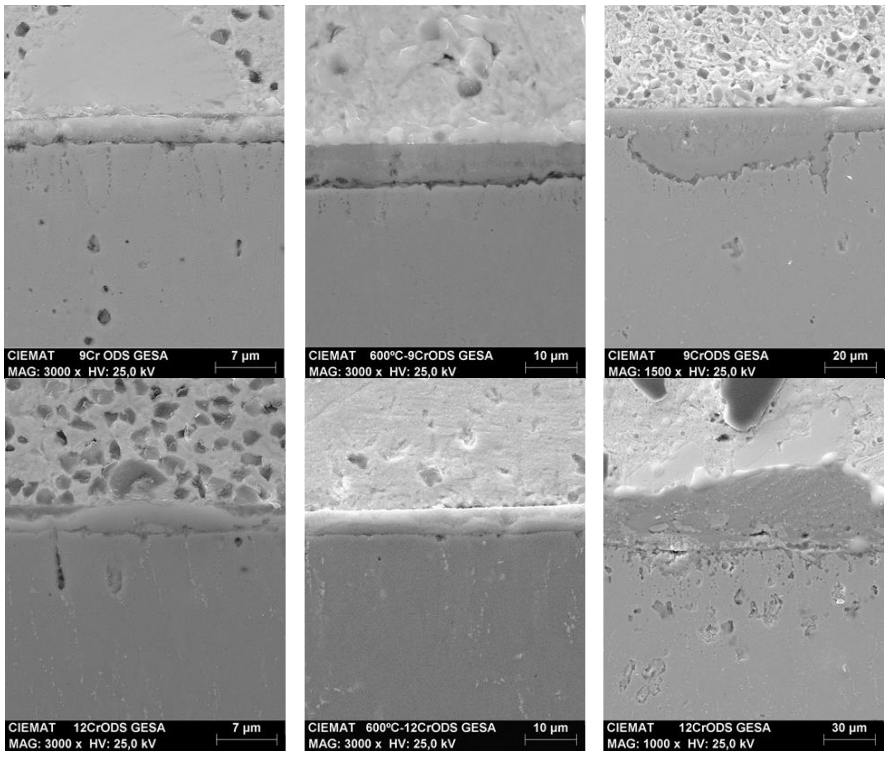

(a) 2000 h (b) 5000h (c) 10000h

Fig. 15: 9CrODS GESA (top) and 12CrODS GESA (bottom) tested at 600°C in lead with 10-6 wt. % O, at different exposure times

The corrosion behavior of 9Cr and 12Cr ODS-GESA at 2000 and 5000 hours was similar. On the surface of both steels an oxide followed by an area with grain boundary oxidation was observed. In the case of 9Cr ODS either Cr-oxide or Fe-Cr spinel containing Mn was formed (depending on location), Fig. 16. At the boarder to the bulk material the Cr and the Mn content is increased (not shown in the figure). The 12Cr ODS specimens showed a Fe-Cr spinel with Cr rich areas or nods, Fig. 17. After 10.000h severe dissolution attack and lead inclusions into the base material were detected in both materials. Especially the 12Cr ODS GESA specimen exhibits dissolution attack nearly at the whole surface. The composition of the detected oxide layers after 10000h are comparable with those after 2000h and 5000h.

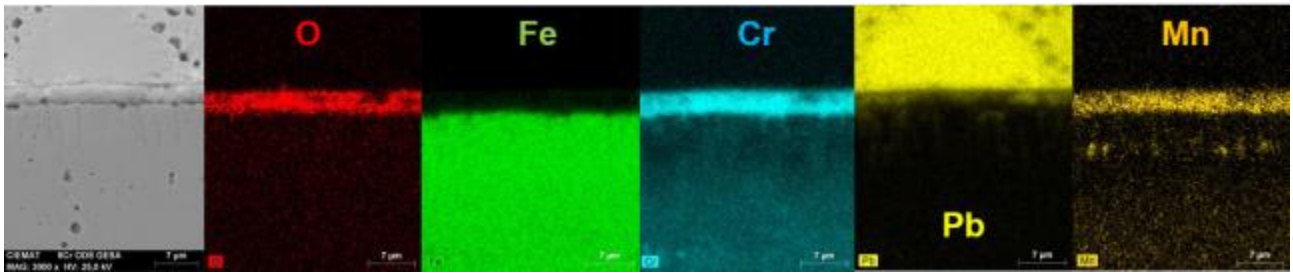

Fig. 16: Elemental mapping in EDX analysis of 9CrODS-GESA tested at 600ºC, 10^{-6} wt.% O and 2000 h.

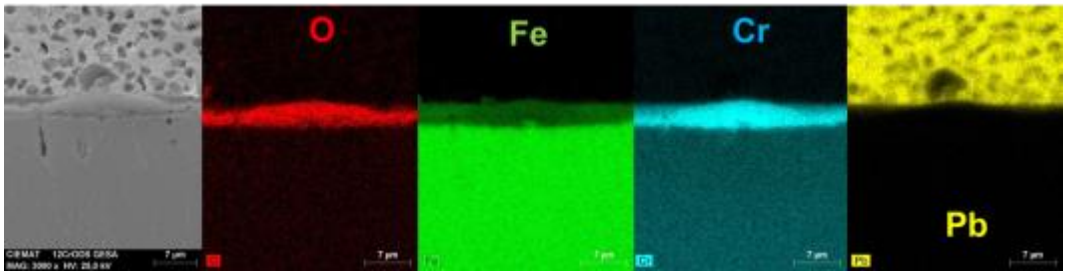

Fig. 17: Elemental mapping of EDX analysis of 12CrODS-GESA tested at 600ºC, 10^{-6} wt.% O and 2000 h.

The average thickness of the oxide layer on both steels is quite similar up to 5000h. After 10.000h the 12Cr ODS steel with GESA treatment shows a strong increase in oxidation rate while the oxidation rate of the 9Cr ODS GESA steel slightly decreases.

600°C		Average thickness (µm)		
		2000 h	**5000h**	**10000h**
9Cr ODS GESA	**Cr-O with Mn**	~3.5	~8	~11
	Grain boundary oxidation	~7	~8	~13
12Cr ODS GESA	**Cr-Fe spinel**	~3	~7	~50
	Grain boundary oxidation	~7	~7	

Tab. 8: Average thickness of the formed oxide layer on the 9Cr ODS GESA and 12Cr ODS GESA steel at 600°C after different exposure times

3.3 650°C - KIT

3.3.1 9Cr and 12Cr ODS

The behaviour of the two steels at 650°C after 2000h and 5000h is depicted in Fig. 18. Both steels are covered at the surface by a spinel layer. In the case of the 9Cr ODS steel it is a ~ 1-2 µm thick Cr-Mn-Si spinel with small amounts of Fe and oxide roots that can extend up to 16µm. In the roots Pb inclusions can appear. In some points dissolution attack is visilble like depicted on the cross section photo in Fig. 18 top left. After longer exposure time the entire

surface is covered by a Cr-Mn-Si spinel with strong Pb inclusions. The layer is around 12-13µm thick and in areas with with roots up to 19.5µm. Areas with dissolution attack looks pretty similar like that after 2000h shown in Figure 18.

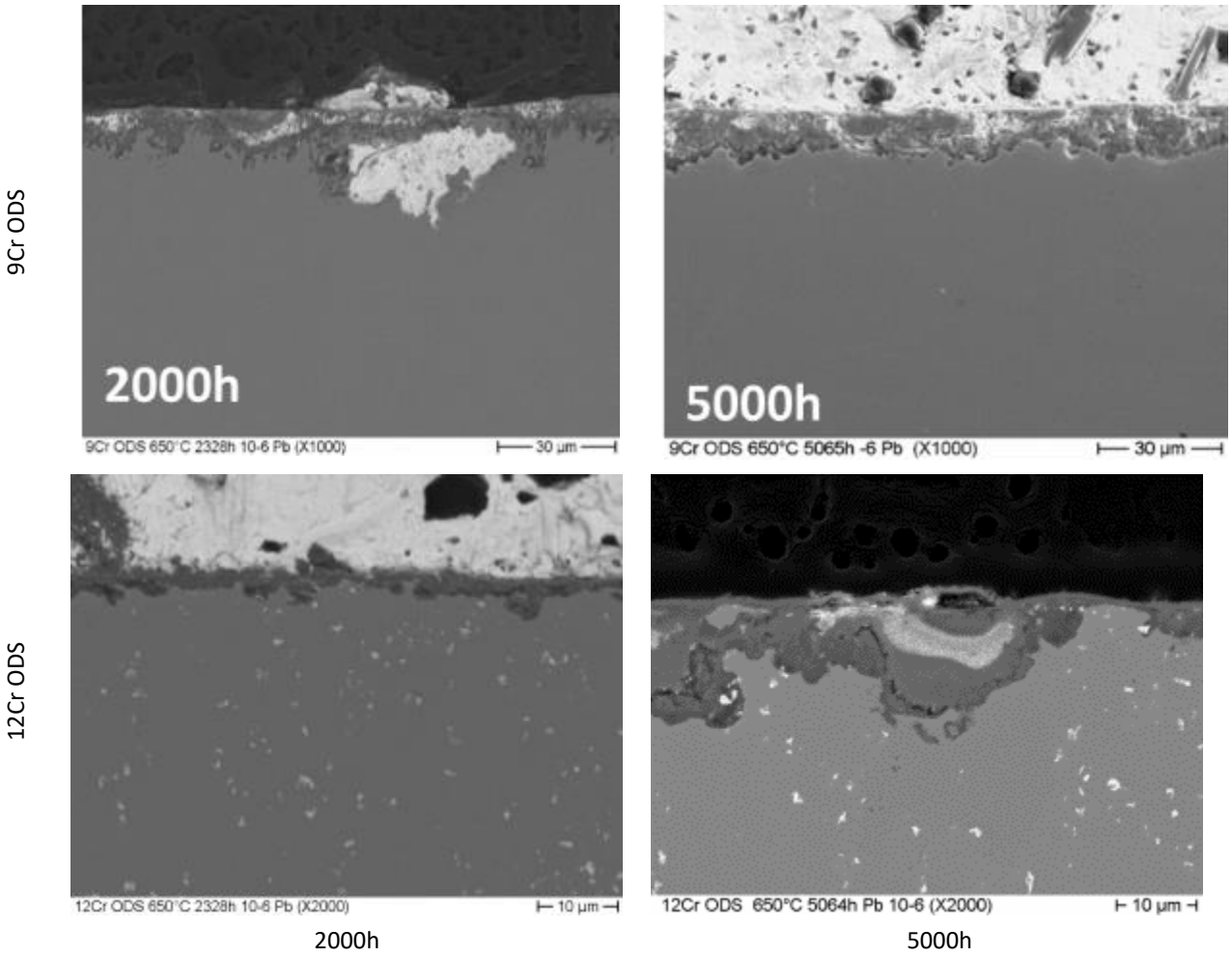

Fig. 18: 9CrODS (top) and 12CrODS (bottom) tested at 650°C in lead with an oxygen content of 10^{-6} wt. % O after 2000 and 5000h exposure

Different to the 9Cr ODS, on the 12Cr ODS specimen, Fig. 18, a 2µm Cr rich Cr-Fe spinel with nods (up to 20µm) was formed at the surface. Only in few areas Pb inclusions in the nods were observed. Fig. 19 depicts an EDS line scan through the oxide layer. Additional to Cr also Si, Ti and Y are enriched. Where as Si and Y are enriched in the whole oxide layer, the Ti content increases towards the boundary to the bulk material. The white dots in the bulk material are W precipitations.

After 5000h occationally Pb is observed in the nods, which can be seen in Fig. 18 bottom right. The oxide thickness reaches between 2µm (thin area) up to up to 26µm (nods).

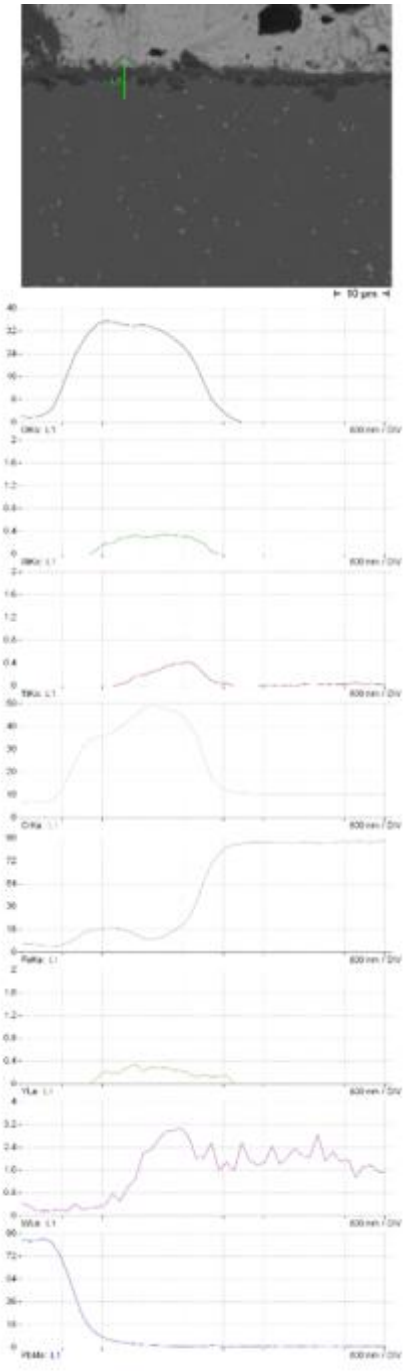

Fig. 19: EDS line scan starting in the LBE region and extending into the 12Cr ODs specimen, which was exposed 2000h at 650°C in Pb with 10^{-6}wt%

3.3.1 9Cr and 12Cr ODS GESA

Fig. 20 shows the behaviour of the ODS GESA treated steels after 2000 and 5000h exposure. On both steels a thin oxide layer is on the top after 2000h. In case of 9Cr ODS GESA it consists of Cr, Mn Si and O and is around 1µm thick. Between the underlying area characterized by grain boundary oxidation and the top Cr-Mn-Si-O layer Pb is enclosed, Fig. 21. The grain boundary oxidation zone is ~3.2µm thick and followed again by a Cr-Mn-Si oxide layer with IOZ (inner oxidation zone) underneath. In the cross section, 4 areas with dissolution attack were observed with a maximum depth of 43µm. After longer exposure times the Pb inclusion into the grain boundary oxidation zone are pronounced.

in the area with grain boundary oxidation, like in Fig. 20 top right. On the sample one area with a dissolution attack was observed. It reachs a depth of 77µm.

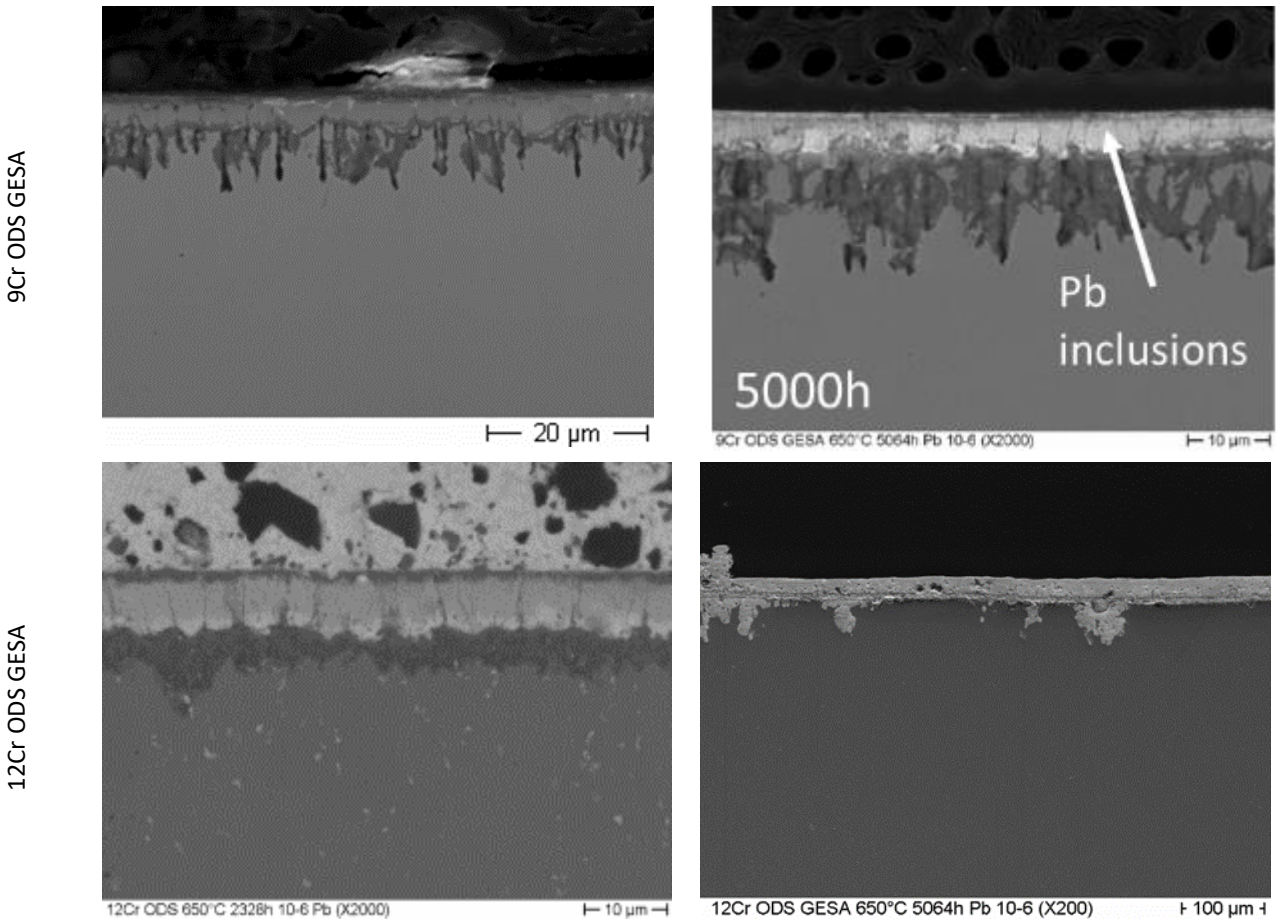

Fig. 20: 9CrODS GESA (top) and 12CrODS GESA (bottom) tested at 650°C in lead with oxygen content of 10^{-6} wt. % O after 2000 and 5000h exposure

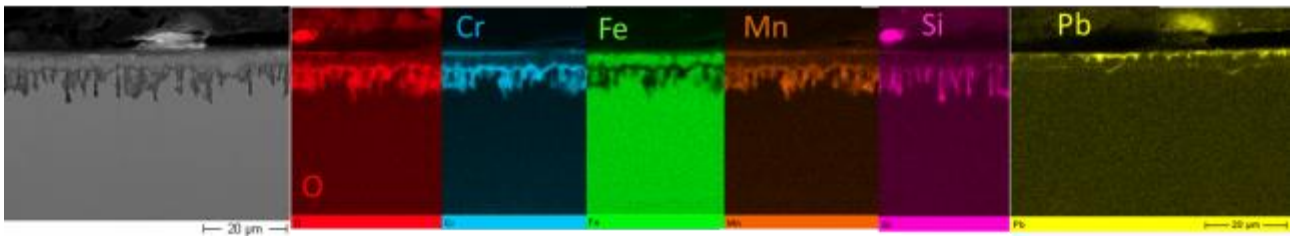

Fig. 21: EDS Element mapping pictures of 9Cr ODS GESA tested at 650°C, 10^{-6} wt% O and 2000 h

The 12Cr ODS specimen shows a Cr rich oxide at the top which is around 1-1.5µm thick, Fig. 22. Ti is slightly enriched in the oxide. Underneath follows an area with grain boundary oxidation (~ 6µm) like at the 9Cr ODS GESA steel, but strong Pb inclusion are observable even after 2000h. Before the bulk starts again, a Cr rich oxide with nods is formed which is around 5µm thick.It is slightly enrichted in Si, Ti and Y.

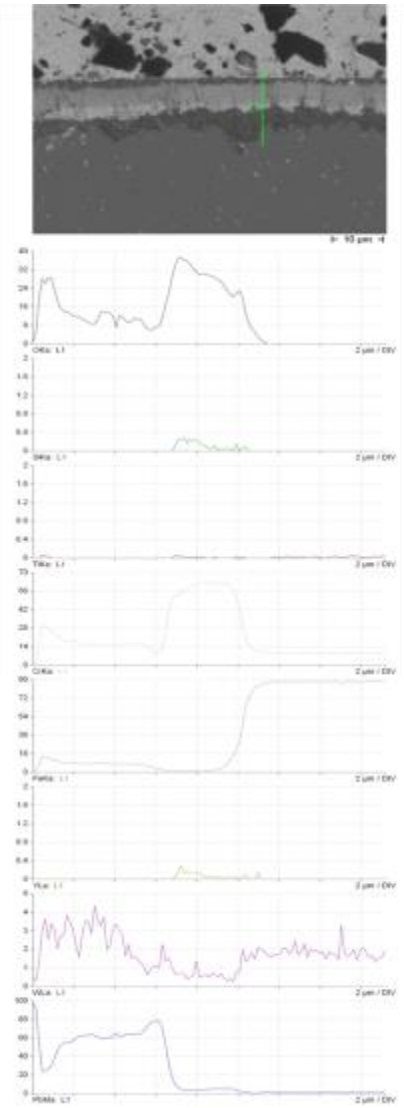

Fig. 22: 12Cr ODS GESA specimen after 2000h exposure at 650°C with marked line for the EDS line scan below

3.3.2 14Cr ODS and 14Cr ODS GESA

14Cr ODS was tested with and without GESA treatment at 650°C. On both specimens an oxide layer was formed and no dissolution attack was visible up to 5000h, Fig. 23. However, the sample without GESA treatment shows often areas with pronounced inner oxidation like in Fig. 23 top left, and after 5000h Pb can penetrate into the oxide layer. The oxide layer formed on the GESA specimen is slightly thicker compared to the 14Cr specimen in pristine state, but very homogenous without any areas of inner oxidation. Here, the idea that the re-melting by the GESA can remove local inhomogeneities that can cause local corrosion (either severe oxidation or dissolution attack) seems to be approved.

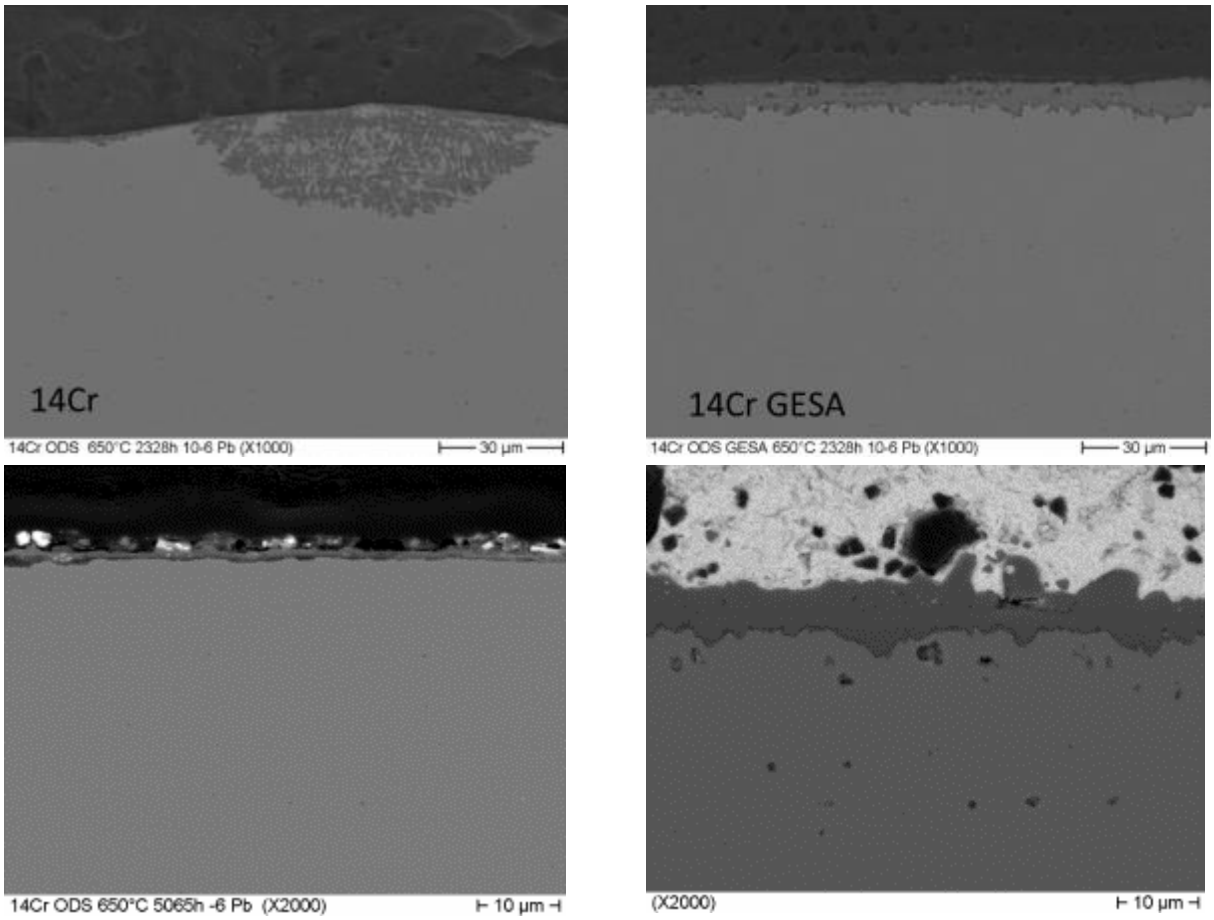

Fig. 23: 14Cr ODS with (right) and without (left) GESA treatment after 2328h (top) and 5000h (bottom) at 650°C in Pb with 10^{-6}wt% O

EDS line scans through the oxide layer on both surface states of the 14Cr ODS steel are despicted in Fig. 23. On the non-treated steel an oxide containing Fe, Cr, Si, Mn and small amount of Ti is grown. After 5000h the scale reaches a thickness of around 1.3µm and Pb inclusions are likely to be observed. In contrast to this, on the GESA treated specimen a multi-layered oxide was formed, which consists of an outward growing Fe- oxide and an inward growing Fe-Cr spinel with Mn and Ti. At the border to the bulk material Si is enriched. After 5000h Kirkendall pores were detected underneath the oxide to a depth of 28µm,which is still inside the treated layer. They are formed most probably due to the fact that the diffusion is faster in the GESA treated layer and the elements could not diffuse fast enough from underneath inside this layer. However no dissolution attack or Pb inclusions were observed.

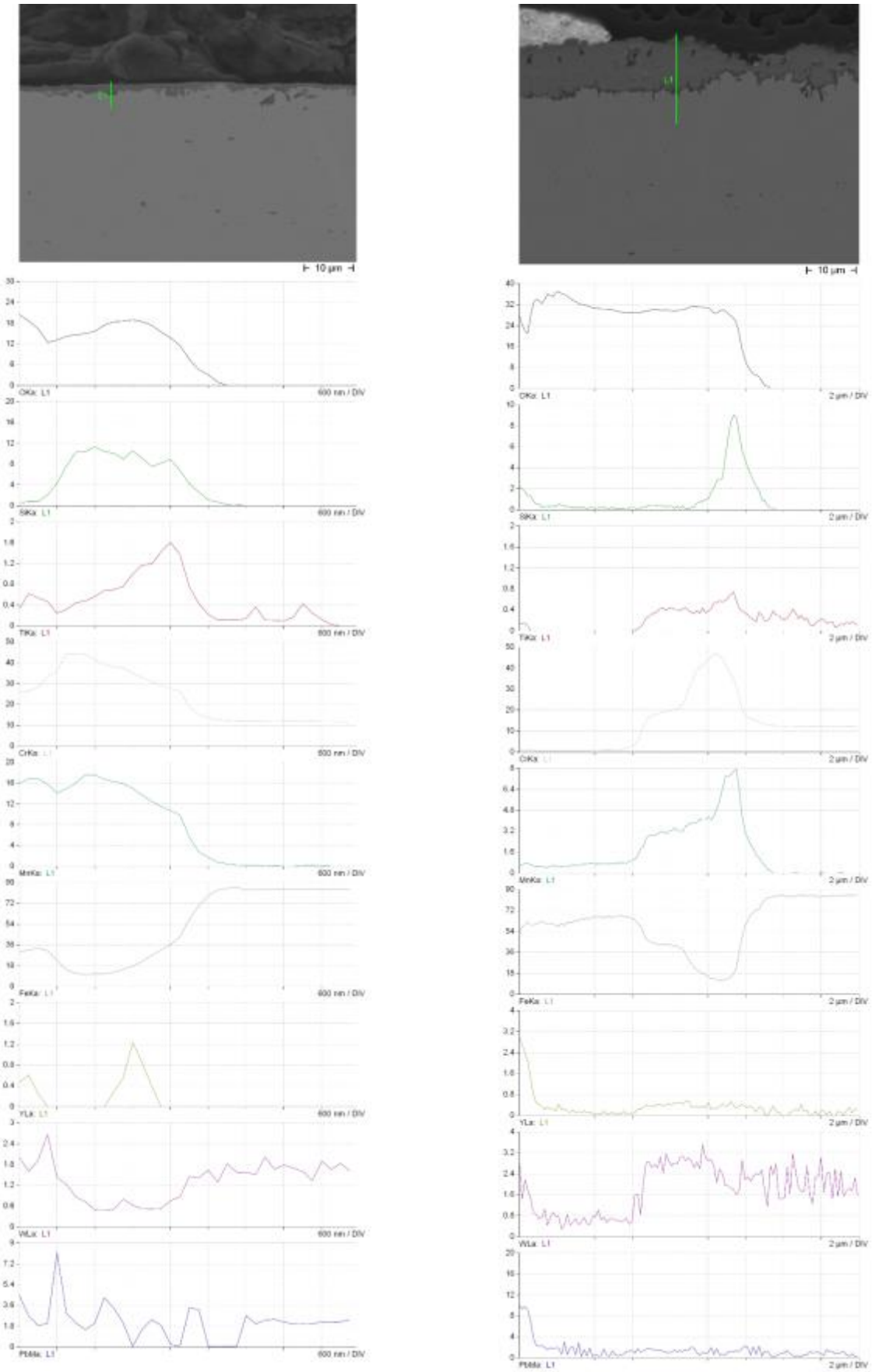

Fig. 24: 14Cr ODS with (right) and without (left) GESA treatment after 2328h at 650°C in Pb with 10-6wt% O, EDS line scan of the marked line below

3.3.3 9Cr and 12Cr ODS Al - GESA surface alloyed

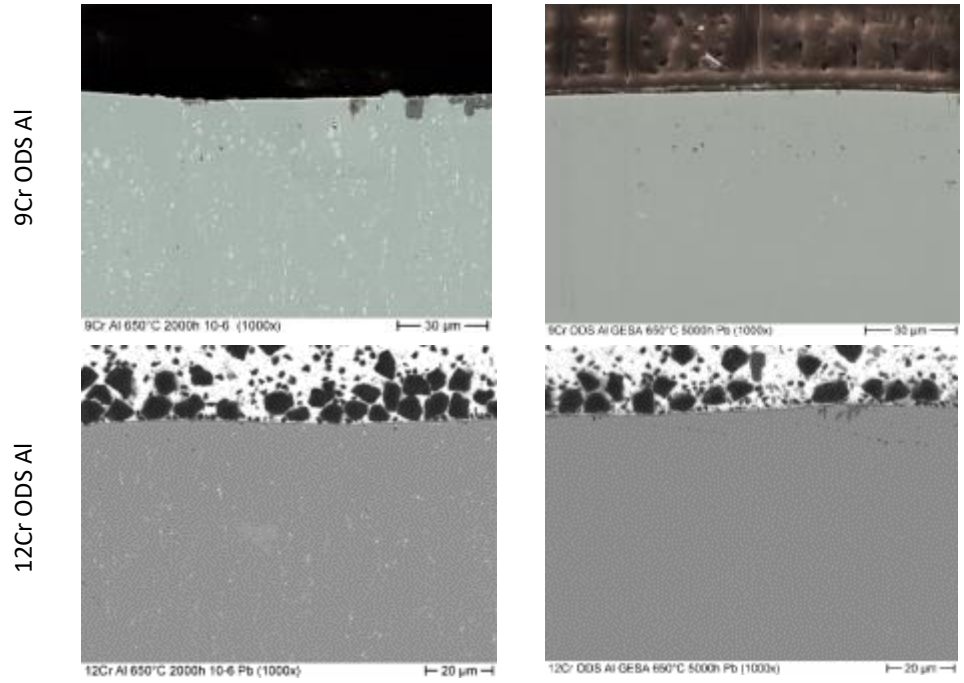

Fig. 25: cross section of 9 and 12 Cr ODS Al after 2000h and 5000h exposure to Pb with 10^{-6}wt% O at 650°C

Fig. 26 shows a micrograph of the cross section of 12Cr ODS Al after 2000h exposure at 650°C in Pb. The EDS line scan measured on the marked line is depicted underneath. Obvious is the increase of Al and O at the surface, which hints on a thin alumina layer at the top that protects the steel. In the bulk material W-Cr precipitations with a low amount of O appear.

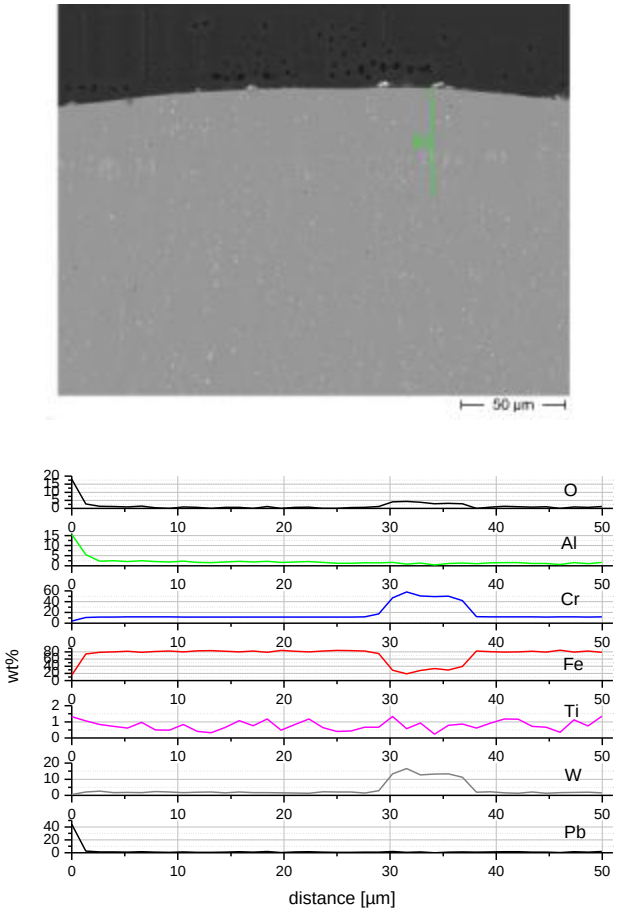

Fig. 26: photo of 12Cr ODS Al after 2000h exposure at 650°C with marked line for EDS line scan, EDS line scan underneath

3.4 700°C – CIEMAT / 9Cr and 12Cr ODS

The development of the oxide layer on 9 and 12Cr ODS steel at 700°C is illustrated in Fig. 27. The layer consists mainly of Cr rich Cr-Fe spinel or Cr oxide, Fig. 28 and Fig. 29. A Fe-based outer oxide layer or nods of it are only visible in some areas on the surface of the 9Cr ODS after 2000 h (see Fig. 27 and Fig. 28). Such Fe-based oxides are not observed after longer exposure times. After 10000h 9Cr ODS shows a thin Cr oxide layer with Mn enrichment at the surface, underneath a grain boundary diffusion area with thicker oxide roots at the transition to the bulk material is formed, Fig. 27 top right. The oxide roots also consist of Cr oxide with Mn. 12Cr ODS steel has a Cr oxide at the top with some Pb inclusions after 2000h and 5000h. Fe-O nods are only visible in the adherent Pb. Nevertheless, for long exposure times, severe dissolution attack and lead inclusions into base material were detected in both materials.

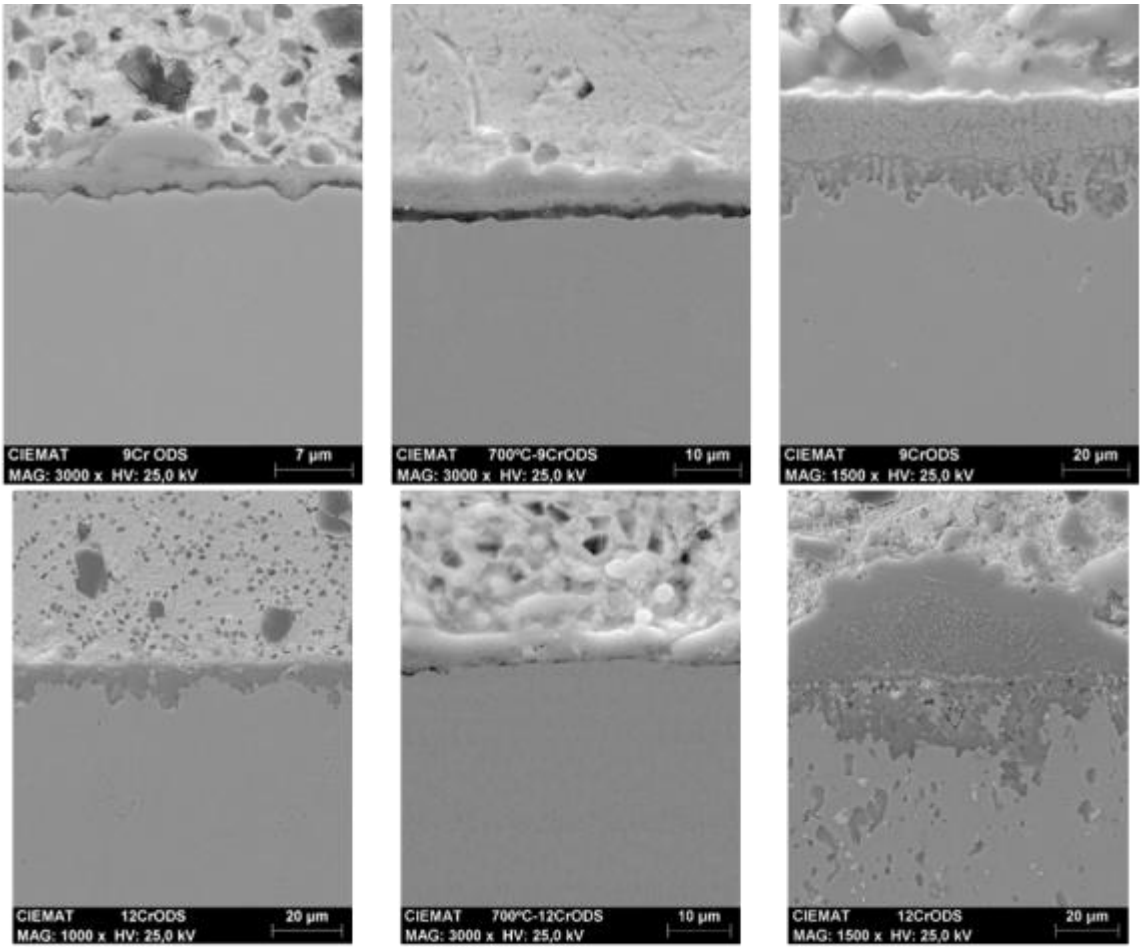

(a) 2000 h (b) 5000h (c) 10000h

Fig. 27: 9CrODS and 12CrODS tested at 700°C in lead with oxygen content of 10^{-6} wt. % at different exposure times.

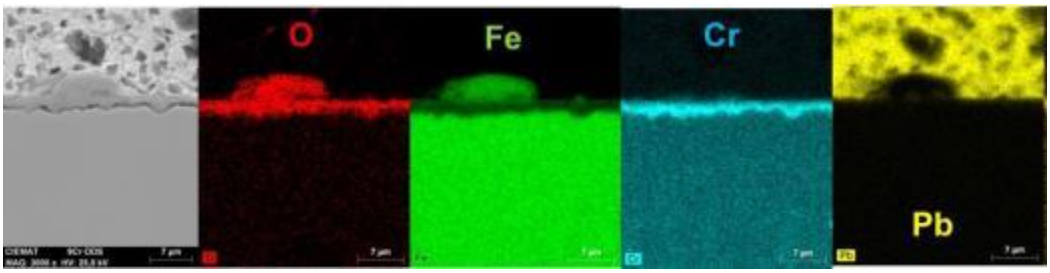

Fig. 28: Elemental mapping of EDX analysis of 9CrODS tested at 700ºC, 10^{-6} wt% O and 2000 h.

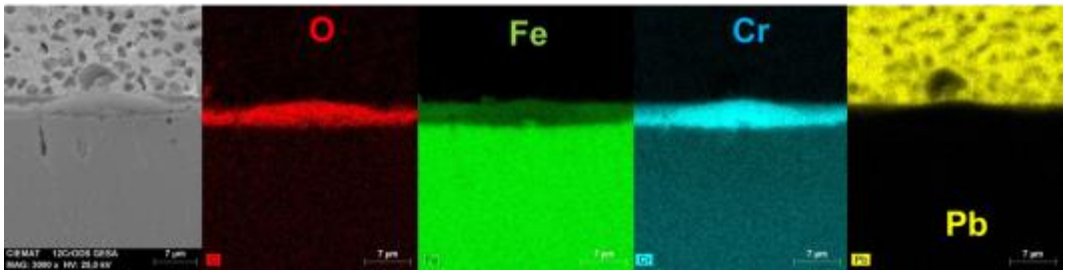

Fig. 29: Elemental mapping of EDX analysis of 12CrODS tested at 700ºC, 10^{-6} wt% O and 2000 h.

The oxide layer thickness of both materials is quite different after 2000h exposure, Tab. 9. While on 9Cr ODS the oxide layer has a thickness between 2-4µm, a 10µm thick oxide layer is found on the 12Cr ODS specimen. After 5000h the thickness is comparable. After 10000h the oxide thickness varies between 20-36µm on the 9 Cr ODS steel, while on the 12Cr ODS steel it amounts to about 40µm.

700°C		Average thickness (µm)		
		2000 h	**5000h**	**10000h**
9Cr ODS	**Cr-O with Mn**	~2-4	~8-9	~20-36
12Cr ODS	**Cr-O**	~10	~8-10	~40

Tab. 9: Average thickness of the formed oxide layer on the 9Cr ODS and 12Cr ODS steel at 700°C after different exposure times

3.4.1 9Cr and 12 Cr ODS GESA

The development of the oxide layer on both GESA treated materials at 700°C can be seen in Fig. 30. Noticable are the around 5µm large Fe-oxide nods on the surface of the 9Cr ODS GESA specimen after 2000h, Fig. 30 top left and Fig. 30 . Underneath a Fe-Cr spinel layer significant enriched with Cr and a higher Mn content at the boarder to the bulk material is visibel. This observation does not change after 5000h exposure . Sometimes Fe-O nods occure as a layer. Nevertheless, Pb inclusions in the oxide layer can be observed in both specimens. After 10000h severe dissolution attack and lead inclusions in the base material were detected in both materials. At 700 °C, this behavior is more evident, especially in the 12Cr ODS-GESA steel.

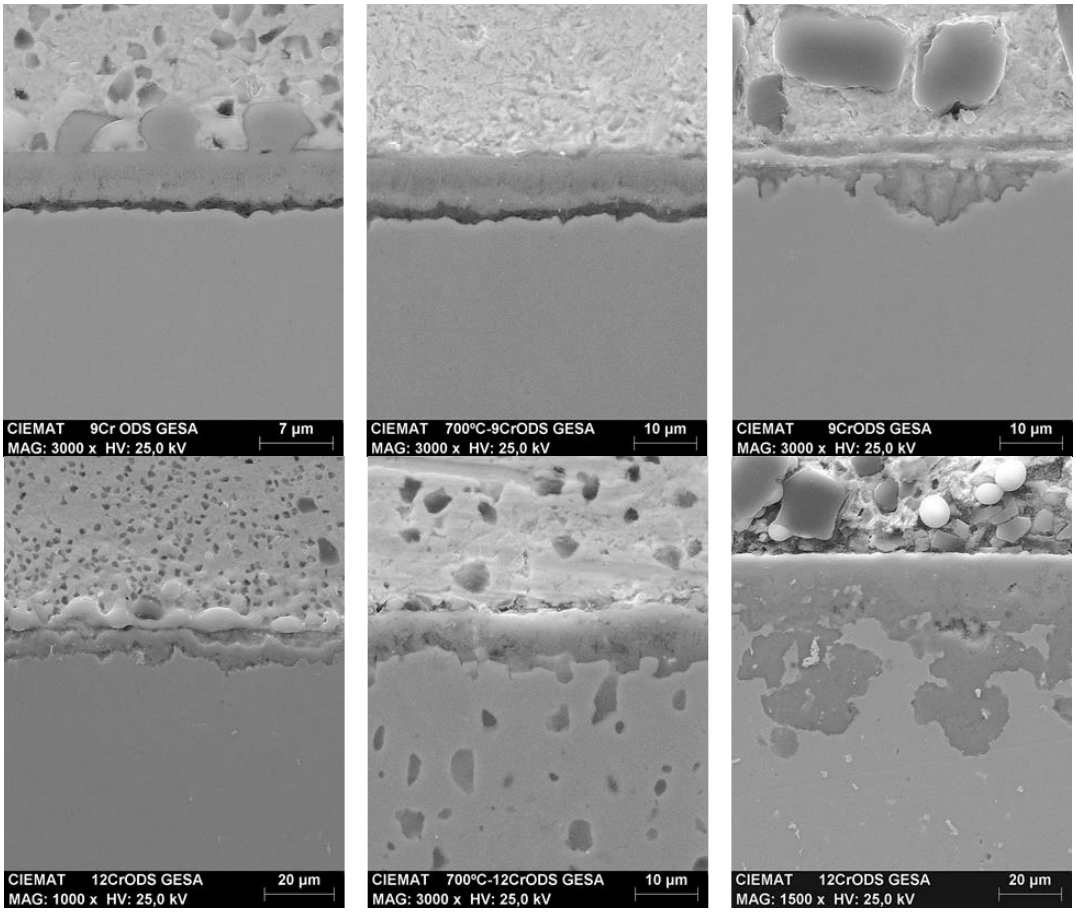

Fig. 30: 9CrODS GESA and 12CrODS GESA tested at 700°C in lead with 10-6 wt. % O after different exposure times

The result of the thickness measurement on the oxide layers is listed in Tab. 10. It is comparable with that measured on the not treated specimens at 700°C. Nevertheless, the oxide cannot prevent the penetration of Pb into the bulk, which leads to severe dissolution attack after longer exposure times.

		Average thickness (µm)		
		2000 h	**5000h**	**10000h**
700 ºC	**9CrODS GESA**	5	9	16
	12CrODS GESA	7	8	60

Tab. 10: Thickness measurements of the oxide layers of ODS GESA steel at 700°C

An EDS element mapping analysis of the oxide layer of 9Cr GESA and 12Cr GESA formed after 2000h exposure at 700°C is shown in Fig. 31 and Fig. 32. They clearly illustrate the described Fe-O nods on the 9Cr ODS GESA specimen and the Cr-oxide layer on the surface of the 12Cr ODS GESA specimen.

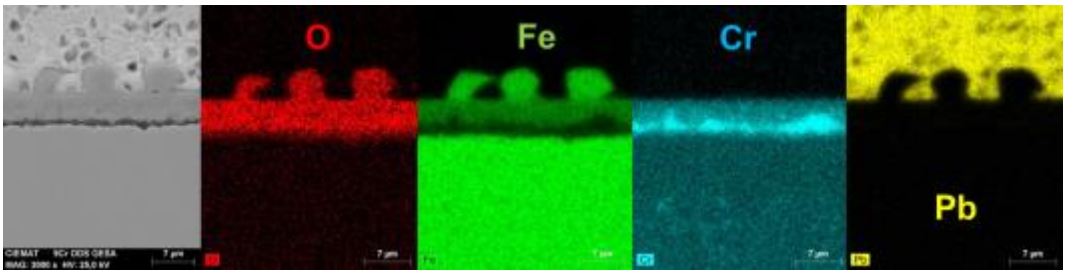

Fig. 31: Elemental mapping of EDX analysis of 9CrODS-GESA tested at 700ºC, 10^{-6} wt% O and 2000 h.

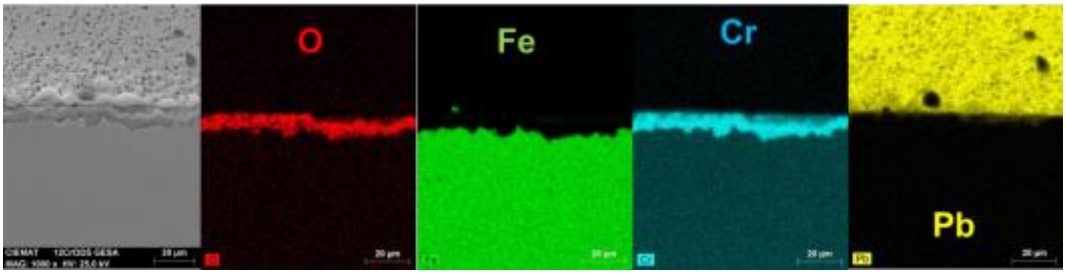

Fig. 32: Elemental mapping of EDX analysis of 12CrODS-GESA tested at 700ºC, 10^{-6} wt% O and 2000 h.

4 Experimental results at 450°C and 650°C with low oxygen contents - CNR

The signal of the Pt-air electrodes measured during the test at 650°C is shown in Fig. 33.

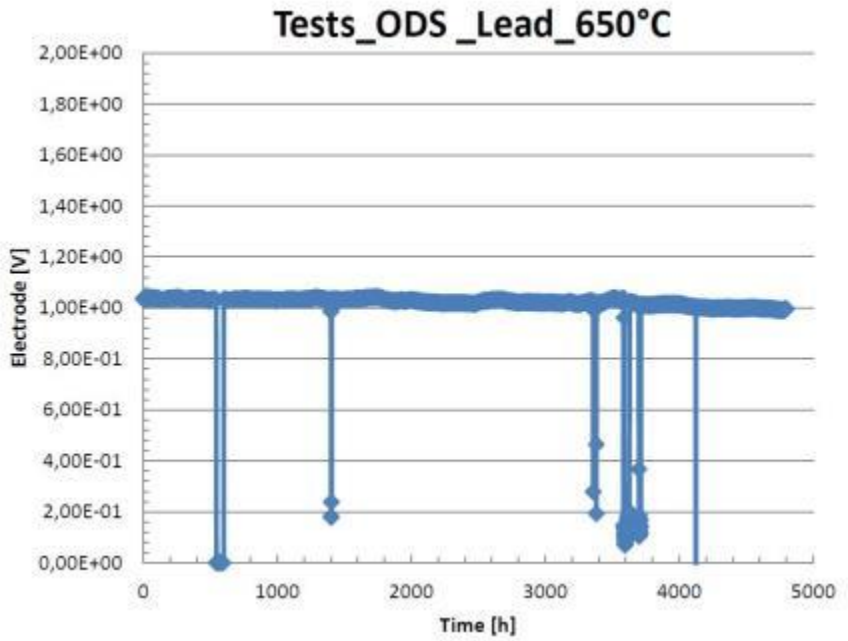

Fig. 33: Signal of the Pt-air electrode in the liquid lead at 650°C under a constant flow Ar-5%H2

The electrode's potential was almost constant during the whole all test times:
At T=450°C, the mean value of the potential was V= 1.09V
At T=650°C the mean value of the potential was V= 1.03V
According to the relation:
Log (Co[wt%]) =-2,3335+6338,1 / T[K] -10080E [V] / T[K] (C. Schroer,J. Konys, FZKA-7364)
the oxygen content mean value during the experiment was calculated:
at T= 650°C Co = 1.9 10^{-7} wt%
at T= 450°C Co= 5.1 10^{-8} wt%

After all corrosion tests, the surface of the solidified Pb baths showed no surface oxidation. The residual lead eventually present on the surface of each sample was not removed. Each sample was embedded in resin, grinded with SiC and polished with diamond paste. Afterwards, the specimens were examined by SEM-EDS.

4.1 450°C/ 5.1 10^{-8} wt%

4.1.1 9Cr ODS / 9Cr ODS GESA / 450°C

Photos of the cross section after the exposure (2000h and 5000h) of the 9Cr ODS steel are depicted in Fig. 34. After 2000h no oxide layer could be detected by EDX.

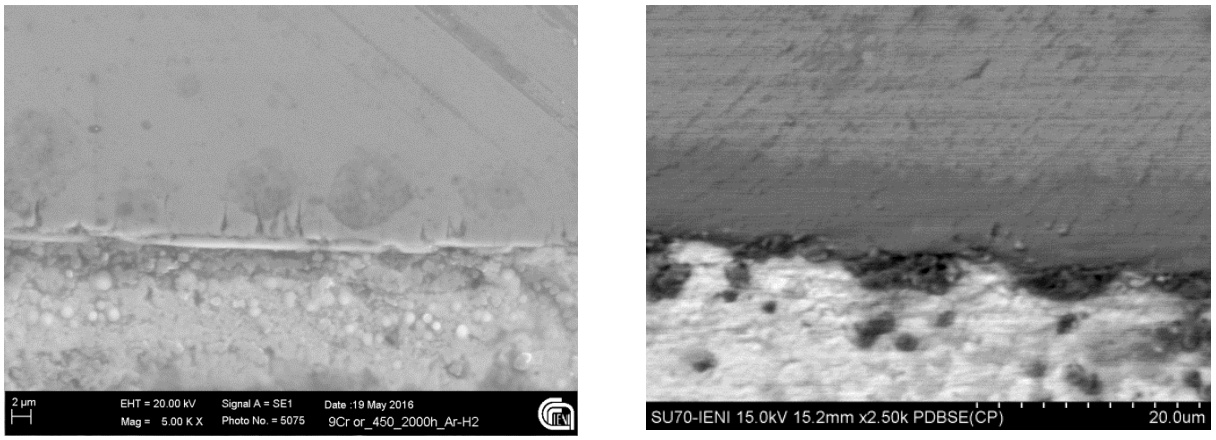

Fig. 34: ODS 9Cr tested in static lead at 450°C for 2000h (left) and 5000 h (right)

The EDS measurements after 5000h exposure revealed an oxide layer consisting of a thin Fe-O area followed by a very thin Cr-Fe spinel layer.

Due to a better diffusion in the GESA treated specimen a 4-5µm thick, homogenous oxide layer was formed on the 9Cr ODS GESA specimen after 5000h, Fig. 35. It consist like on the 9Cr ODS specimen of a Fe-O outer layer (magnetite) and a Cr-Fe spinel layer. Parts of the magnetite seems to spall off.

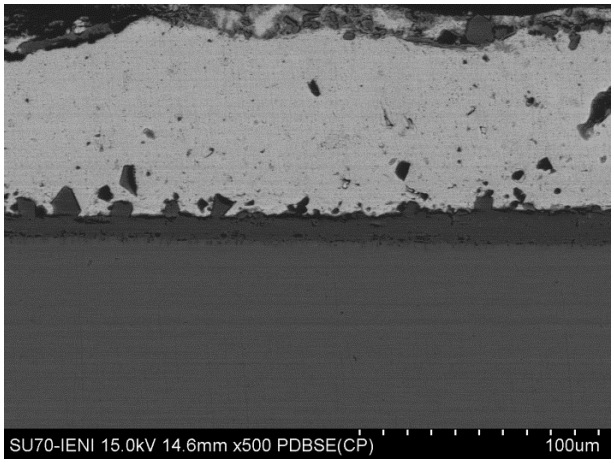

Fig. 35: ODS 9Cr ODS GESA tested in static lead at 450°C for 5000h

4.1.2 12Cr ODS / 12Cr ODS GESA / 450°C

After 2000h exposure, only small oxide nods were detectable on the surface. In some areas grain boundary oxidation happens like in Fig. 36 top left.

A very thin oxide layer was found after 5000h exposure on the 12Cr ODS specimen. It seems to consist similar as on the 9Cr ODS specimen of an outer Fe-O and a Fe-Cr spinel layer underneath, Fig. 36. Like after 2000h in some area grain boundary oxidation was observed. The small particles in the lead above the steel surface are abrasive grains from the sample preparation.

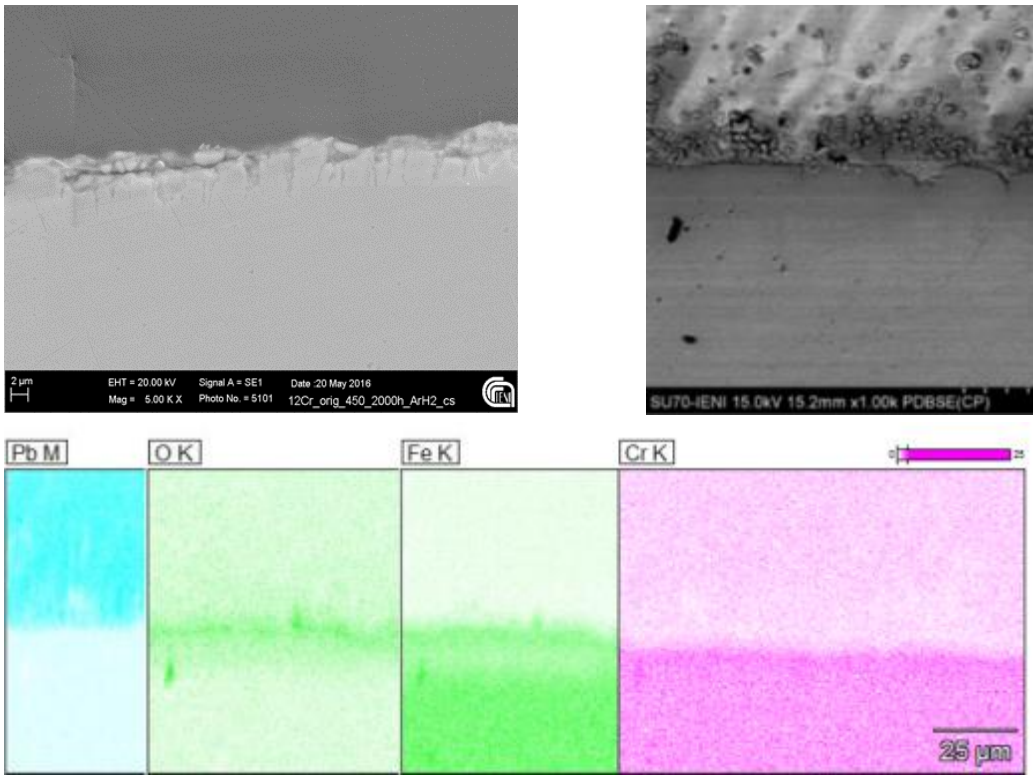

Fig. 36: ODS 12Cr tested in static lead at 450°C for 2000h (top left) and 5000 h (top right); EDS mapping (bottom) of Pb, O, Fe and Cr on the 5000h specimen

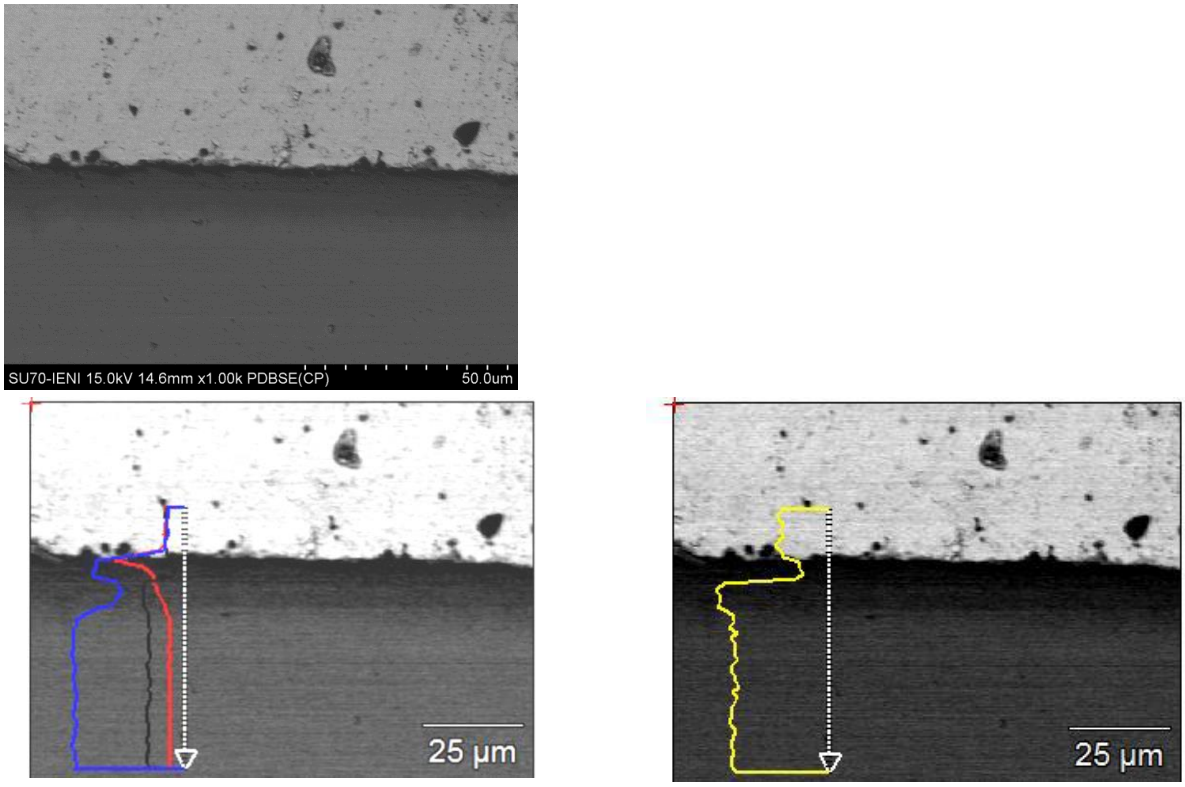

Fe: blue; O. red; Cr: black

Cr

Fig. 37: 12 Cr ODS GESA tested in lead at 450°C for 5000 h (top), with EDS line scan trough the oxide layer (bottom)

The behavior of the GESA treated 12Cr ODs specimen can be seen in Fig. 37. There is a multi-layered oxide on the surface. It consists of a Fe-O layer on top with a Fe-Cr spinel underneath. Areas with grain boundary oxidation were no observed.

4.1 650°C/ 1.9 10^{-7} wt%

4.1.1 9Cr ODS / 9Cr ODS GESA / 650°C

A very thin oxide layer and dissolution attack together with parts with inner oxidation could be observed on the 9Cr steel at 650°C after 2000h, Fig. 38 top left.

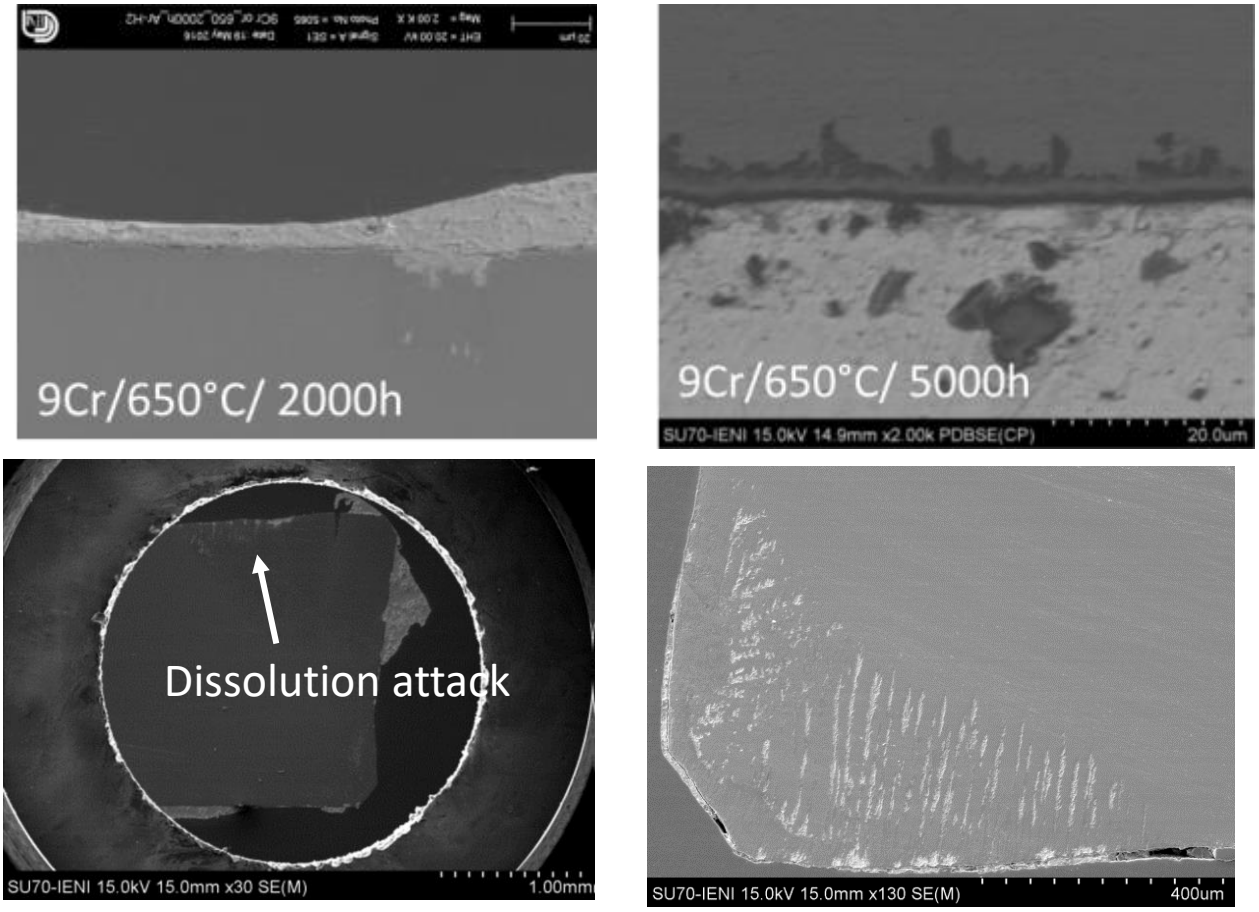

Fig. 38: ODS 9Cr tested in static lead at 650°C for 2000h (top left) and 5000 h (top right, bottom)

After 5000h the oxide layer grows further and reaches a thickness of around 3µm with roots going up to 8.4µm into the depth, Fig. 38 top right. The oxide layer consists of a Cr rich Fe-Cr-Mn spinel. Undeneath an area with higher Fe and lower oxygen content results in a brighter appearance on the SEM picture. It is followed by oxide roots consisting of a Si rich Cr-Mn-Fe oxide. Also here areas with dissolution attack were observed (bottom left and right), very severe especially at the edges of the specimen.

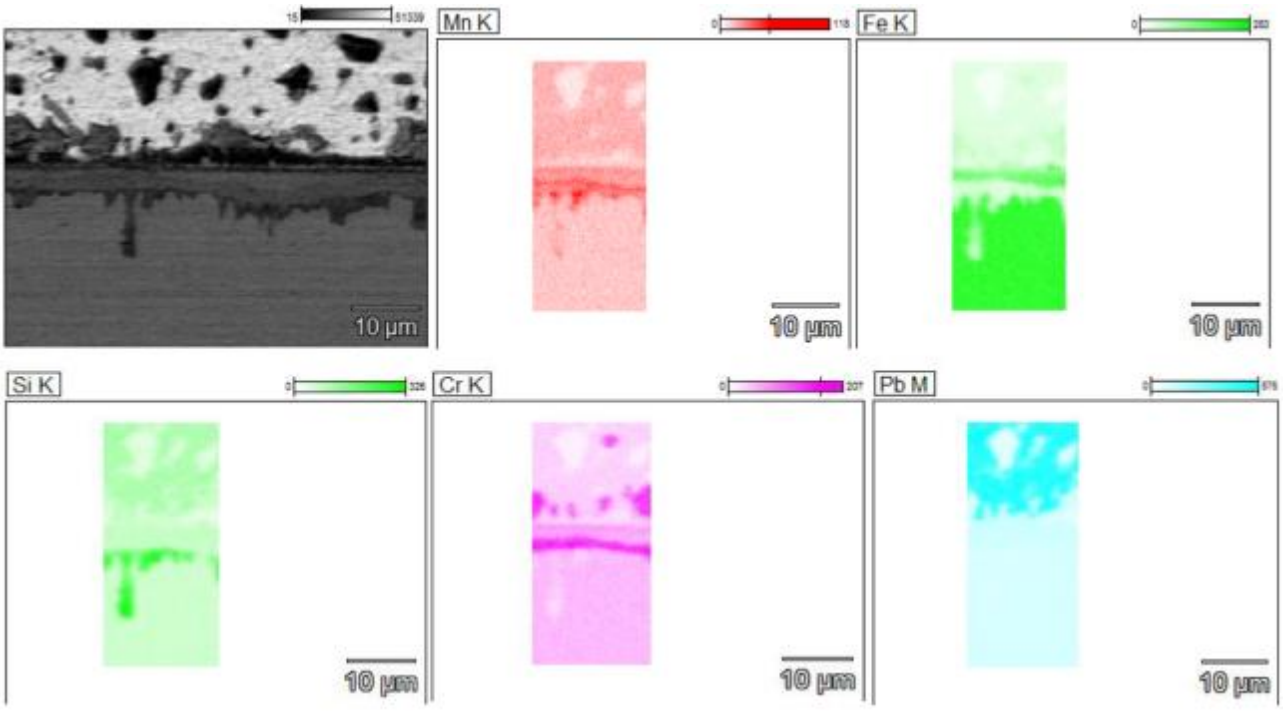

Fig. 39: 9Cr ODS GESA tested in static lead at 650°C for 5000h (top left) and EDS mapping photos of Mn, Fe, Si, Cr and Pb

The GESA treated specimen behaves better, no dissolution attack was observed. The surface is covered with a multilayered oxide, which consists of a Fe-oxide on top, underneath a Fe-Cr-Mn oxide with increased content of Cr and Mn to the boarder of the oxide roots and bulk material. The oxide roots consist of Si and Mn. The oxide layer has a thickness of around 6-7µm, together with the roots up to 13-14µm.

The specimen shows at the bottom that was not GESA treated a similar worse behavior like the 9Cr ODS specimen in pristine state.

4.1.2 12Cr ODS / 12Cr ODS GESA / 650°C

Already after 2000h at 650°C (1.9 10^{-7}wt% in the liquid Pb) the 12Cr ODS specimen shows deep dissolution attack, Fig. 40 top. After 5000h, the specimen exhibits large areas with dissolution attack of up to 88µm, Fig. 40 middle right. Nevertheless, also a 24-42µm thick oxide layer consisting of Cr-oxide can be seen on part of the surface, Fig. 40 bottom.

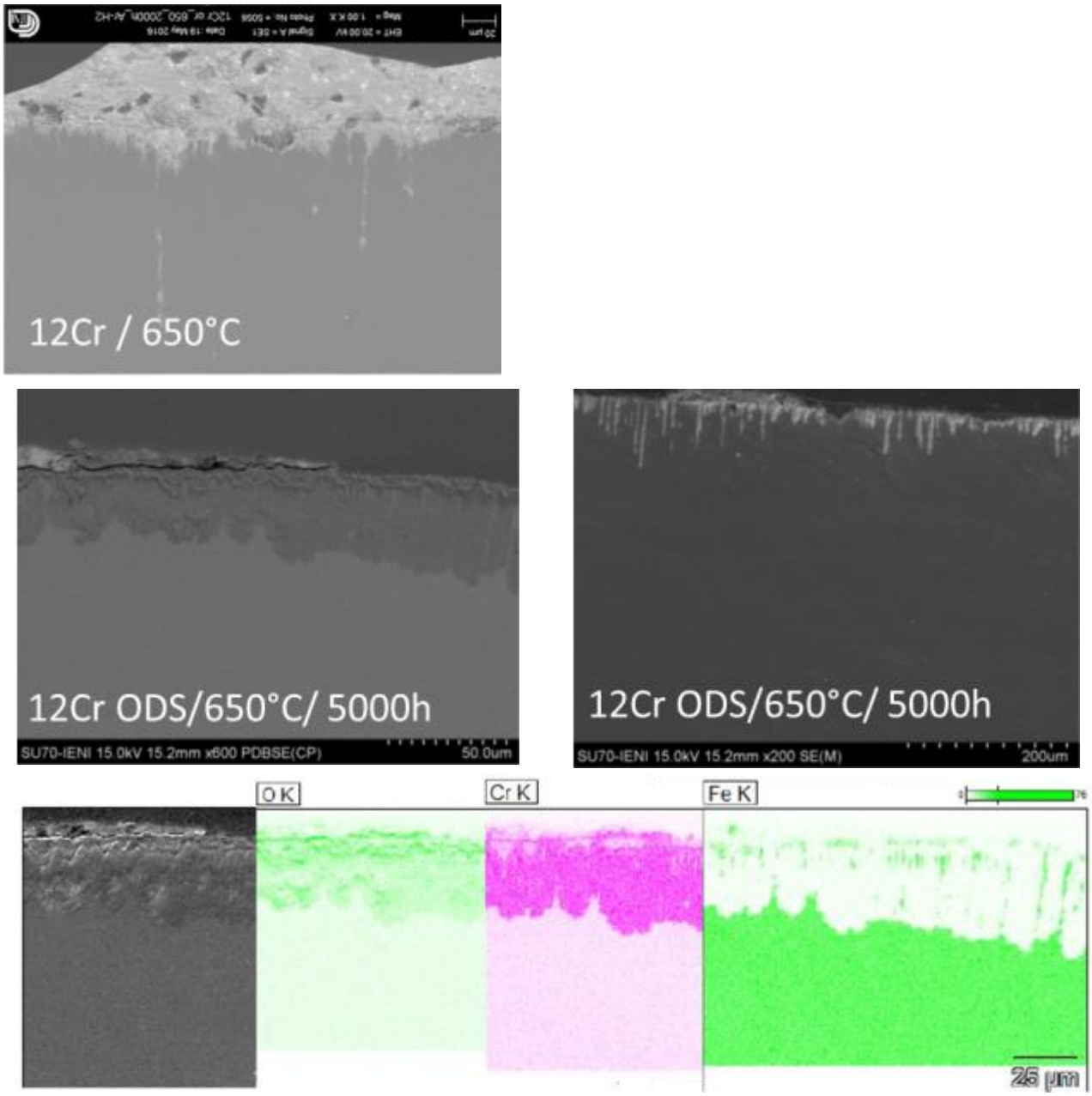

Fig. 40: ODS 12Cr tested in static lead at 650°C for 2000h (top) and 5000h (middle) with EDS mapping photos (bottom)

The behavior of the 12Cr ODS GESA treated specimen is depicted in Fig. 41. After 2000h a mixture between areas with dissolution attack and oxide layers can be seen, Fig. 41 top left. The oxide layer is growing. After 5000h parts with an around 7-8µm thick Fe-Cr spinel at the top with Pb inclusions (Fig. 41 top right) and pores underneath occur. As well, the dissolution attack is progressing. It is growing up to a depth of 135µm, Fig. 41 bottom.

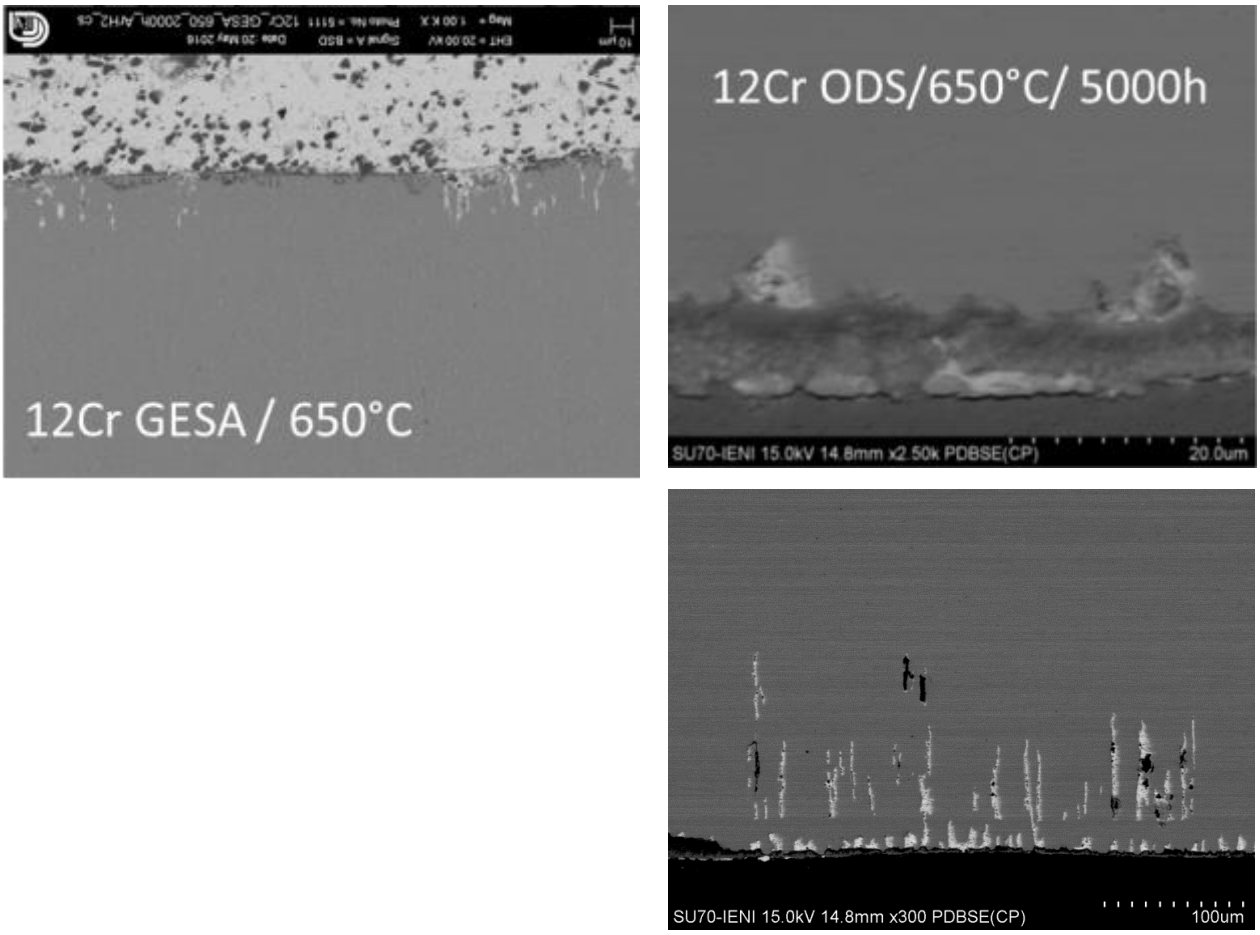

Fig. 41: ODS 12Cr tested in static lead at 650°C for 2000h (top left) and 5000h (top right, bottom)

5 Experimental results under transient conditions

5.1 550°C -750°C (24h)-550°C

After the test, all specimens showed a similar behaviour like after exposure at constant 550°C. The 9Cr ODS showed a multi-layered oxide with a thickness of around 13µm and with roots up to 19µm depth. Fig. 43 left shows an EDS line scan though the oxide layer. It consists on top mainly of Fe and O. Underneath follows a Fe-Cr spinel with Mn and Si. The Cr, Mn and Si content increases to the border to the bulk material.

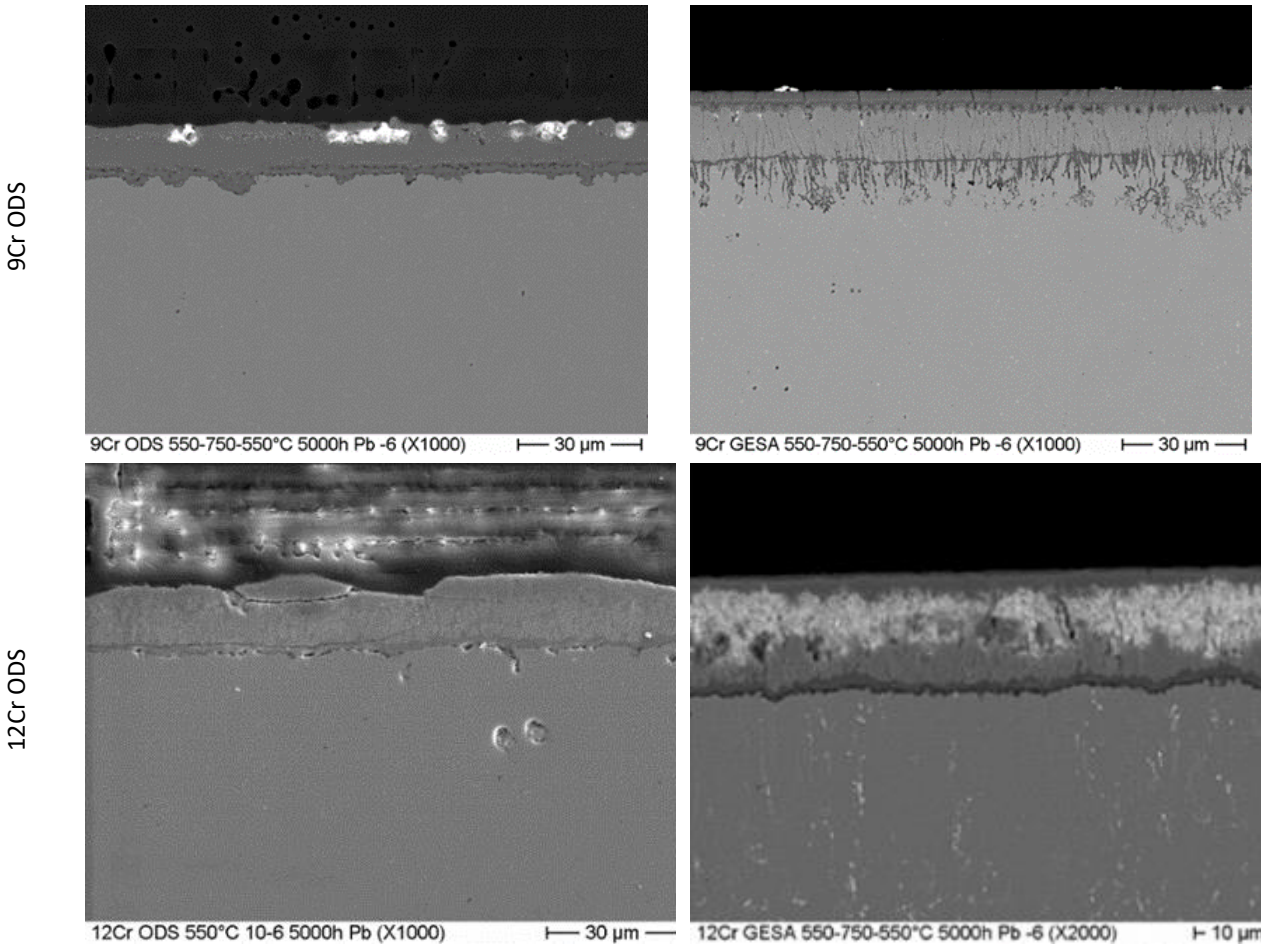

Fig. 42: 9Cr and 12Cr ODS with (right) and without GESA (left) after exposure test under transient conditions (550°C-750°C-550°C-5000h)

An EDS line scan though the oxide layer on the 9Cr ODS GESA specimen is depicted in Fig. 43 right. On top a homogenous oxide of 3.5-5 µm was formed consisting of Fe-Cr-O and a slight enrichment in Si and Y. This oxide layer has some cracks. Underneath this oxide scale the area with columnar grains exhibits oxidation of the longitudinal oriented grain boundaries with pores in the boundary region to the scale that are partly filled with Pb. The zone with oxidized columnar grain boundaries is around 8-12 µm thick and followed by a Cr rich spinel band with increased Si content. Below, an area with grain boundary oxidation having a thickness between 13-20µm is observed. The oxide layer in total has a thickness between 30-35µm.

Fig. 44 shows EDS line scans through the formed oxide layer on the 12Cr ODS steel with (right) and without (left) GESA treatment. The thick oxide layer, which was observed in the test with constant temperature after 2000h exposure at 550°C, is spalled off. Only rests of the diffusion zone can be found, sometimes with minor rests of the Cr-Fe spinel on top. In the inner diffusion zone Pb inclusions can be observed as well as cracks parallel to surface, Fig. 42

bottom left. At the end of this area the Cr content and slightly the Si and Ti content increases and form a border strip to the bulk. Between the border strip and the bulk Kirkendal pores appear which reduces the adherence of the oxide.

The oxide layer on the 12CrODS GESA layer is still there. The Fe-Cr spinel on top has two distinct layers. The first layer is denser but exhibits cracks, similar like the upper part of the oxide layer on the 9Cr ODS GESA specimen. The second part has strong Pb inclusions, which can be seen on Fig. 42 bottom right. Underneath follows an area with grain boundary oxidation. In this area the Fe content is higher than in the Cr-Fe spinel above, Fig. 44 right. In addition, a Cr rich oxide boarder strip is observed. Sometimes underneath the border strip a small area of inner diffusion can be seen, Fig. 44 right.

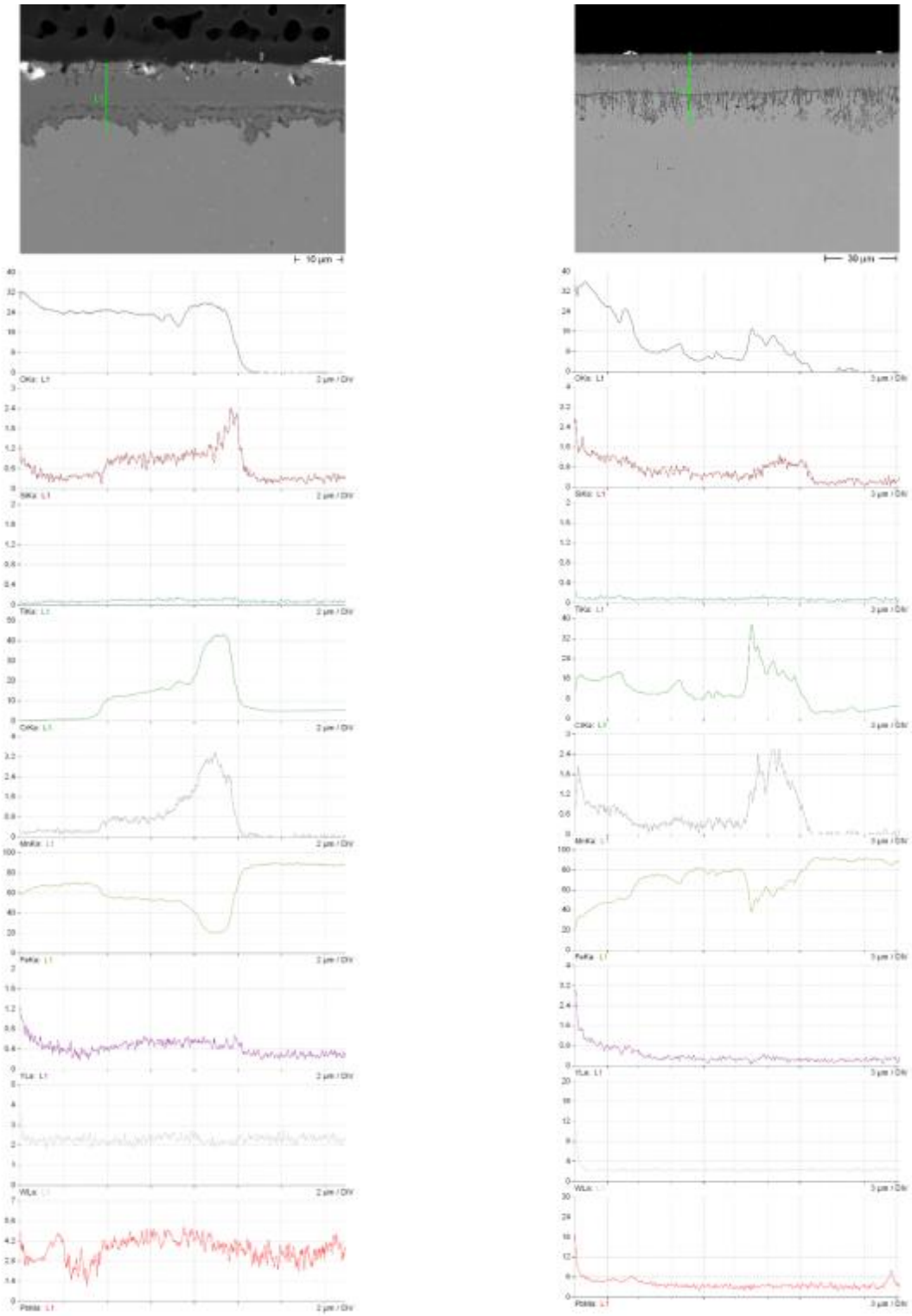

Fig. 43: EDS line scan (wt%) though the formed oxide layer on 9Cr ODS with (right) and without (left) GESA treatment exposed to Pb with transient temperature condition (550°C-750°C-550°C-5000h)

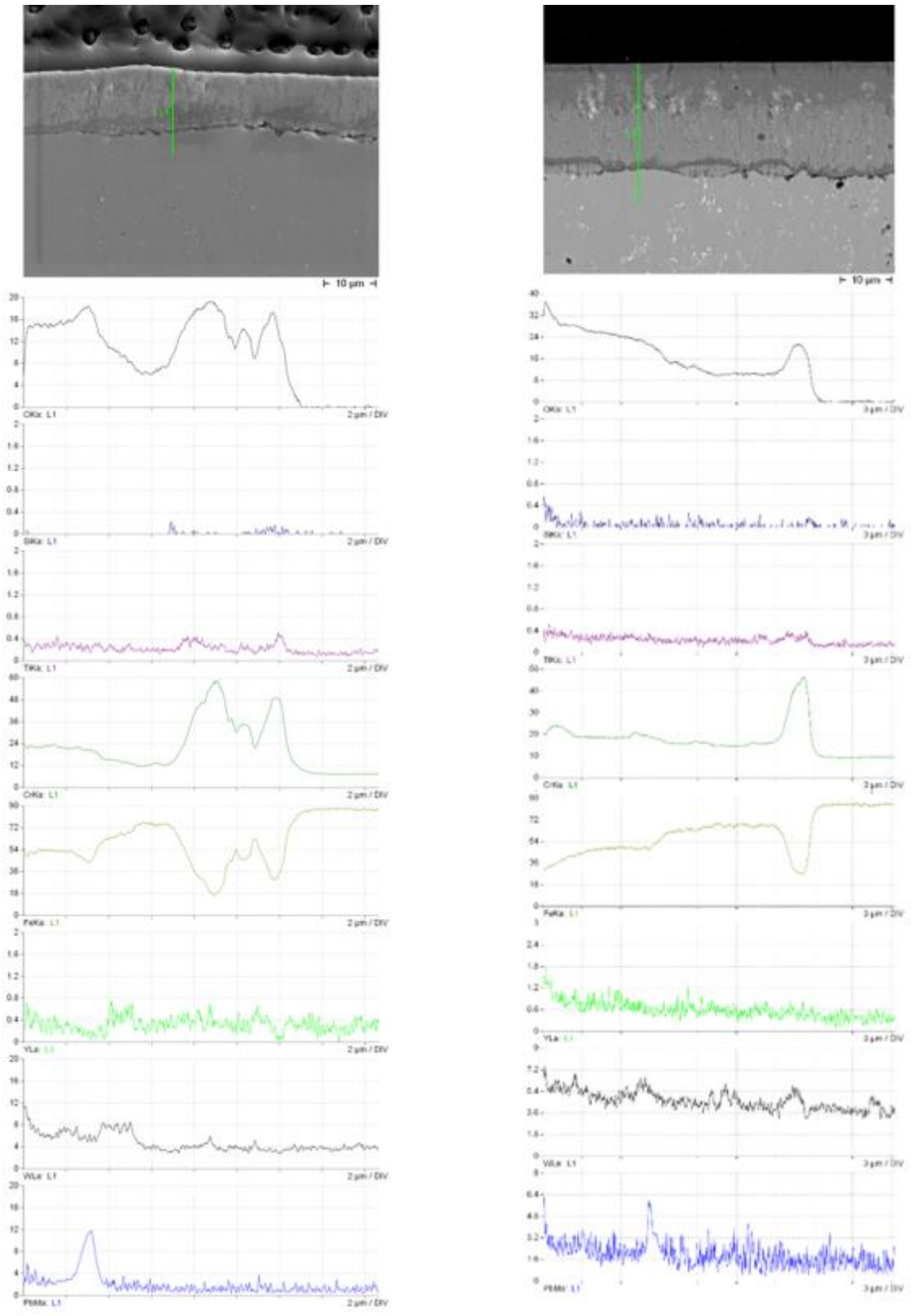

Fig. 44: EDS line scan (wt%) though the formed oxide layer on 12Cr ODS with (right) and without (left) GESA treatment exposed to Pb with transient temperature condition (550°C-750°C-550°C-5000h)

The cross sections of the 14Cr ODS specimens with and without GESA treatment are shown in Fig. 45. Like in the test at constant temperature, an 800nm thin oxide layer was formed on the specimen in pristine state. In contrast, the

modified sample exhibit a multi-layered oxide consisting of magnetite and a spinel. The magnetite layer has Pb inclusions and starts to spall off. Dissolution attack was not observed on both specimens.

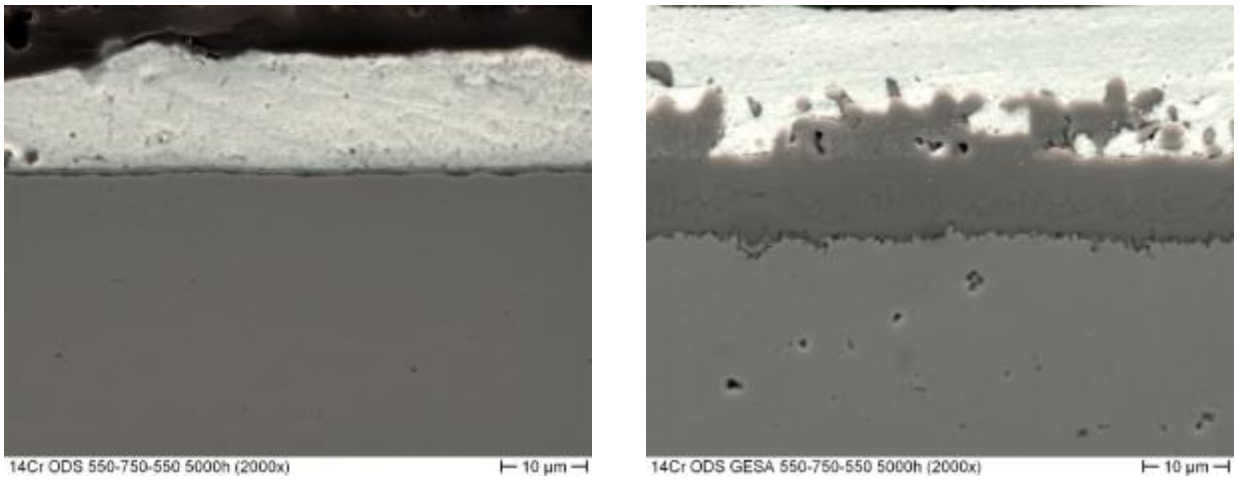

Fig. 45: 14Cr ODS with (right) and without GESA (left) after exposure test under transient conditions (550°C-750°C-550°C-5000h)

5.2 550°C -1000°C (24h)-550°C

The temperature transient test was stopped after the temperature was reduced to 550°C following the 24h 1000°C period. Finally, the total testing time was 2072 hours. The specimens were analyzed and the behaviors observed are presented in Fig. 46 and Fig. 47 for both steels, with and without GESA treatment, respectively.

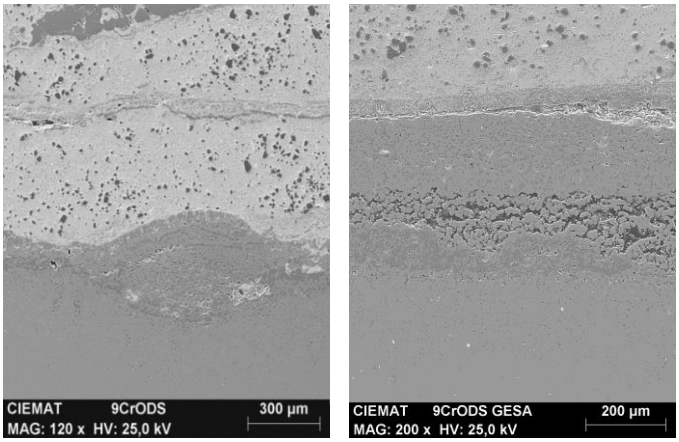

Fig. 46: 9CrODS (left) and 9CrODS GESA (right) after the temperature transient test (2072 hours)

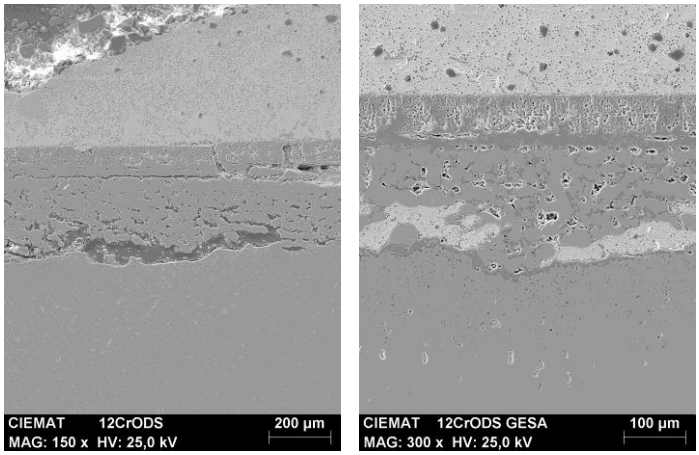

Fig. 47: 12CrODS (left) and 12CrODS GESA (right) after the temperature transient test (2072 hours)

The composition of the oxide films of each of the specimens were characterized by SEM-EDS. The element mapping micrographs can be seen in Fig. 48 and Fig. 49.

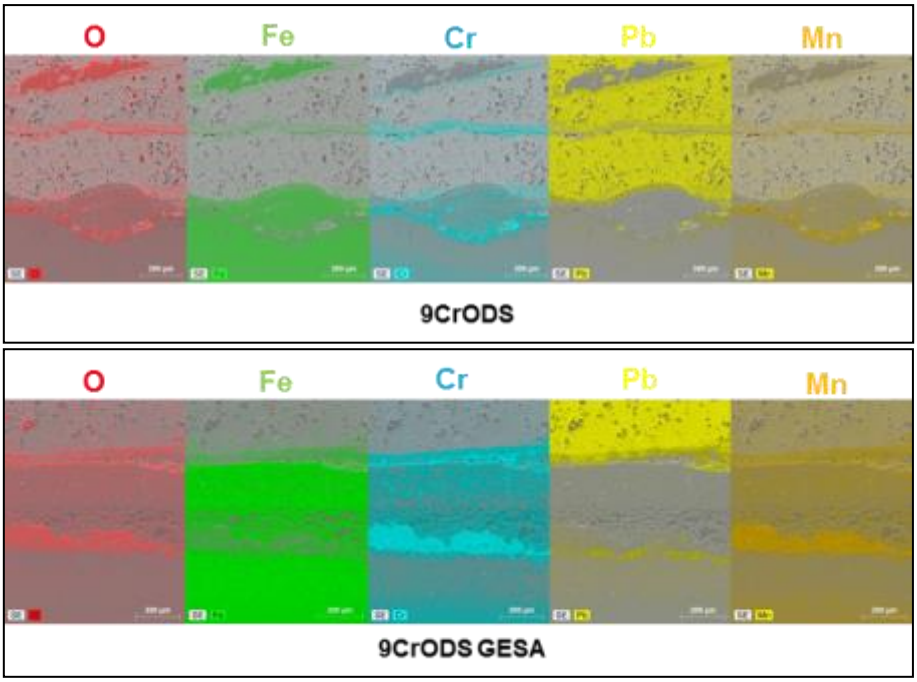

Fig. 48: Elemental mapping of EDX analysis of 9CrODS after the temperature transient test (2072 hours)

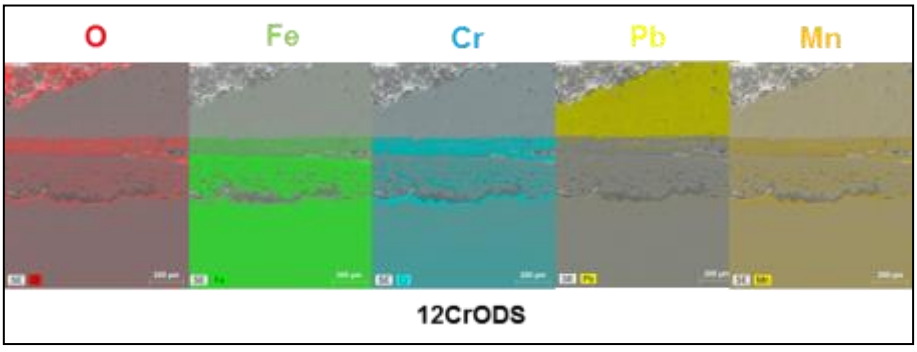

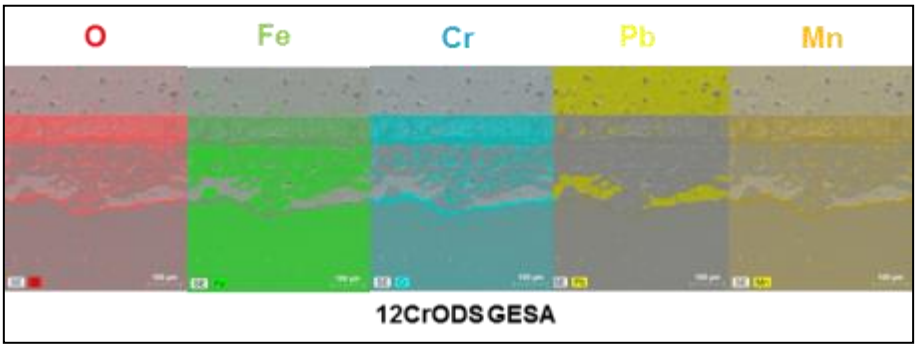

Fig. 49: Elemental mapping of EDX analysis of 12CrODS after the temperature transient test (2072 hours)

In all cases the oxide layer is damaged and started to spall off. With the exception of 12Cr ODS, Pb is found at the border to the bulk material, Fig. 48 and Fig. 49.

6 Loss of oxygen control system

6.1 9Cr ODS original

After the test, the sample showed a 4-5µm thick oxide layer at the surface (Fig. 51 + Fig. 50). EDS analysis are depicted inside the micrographs. In Fig. 50 a thin internal layer enriched in Cr and a layer of Fe-Cr-O is observed. The Fe content increases to the surface.

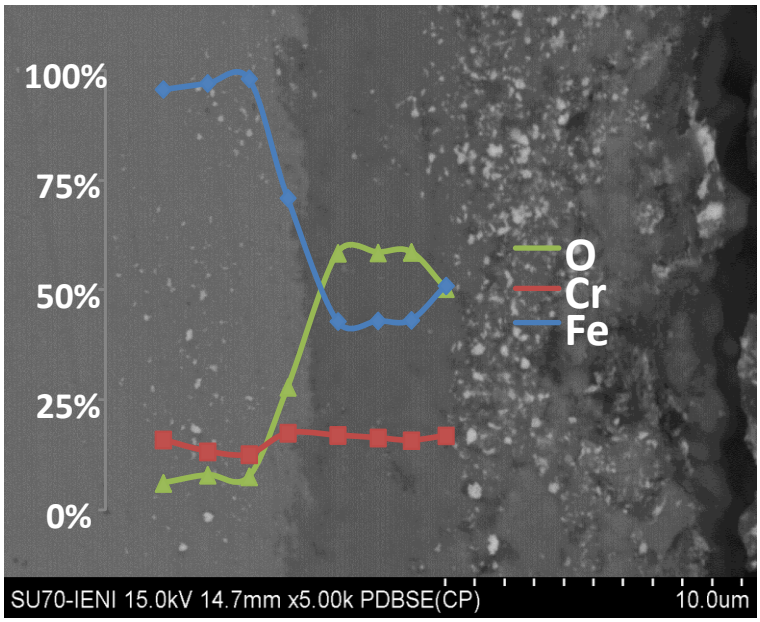

Fig. 50: ODS 9Cr, tested in static lead at 450°C under oxygen transient conditions. The composition of the different layers observed is in at%.

The measurement in Fig. 51 shows also a Cr enrichment at the border to the bulk and a Fe-Cr-O above. The Fe enrich layer at the surface is thicker in this area than in Fig. 50. A dissolution attack was not observed.

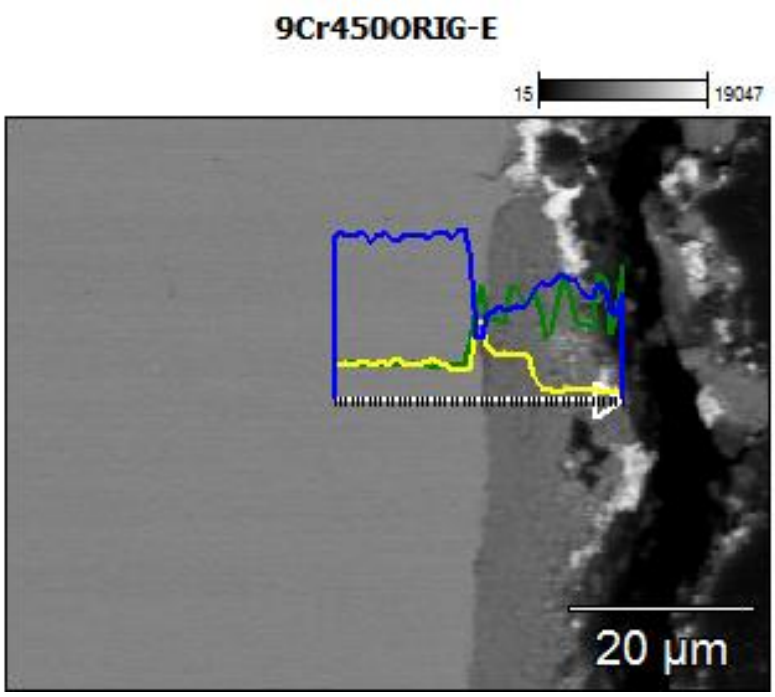

Fig. 51: ODS 9Cr, tested in static lead at 450°C under oxygen transient conditions. Lines scan: blue= Fe; yellow = Cr; green = O.

6.1 9Cr ODS GESA

A significant zone of the sample is shown in Fig. 52 (left-SEM image, right obtained by PDBSE.

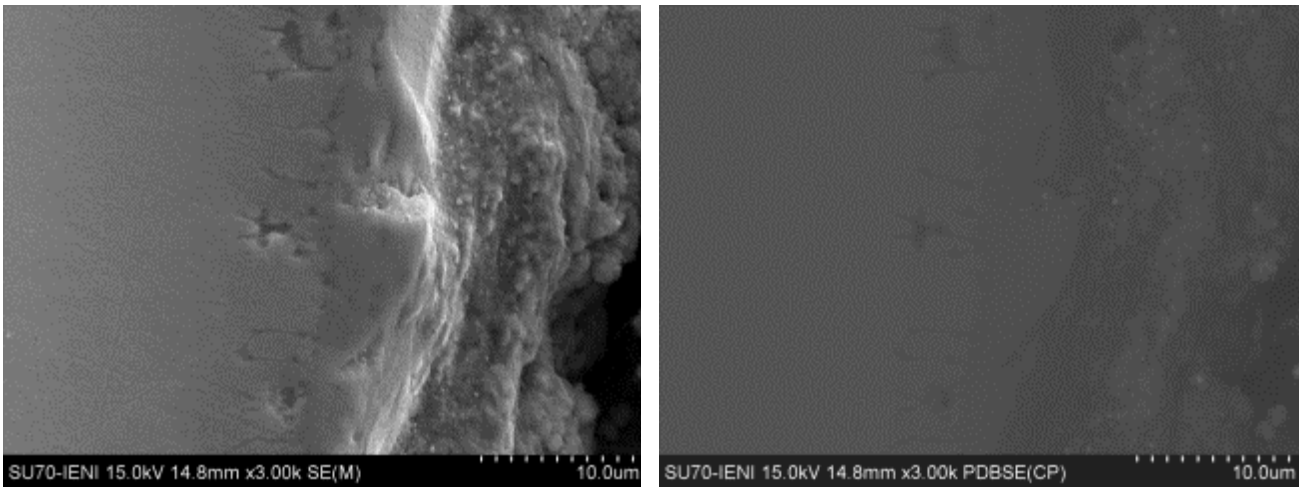

Fig. 52: Fig 6: ODS 9Cr treated GESA, tested in static lead at 450°C under oxygen transient conditions: SEM and BSE images

The sample shows a Cr-enrichment in the inner layer towards the matrix. A Fe-Cr-Mn spinel is detected and the grain boundary oxidation is clearly visible. The iron oxide is located in the outer layer. The EDS analysis of the main components is shown within Fig. 53.

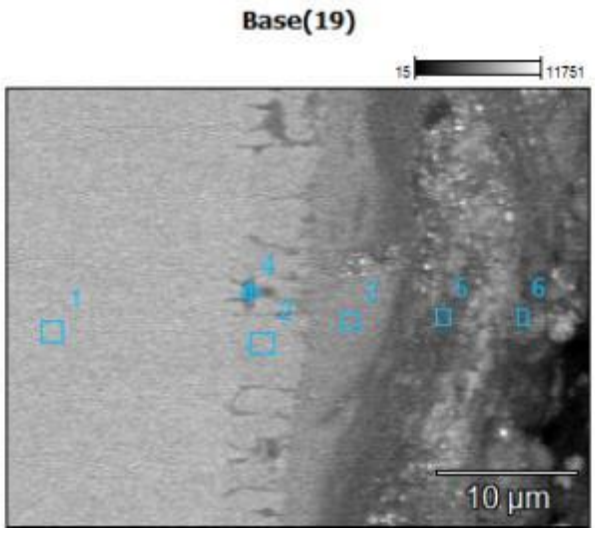

		Cr-K	Mn-K	Fe-K	W-L
9CrGesa450-C_pt1		10.17	1.16	88.11	0.56
9CrGesa450-C_pt2	18.26	9.64	1.20	70.89	0.00
9CrGesa450-C_pt3	48.57	9.99	0.52	40.92	0.00
9CrGesa450-C_pt4	23.55	27.62	1.58	47.26	
9CrGesa450-C_pt5	18.08	3.41		60.82	1.52
9CrGesa450-C_pt6	11.71	0.64		85.22	

Fig. 53: bottom: ODS 9Cr GESA, tested in static lead at 450°C under oxygen transient conditions; top: EDS analysis results of the marked points

A similar microstructure was found in other areas of the sample, as shown in Figure 8.

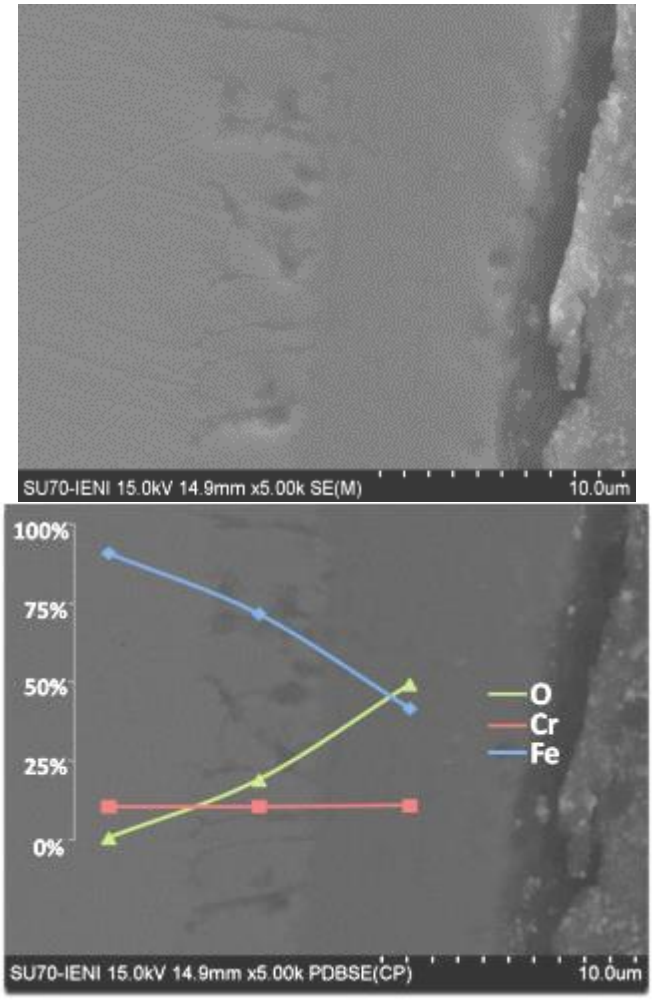

Fig. 54: ODS 9Cr treated GESA, tested in static lead at 450°C under oxygen transient conditions: SEM and BSE images. BSE image with line scan of the composition (in at%).

The EDS analysis of the different layers observed in the sample of Fig. 54 shows an inner oxidation zone with a thickness of 4-5 μm and an outer layer with a thickness of 7-8 μm; most probably the outer layer consist of Fe-Cr spinel with an magnetite above.

6.2 12Cr ODS original

An oxide layer of around 24.8μm thickness (inner oxidation zone and oxide layer together) is formed on the surface of 12Cr ODS under these condition, Fig. 55.

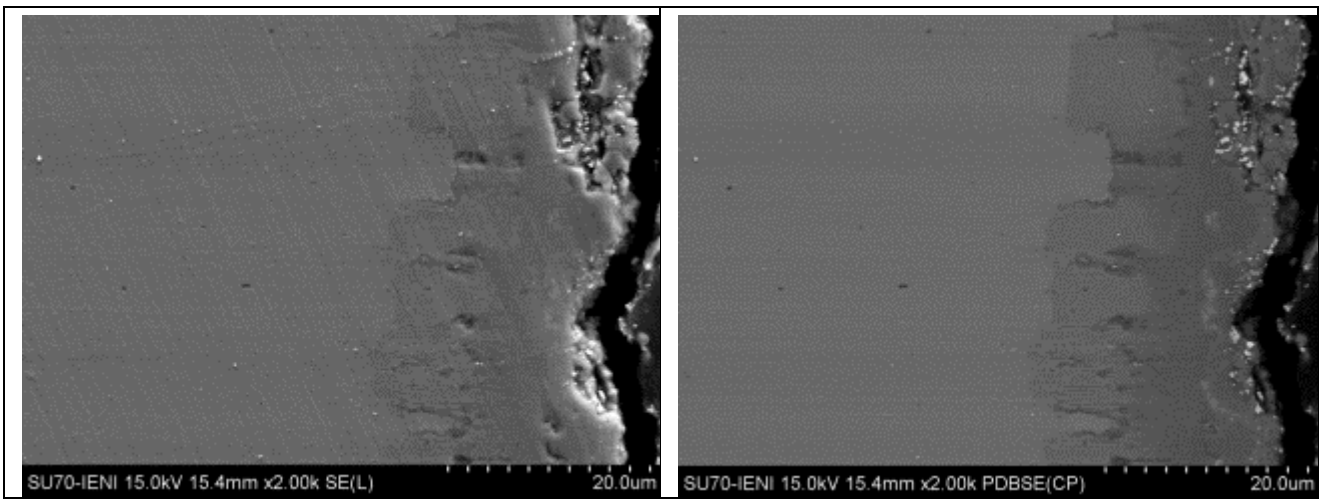

Fig. 55: ODS 12Cr, tested in static lead at 450°C under oxygen transient conditions: SEM (left) and BSE (right) images of the same area

EDS analysis results are shown in Fig. 56. The sample shows inner areas characterized by Cr-enrichment and larger portions with FeCr oxides and iron oxide in the outer layers.

	O-K	***Ti-K***	***Cr-K***	***Fe-K***	***W-L***
12Cr450ORIG-A_pt1	45.82		0.49	53.69	
12Cr450ORIG-A_pt2	46.94		0.90	50.70	
12Cr450ORIG-A_pt3	50.92	0.19	10.58	37.27	0.75
12Cr450ORIG-A_pt4	27.50	0.25	13.14	58.53	0.58
12Cr450ORIG-A_pt5	44.59	0.46	20.69	33.05	1.21
12Cr450ORIG-A_pt6	48.05		0.49	16.90	
12Cr450ORIG-A_pt7	26.34	0.20	13.38	59.27	0.81
12Cr450ORIG-A_pt8		0.20	13.44	85.41	0.95

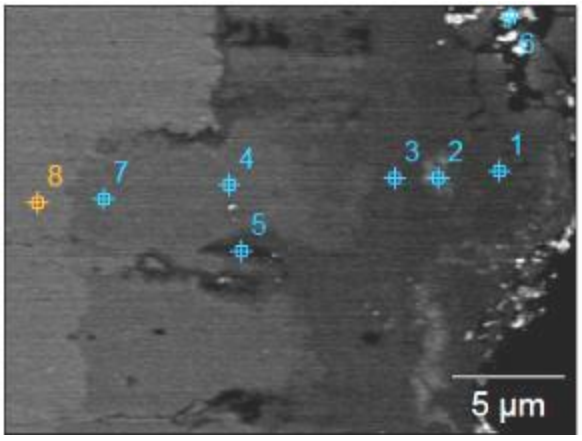

Fig. 56: ODS 12Cr, tested in static lead at 450°C under oxygen transient conditions: EDS analysis (at%) of the portion of the sample shown in figure 11.

In some areas the grain boundary oxidation is more pronounced as seen in Fig. 57. Here, strong Cr enrichments are found along the grain boundaries, which are visible as dark roots. The outer layer consist mainly of iron oxide. Additionally, nodules enriched in Ti and Y are detected.

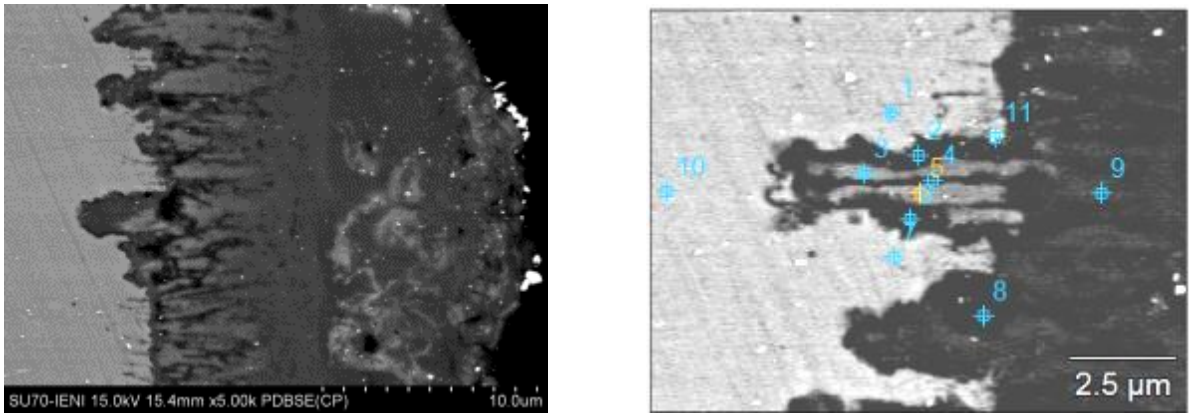

Fig. 57: PDBSE images of ODS 12Cr, tested in static lead at 450°C under oxygen transient conditions.

	O-K	*Ti-K*	*Cr-K*	*Mn-K*	*Fe-K*	*W-L*
12Cr450ORIG-D_pt1			7.32	0.08	91.97	0.64
12Cr450ORIG-D_pt2	42.91	0.26	29.32		26.86	0.65
12Cr450ORIG-D_pt3	33.33	0.19	15.55		50.03	0.90
12Cr450ORIG-D_pt4	36.09	0.23	17.74		45.34	0.60
12Cr450ORIG-D_pt5	30.10	0.25	13.57		55.64	0.44
12Cr450ORIG-D_pt6	43.52	0.87	30.93		24.02	0.67
12Cr450ORIG-D_pt7		0.33	5.96		92.78	0.93
12Cr450ORIG-D_pt8	43.56	0.26	25.09		29.59	1.50
12Cr450ORIG-D_pt9	52.66	0.22	13.59		32.71	0.82
12Cr450ORIG-D_pt10			11.43		87.78	0.79
12Cr450ORIG-D_pt11	39.19		21.27		39.54	

Tab. 11: EDS analysis results of marked point in Fig. 57 right image (at%)

6.3 12Cr ODS GESA

An oxide layer is also formed in the 12Cr ODS GESA sample in lead at 450°C and oxygen transient conditions, Fig. 58. The oxide layer consist of an outer Fe-O oxide with a Fe-Cr-O layer (clearly discernible by the increase of the Cr content, right image). In most cases at the interface to the inner oxidation zone a Cr and Mn enriched zone is visible (darker line- right micrograph). The inner oxidation zone is characterized by a strong Cr enrichment along the grain boundaries. In some cases these zone is also separated from the bulk by a Cr rich band areas, dark broken line visible in both micrographs. The average thickness of the completely oxidized area is 17.1µm (Fe-O ~6.8µm, Fe-Cr-O ~3.2µm and IOZ ~7.1).

In comparison with the non-treated specimen is the oxide layer more homogenous grown on the treated one. However, in both cases no corrosion attack is visible.

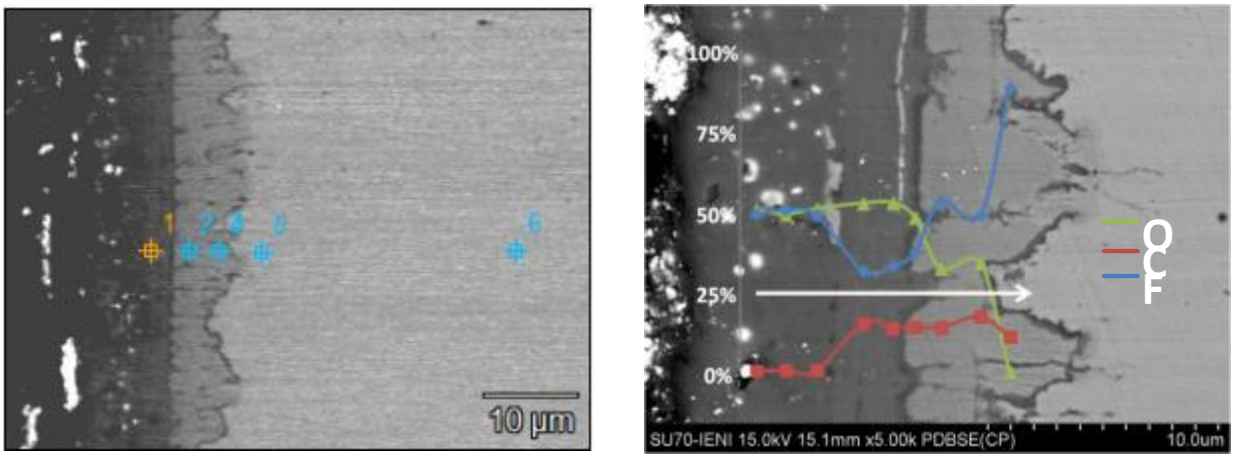

Fig. 58: ODS 12Cr treated GESA, tested in static lead at 450°C under oxygen transient conditions. Left side with marked point for the EDS analysis (Tab. 12, right side with EDS analysis results

	O-K	Ti-K	Cr-K	Mn-K	Fe-K	W-M
12Cr450GESA-A_pt1	51.51	0.43	17.35		29.84	0.87
12Cr450GESA-A_pt2	29.43	0.15	12.63	0.07	57.07	0.65
12Cr450GESA-A_pt3	25.31	0.37	17.11		56.66	0.55
12Cr450GESA-A_pt4	28.22	0.38	17.88		52.92	0.60
12Cr450GESA-A_pt5		0.11	11.11	0.13	88.13	0.53
12Cr450GESA-A_pt6		0.16	13.09	0.28	85.82	0.65

Tab. 12: EDS analysis of marked points in Fig. 58 left side

7 Summary and Conclusion part 1 corrosion

The behaviour of the steel at constant temperature is listed in Tab. 13 and Tab. 14.

°C	550°C		600°C			650°C		700°C		
Time [h]	2000	5000	2000	5000	10000	2000	5000	2000	5000	10000
9Cr		(+)	+	+	-	-	-	+	+	-
9Cr GESA		(+) -	+	+	+	-	-	+	+	-
9Cr Al		Not enough Al				+	+			
12Cr	(+)	(+) -	-	-	-	+	-	+	+	-
12Cr GESA	(+) -		+	+	-	-	-	+	+	-
12Cr Al		+				+	+			
14Cr	+					+	+			
14Cr GESA						+	+			

Tab. 13: Rating of the behavior of 9 and 12Cr steel in Pb (10^{-6}wt% O) at different temperatures and exposure times; += good behavior,(+)= up to now good behavior, but thick oxide layer,_(+) -_ = sign of changing the behavior, - = dissolution attack

°C	450°C		650°C	
Time [h]	2000	5000	2000	5000
9Cr	+	+	-	-
9Cr GESA	+	+	-	-
12Cr	+	+	-	-
12Cr GESA	+	+	-	-

Tab. 14: Rating of the behavior of 9 and 12Cr steel in Pb with a low amount of oxygen at different temperatures and exposure times

After longer exposure times at higher temperature (650 and 700°C) both steels, 9 and 12Cr ODS, with and without GESA treatment showed dissolution attack. Therefore, they can´t be used without additional corrosion protection at these temperatures. Al-surface alloying by GESA was tested as additional corrosion protection. As expected, a clear positive effect was visible. If the Al content in the surface area is sufficiently high, a thin and protective alumina layer is formed.

A slightly positive effect of GESA was observed at the 14Cr ODS steel. The steel exhibits in both variants, pristine and GESA treated, good corrosion resistance at 550 and 650°C. However, at the non-treated steel (pristine) inner oxidation was observed locally at 650°C, which was not detected at GESA treated samples.

At the GESA affected zone an increased diffusion was noticed. The formed columnar structure seems to favour diffusion along grain boundary, which leads to a worse behaviour in most cases. This columnar structure was typically formed in the modified layer of 9 and 12Cr ODS steel. The columnar structure, which is formed at the 14Cr steel specimen, is not reaching the surface and has therefore not the same negative impact. Nevertheless, 12Cr GESA showed a better behaviour than the non-treated steel at 600°C. This could be due to the fact that the corrosion protection seems to be weak during the change of the oxidation mechanism from multil-layered oxide to a single spinel type oxide. This transition in oxidation behaviour seems to be shifted to higher temperatures using GESA treated specimens due to an increased diffusion, which fosters enhanced oxide growth. For 9Cr ODS this change in oxidation is observed between 600 and 650°C and for 12Cr ODS between 550°C and 600°C.

The enhanced diffusion due to the GESA process leads to a slightly better behaviour in the liquid Pb at 450°C having a low oxygen concentration ($5.1*10^{-8}$wt% O). At 650°C all specimens showed a dissolution attack already after 2000h and low oxygen concentrations of $1.9*10^{-7}$wt% . This situation has to be avoided, especially during the start of the reactor, where a high oxygen consumption can be expected.

The temperature transient test 550°C-750°C (24h) -550°C showed no influence on the corrosion behaviour. After an increase to 1000°C, the thick oxide layers spalled off. The thinner oxide layer on the GESA samples seems to be a bit more stable.

Furthermore, no negative effect was observed due to a decreasing oxygen content at 450°C. However, the oxygen content in Pb was after 6700h still in the range of 10^{-6}wt%, which is still high enough to form Fe_3O_4.

8 Literature part 1 corrosion

1. V. Engelko, B. Yatsenko, G. Mueller, H. Blum ; Vaccum 62 (2001) 211-216
2. C. Schroer, J. Konys l, Report FZKA-n° 7364 (http://bibliothek.fzk.de/zb/berichte/FZKA7364.pdf)
3. G. Müller, G. Schumacher, A. Weisenburger, A. Heinzel, F. Zimmermann, T. Furukawa, K. Aoto, Study on Pb/Bi Corrosion of Structural and Fuel Cladding Material for Nuclear Application, Part I, JNC TY 9400 2002-016
4. G. Müller, A. Heinzel, G. Schumacher, A. Weisenburger, J. Nucl. Mater. 321 (2003) 256

9 Investigation of ODS steels susceptibility to liquid metal embrittlement in LBE environment

Susceptibility of 9%Cr-, 12%Cr-, 14%Cr-ODS steels and 14%Cr model alloy to liquid metal embrittlement (LME) in liquid lead-bismuth eutectic environment were investigated by SSRT tests. Additionally two specimens of 9%Cr- and 12%Cr-ODS steels with GESA treated surface were tested to investigate effect of surface alloying on appearance of LME in SSRT tests. All specimens tested in LBE environment did show evidences of LME. However, 14%Cr-ODS steel shows less susceptibility than other tested materials and only few surface cracks were found in the necking area. To check if 14% of chromium content is the reason for low susceptibility 14%Cr laboratory steel has been tested. It demonstrated significant susceptibility to LME. Two specimens with GESA treated surface shows very clear evidences of LME and in case of 12% Cr steel the elongation reduction due to LME was more significant in comparison with not treated specimens tested in LBE.

9.1 Materials

The list of tested materials is given in Table 9.1. All tested materials except T91 steel were fabricated in framework of EURATOM FP7 GETMAT project. The exact specification of the materials was not available so the chemical composition provided in Table 9.1 is composition from different sources and might be not complete. For 12%Cr-and 14%Cr-ODS steels tensile and fracture toughness tests at various temperatures have been performed in framework of FP7 GETMAT [1]. 14%Cr steel was used to check a hypothesis on effect of chromium content on susceptibility of steels to LME. This steel was produced by OCAS in framework of FP7 GETMAT and basic characterization has been performed at SCK•CEN [2].

Two tested specimens one of 9%Cr- and one of 12%Cr-ODS steels were surface alloyed with GESA technology at KIT[6].

T91 steel was produced and basic characterization performed in framework of FP6 EUROTANS DEMETRA project [3].

Table 9.1. Summary of tested materials for LME susceptibility

Material	C	Si	Mn	P	S	Cr	Mo	Ni	Nb	Ti	V	W	Y_2O_3
T91	0.097	0.218	0.386	0.020	0.0005	8.873	0.871	0.115			0.080		
9%Cr ODS KIT-Kobelco	0.095					8.9	0.76						0.36
12%Cr ODS Kobelco		0.1	<0.01			11.59		<0.01		0.22		1.87	0.23
14%Cr ODS CEA			0.33			13.65		0.16		0.30		1.17	
14%Cr steel OCAS	0.09	0.29	0.74	0.01	0.01	14.72	1.08	0.14	0.07		0.22	0.01	

9.2 Tests approach

The procedure for LME susceptibility tests in LBE environment has been used in framework of FP7 GETMAT project to investigate susceptibility of T91 steel to LME in LBE [4]. In framework of FP7 MATTER project this procedure was verified with collective exercise and the guidelines for this testing have been proposed [5].

Round tensile specimens with the diameter of 2.4 mm and gage length of 12 mm as shown in Figure 3 were used. To provide intimate contact between steel and liquid metal the pre-exposure of the specimens in LBE with low to medium (up to 10^{-6} wt.%) oxygen content at 450 °C prior for at least 20 hours was performed.

At SCK•CEN the reference tests are performed in air on electromechanical test bench Instron-1362 and in LIMETS1 (Figure 1) and LIMETS4 (Figure 2) in Ar+5%H_2 atmosphere. The tests in LBE are performed in LIMETS1 and LIMETS4. The description of the tests benches and more details on the testing procedure are provided in [5].

One T91 tensile specimen has been tested during ODS steel testing campaign. It is done in order to verify if all the parameters of the test installation are still corresponds to the state where LME of T91 appears.

The following criteria are used to conclude on LME susceptibility:

- Reduction of total elongation in comparison with the reference tests performed in inert environment;
- Presence of surface cracks;
- Presence of quasi cleavage pattern or other evidences of brittle fracture on fracture surface.

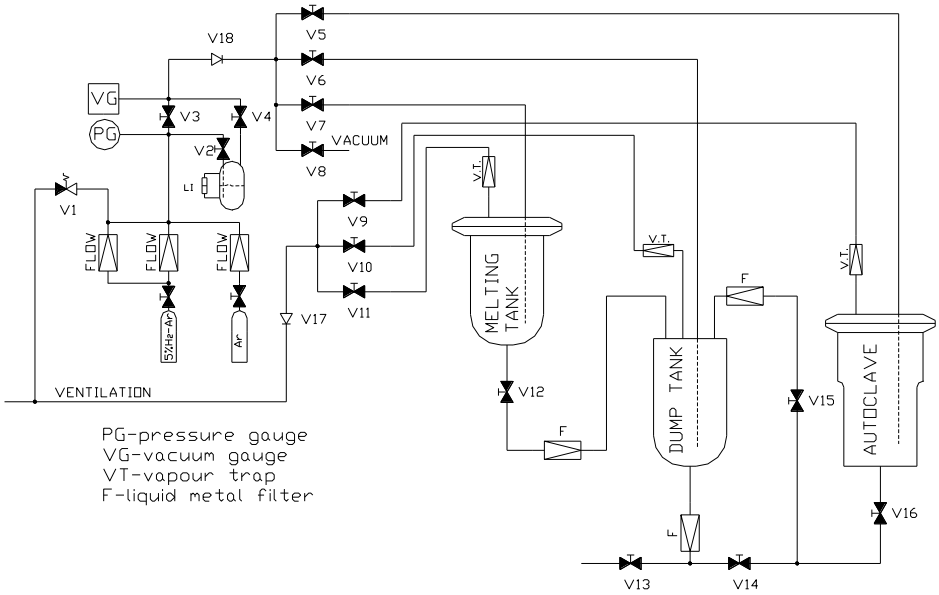

Figure 1. Principle scheme of LIMETS1 installation

Figure 2. LIMETS4 installation

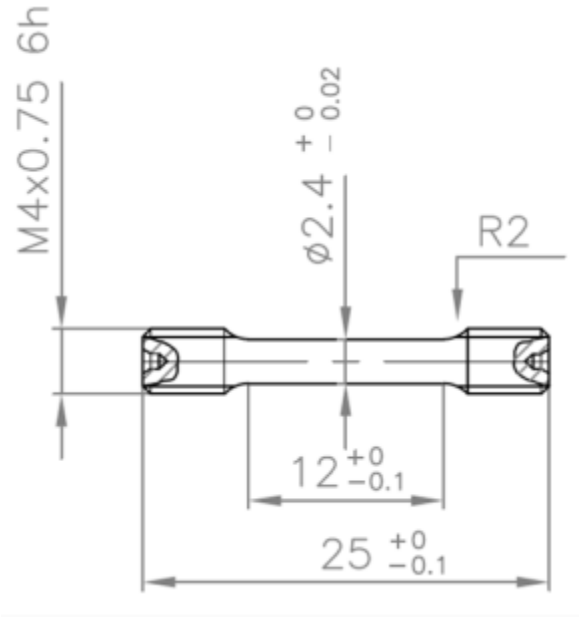

Figure 3. Geometry of round tensile specimens

9.3 Results of SSRT tests

The summary of all SSRT tests discussed in this work is given in Table 9.2. Majority of the tests have been performed for Task 4.3 of FP7 MATISSE. Few tests performed in inert environment and used here as the reference tests were done in framework of FP7 GETMAT as in-kind contribution.

9.3.1 SSRT tests of 9%Cr-ODS steel

For 9%Cr-ODS steel no additional specimens were available at SCK•CEN to perform susceptibility test of bare surface material to LME. One specimen of this steel with GESA type surface treatment provided by KIT was tested in LBE at 300 °C and compared with the results of tensile tests in air performed before in framework of FP7 GETMAT. It was not known the orientation of the specimen provided by KIT and it was compared with the results obtained for T- and L-orientations. The results of these tests are given in Table 9.2 and shown in Figure 4. As one can see there is significant reduction in total elongation of specimen tested in LBE environment in comparison with the tests in air. The bend in the final part of stress-strain curve for specimen tested of LBE is typical for appearance LME. It formed due to multiple surface cracks formed due to LME and arrested so the fracture doesn't happen instantly as in the case of test in inert environment.

The fractured surfaces of the specimen tested in LBE are shown in Figure 5. The surface shows evidences of both ductile and brittle fracture. The gage of the specimen has row of burls (Figure 5b) which are probably artefacts of surface alloying. Typical for LME quasi-cleavage pattern is observed on fracture surface of these burls (Figure 5c and d) One can guess that the cracks might initiate at these burls and propagate further to the bulk of the material. Part of the fracture surface shows evidences of decohesive rupture of laminar layers. The nature of these layers requires further investigation but probably it is the artefact of the material fabrication and the plate rolling in particular.

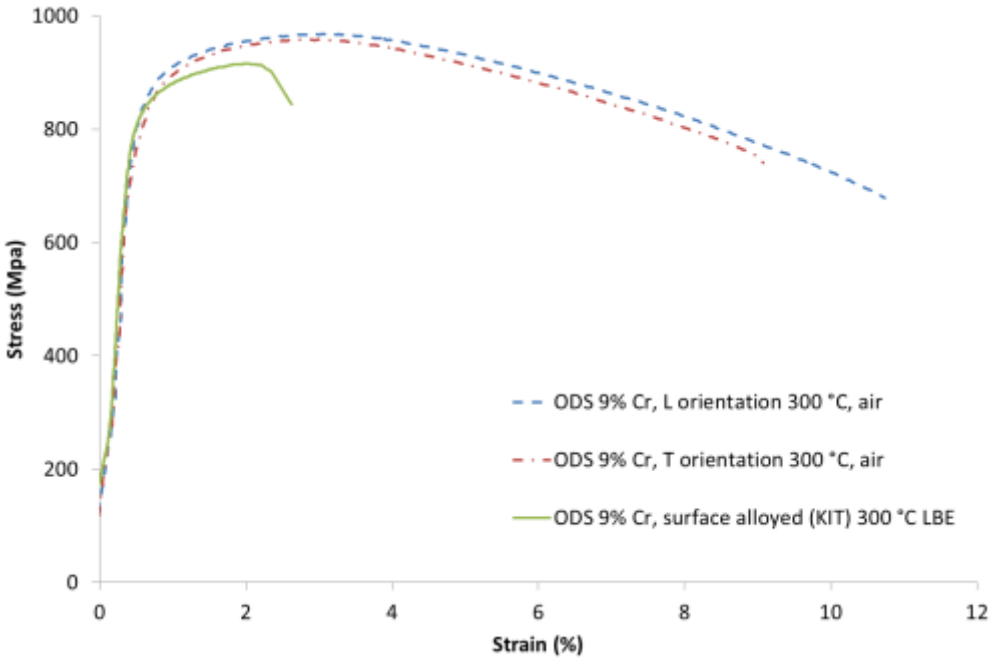

Figure 4. Engineering stress-strain curves of 9% Cr – ODS (KIT-Kobelco) at 300 °C.

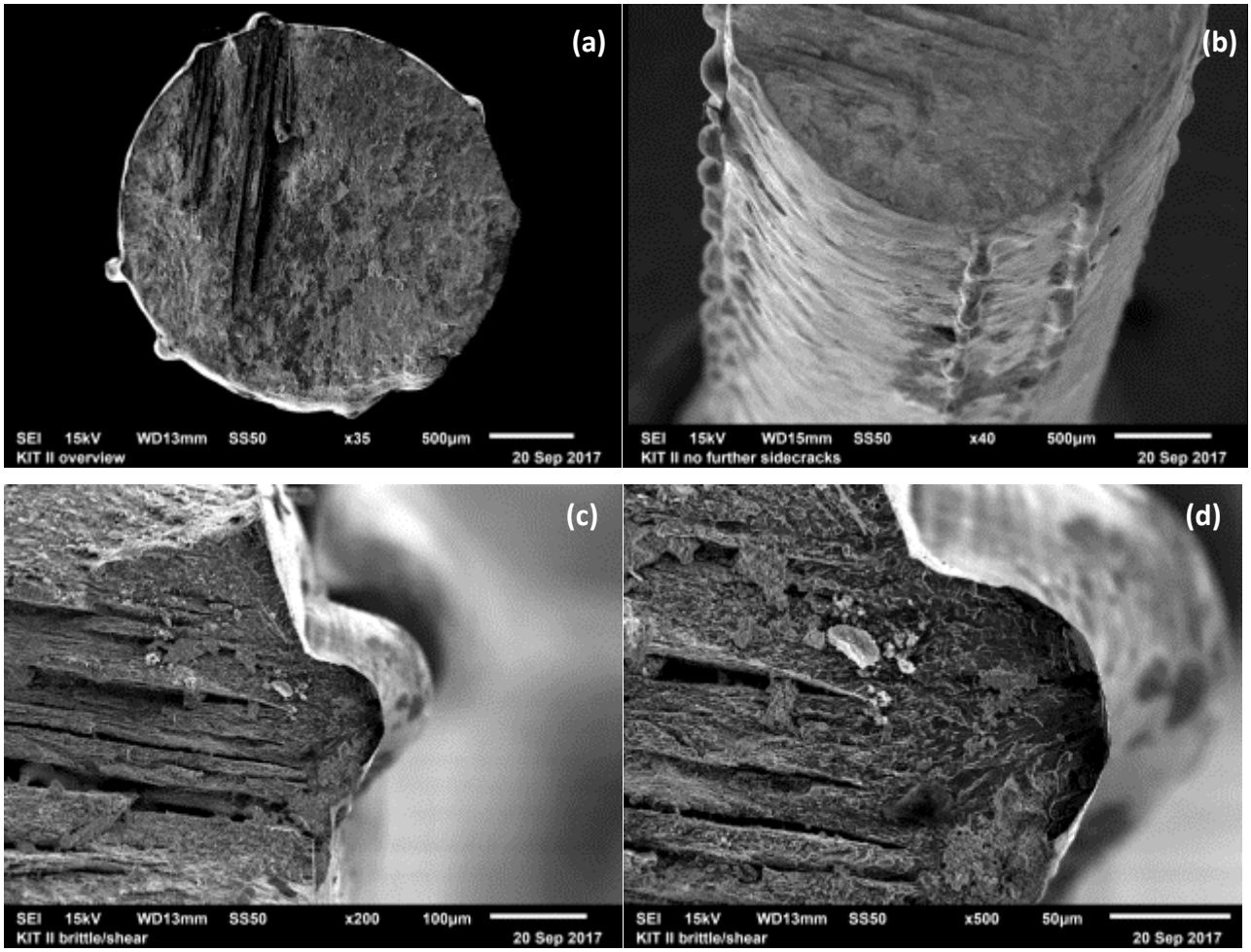

Figure 5. Fracture surfaces of 9% Cr – ODS (KIT-Kobelco) with GESA surface treatment tested in LBE at 300°C

9.3.2 SSRT tests of 12%Cr-ODS steel

Five tensile specimens made of 12%Cr-ODS steel were tested in LBE at 300 °C. Two specimens with L orientation, two with T orientation and one specimen of this steel with GESA type surface treatment provided by KIT. The results were compared with the results obtained in inert environment for T- and L-orientations. The results of these tests are given in Table 1.2 and shown in Figure 6. From comparison of the two tensile curves obtained in inert environment for two different orientations it is evident that material is anisotropic. While the strength does not depend on specimen orientation, the ductility (total elongation) in the T–orientation is clearly smaller than in the L–orientation. As one can see there is significant reduction in total elongation of specimen tested in LBE environment in comparison with the tests in air and the final parts of the curves obtained in LBE bended typically for LME. The GESA treated sample tested in LBE demonstrated lowest elongation and apparently start to fracture before reaching ultimate tensile strength.

One of the fractured tensile sample tested in LBE and cleaned afterwards from the LBE residuals is shown in Figure 9. The fractured surfaces of the specimen tested in LBE are shown in Figure 7. The surface shows evidences of both ductile and brittle fracture. Similar to 9%Cr-ODS steel one can find clear evidences of decohesive rupture between laminar layers (Figure 7a and b). Number of surface crack typical for LME were found on the gage surface (Figure 7c). The fracture surface of the specimen with GESA treatment shows presence of two step wise brittle cracks (Figure 8).

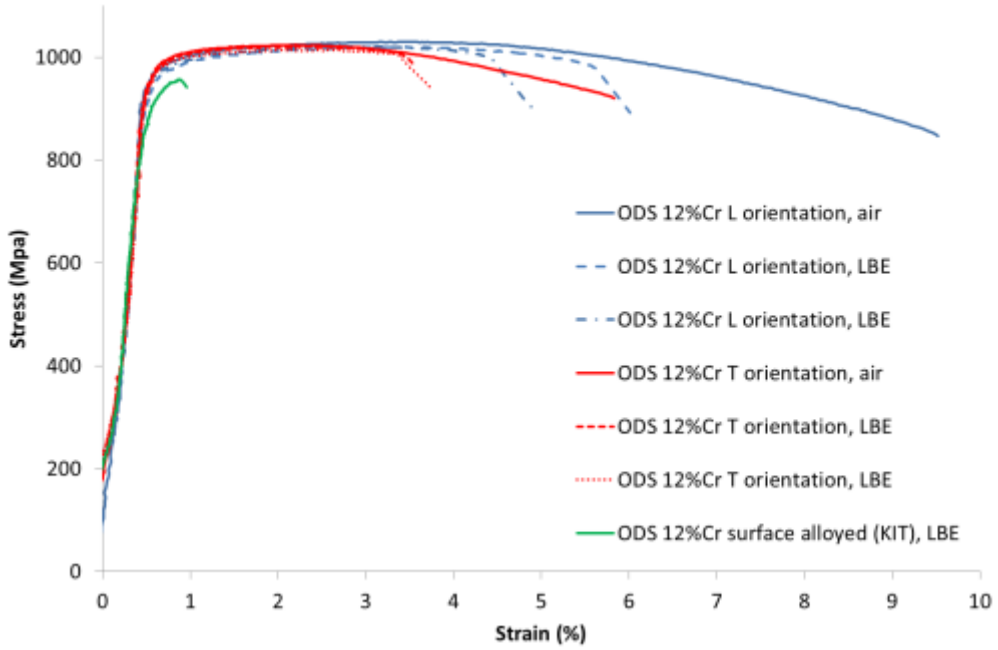

Figure 6. Engineering stress-strain curves of 12% Cr – ODS (KIT-Kobelco) at 300 °C.

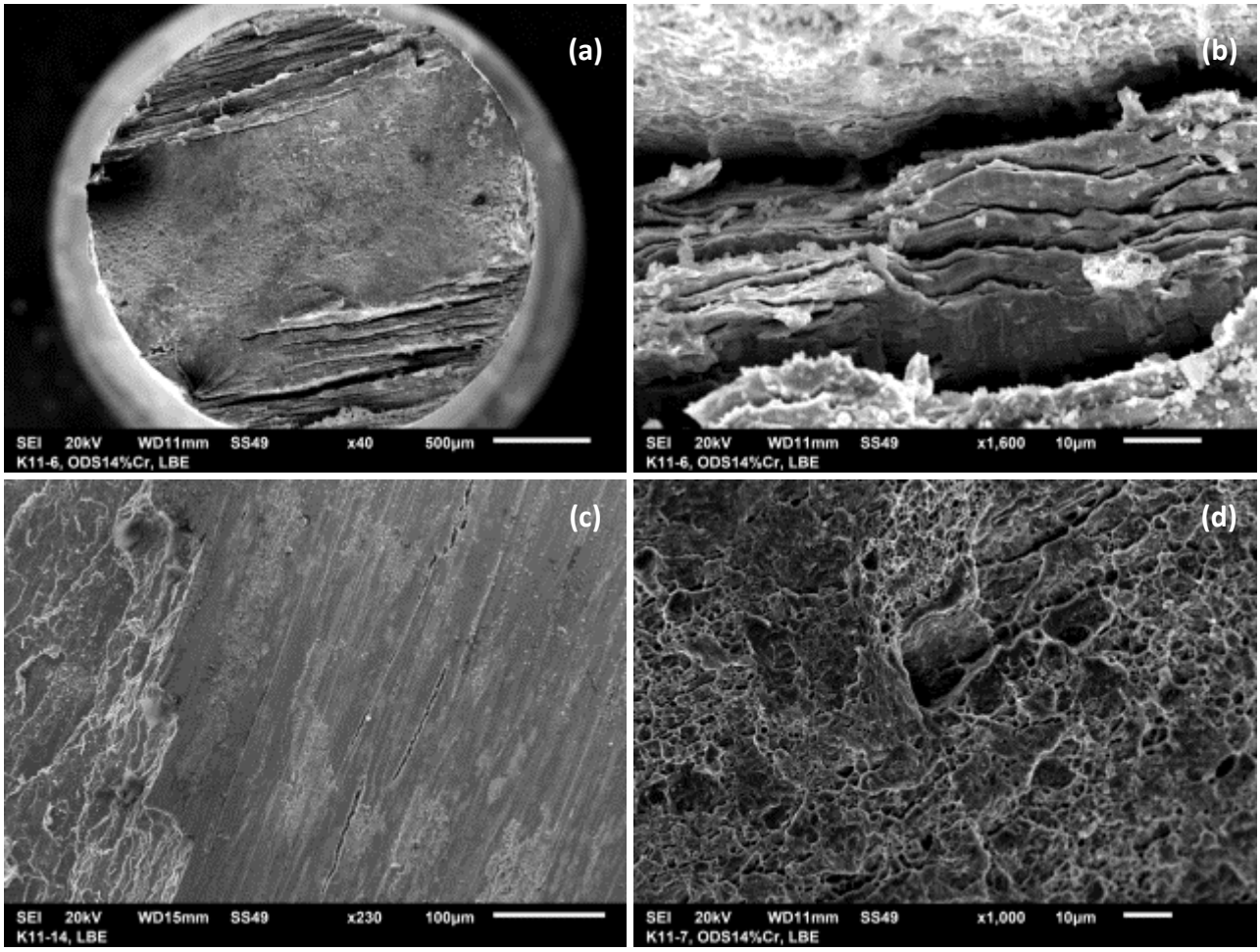

Figure 7. Fracture surfaces of 12% Cr – ODS (Kobelco) tested in LBE at 300 °C

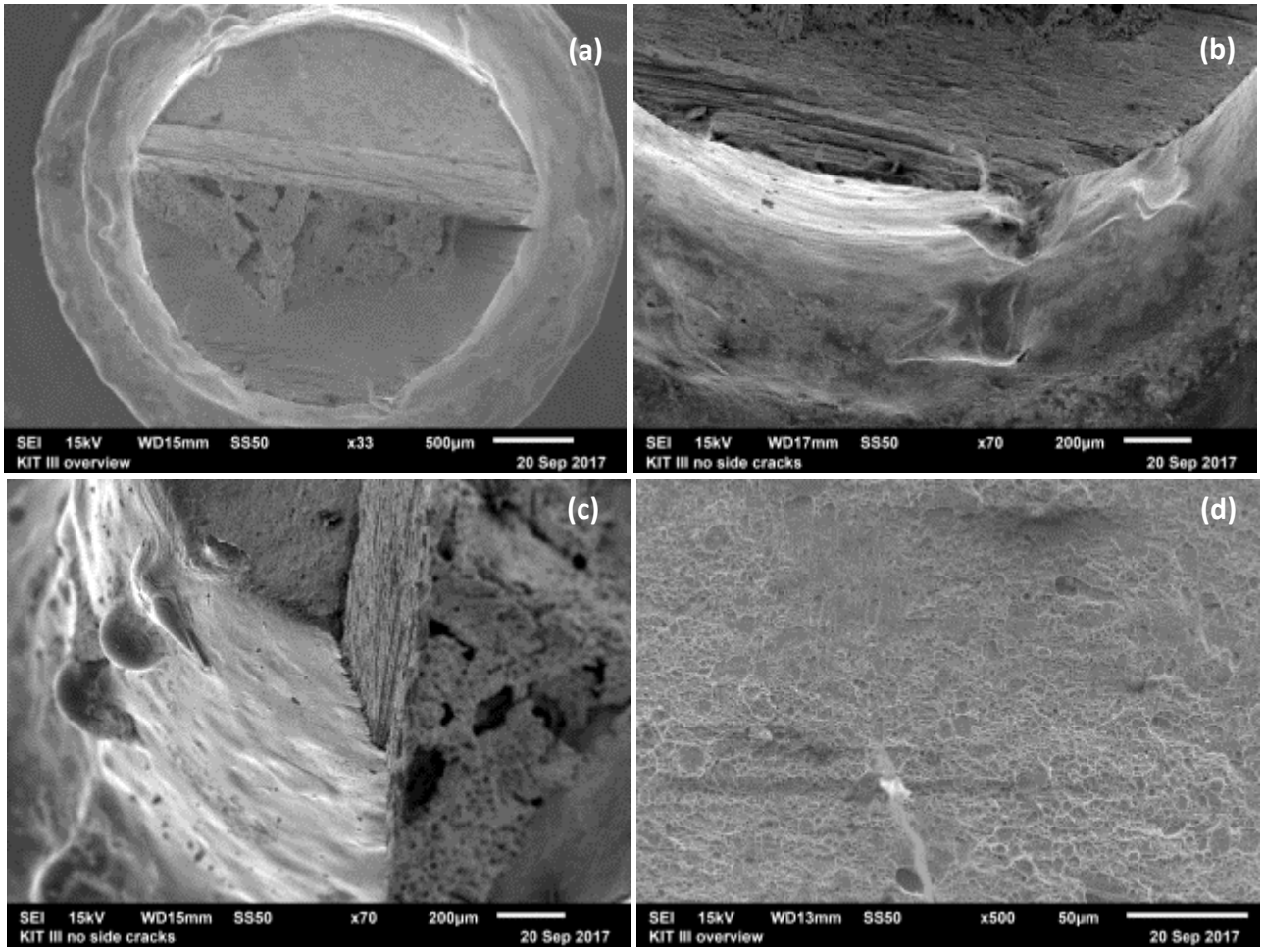

Figure 8. Fracture surfaces of 12% Cr – ODS (Kobelco) with GESA surface treatment tested in LBE at 300 °C

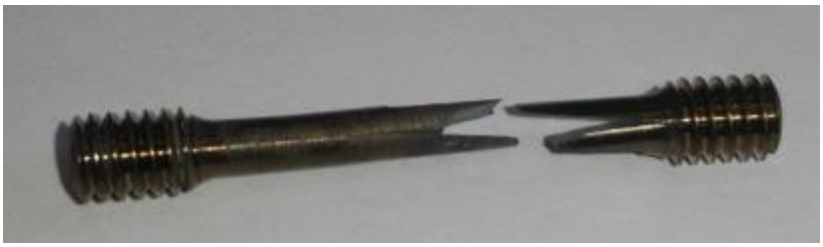

Figure 9. Tensile specimen of 12%Cr-ODS steel after SSRT test in LBE at 300 °C

9.3.3 SSRT tests of 14%Cr-ODS steel

Five tensile specimens made of 14%Cr-ODS steel were tested in LBE at 300, 350 and 450 °C. Two specimens were tested at 300 °c and compared with the test performed in air at the same temperature. The results are shown in Figure 10 and in Figure 11. No reduction of total elongation was observed. The specimens tested in LBE even shows more elongation than those tested in air. However, this is probably due to the difference between two pieces of 14%Cr-ODS steel from which two batches of tensile specimens were made. The final parts of the stress-strain curves obtained in LBE at 300 and 350 °C bended typically for LME.

The fractured surfaces of the specimen tested in LBE at 350 °C and 300 °C are shown in Figure 12 and Figure 13 respectively. There are clearly visible brittle cracks (Figure 12b), some of them initiated at the surface (Figure 12c). Decohesive rupture cracks along loading direction are also observed (Figure 13a). At higher magnification columnar structure of the material is visible and cracks propagate along these columns boundaries (and Figure 13c). The fracture surface clearly shows evidences of LME. However, it seems that LME cracks are arrested more effectively in 14%Cr-ODS steel and therefore have lesser impact on total elongation. One can speculate that this LME retarding effect is due to the inhomogeneity (e.g. columnar microstructure) of this steel.

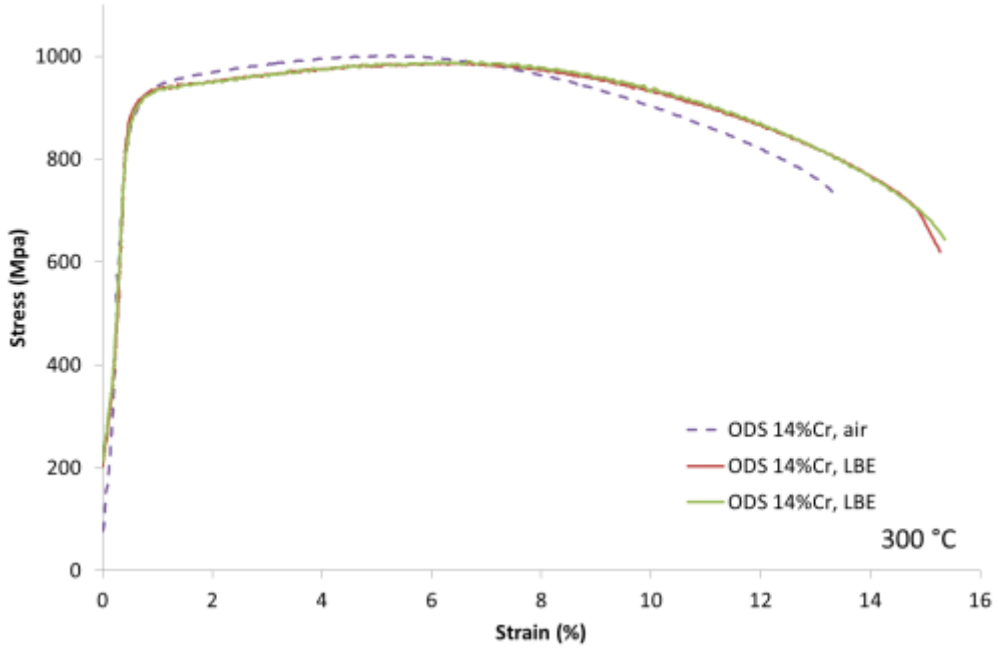

Figure 10. Engineering stress-strain curves of 14% Cr – ODS (CEA) at 300 °C

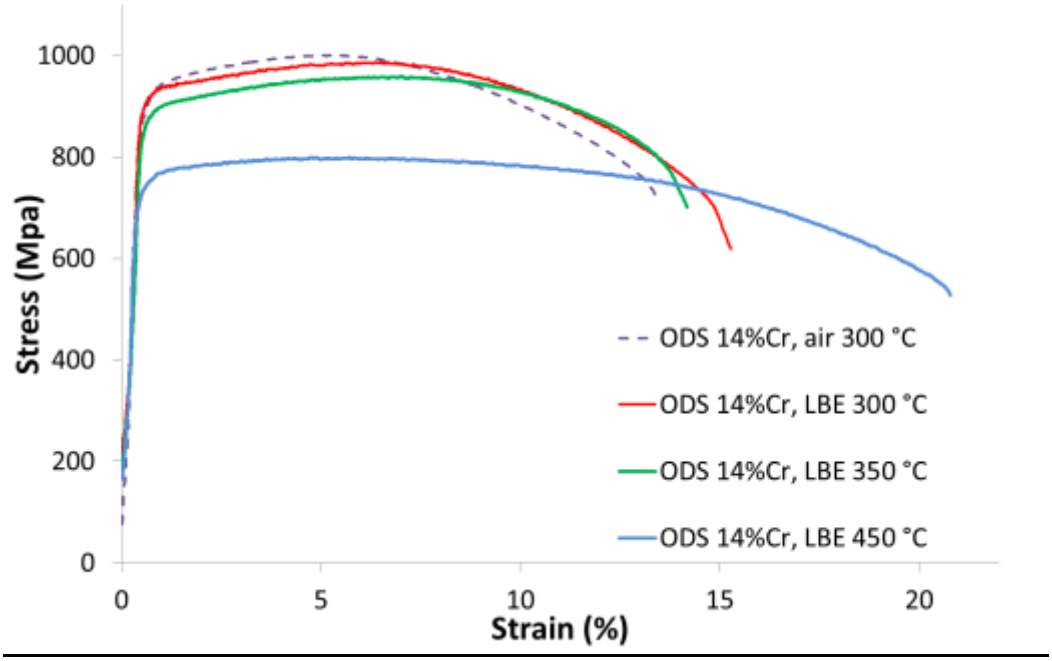

Figure 11. Engineering stress-strain curves of 14% Cr – ODS (CEA) tested at different temperatures in LBE

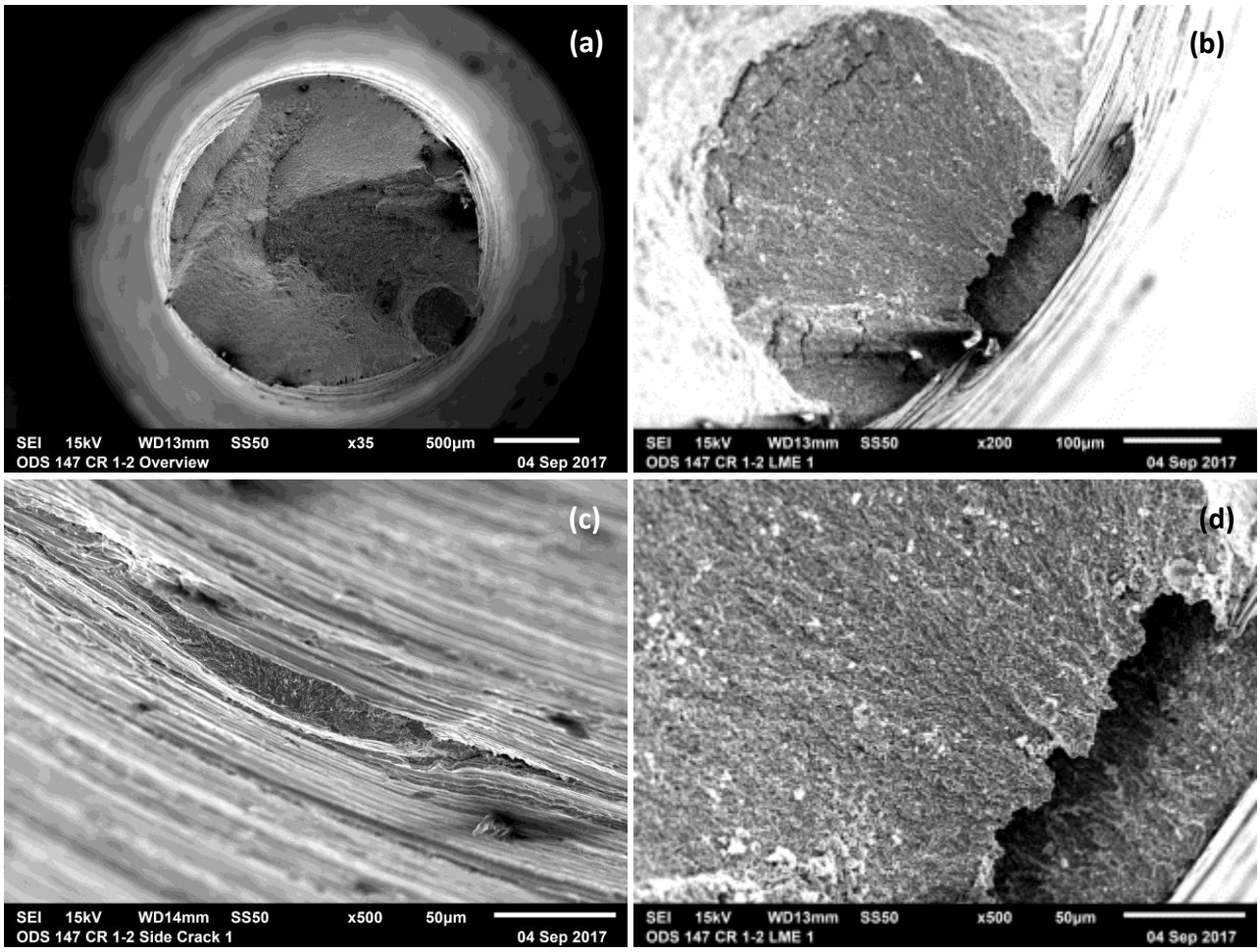

Figure 12. Fracture surfaces of 14% Cr – ODS (CEA) tested in LBE at 350 °C

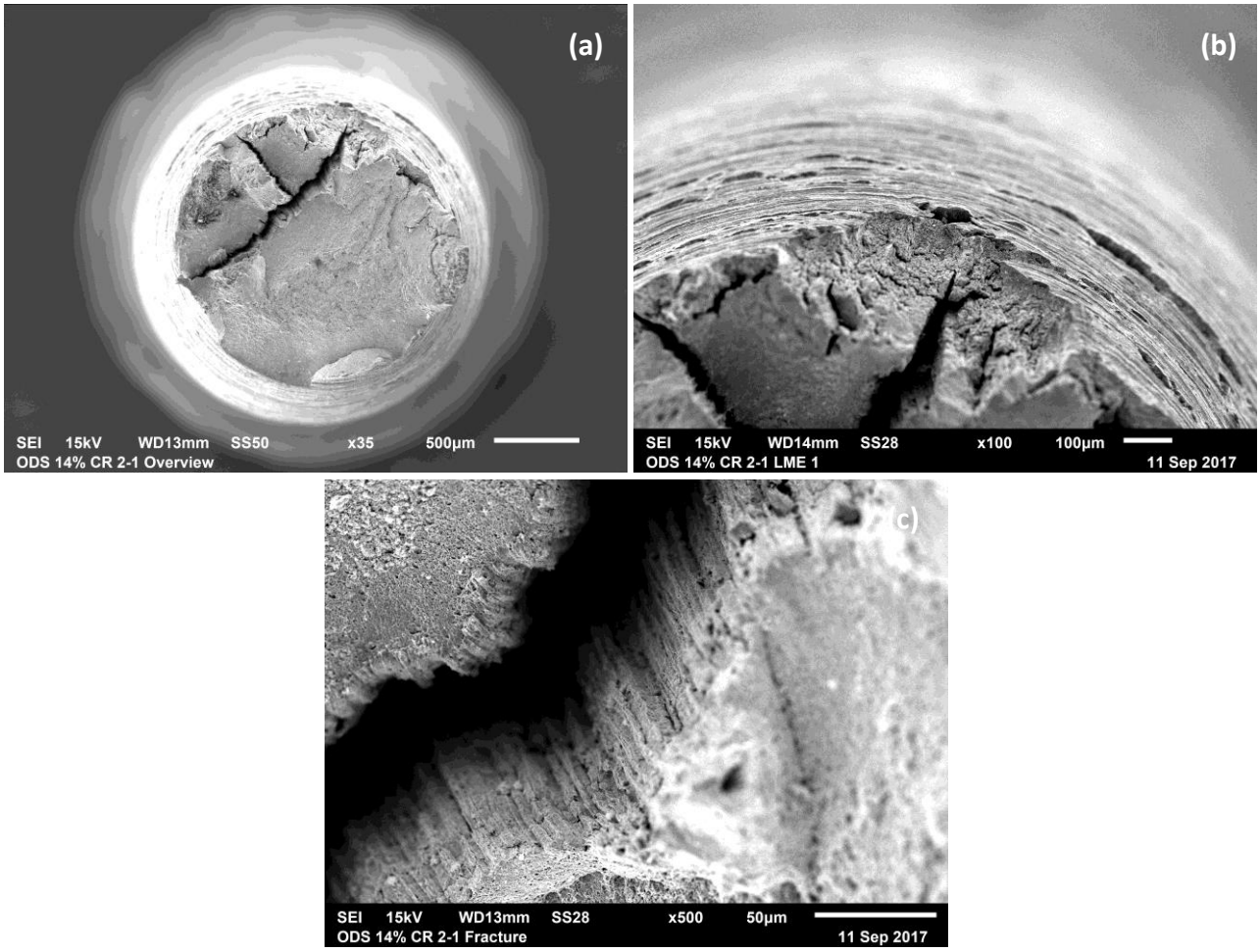

Figure 13. Fracture surfaces of 14% Cr – ODS (CEA) tested in LBE at 300 °C

9.3.4 SSRT test of T91 steel

One specimen of T91 steel was tested in LBE at 350 °C to verify if the set-up is still in the state to observe LME of T91 steel in LBE. The obtained stress-strain curve is compared with the tests performed before at 350 °C in both LBE and air environments (Figure 14). The results of the tests performed in this work is within the scatter of the results obtained before. The fracture surfaces of T91 steel tested in this work are shown in Figure 15. Typical for LME quasi cleavage fracture surface (Figure 15b) and surface cracks (Figure 15c) were observed.

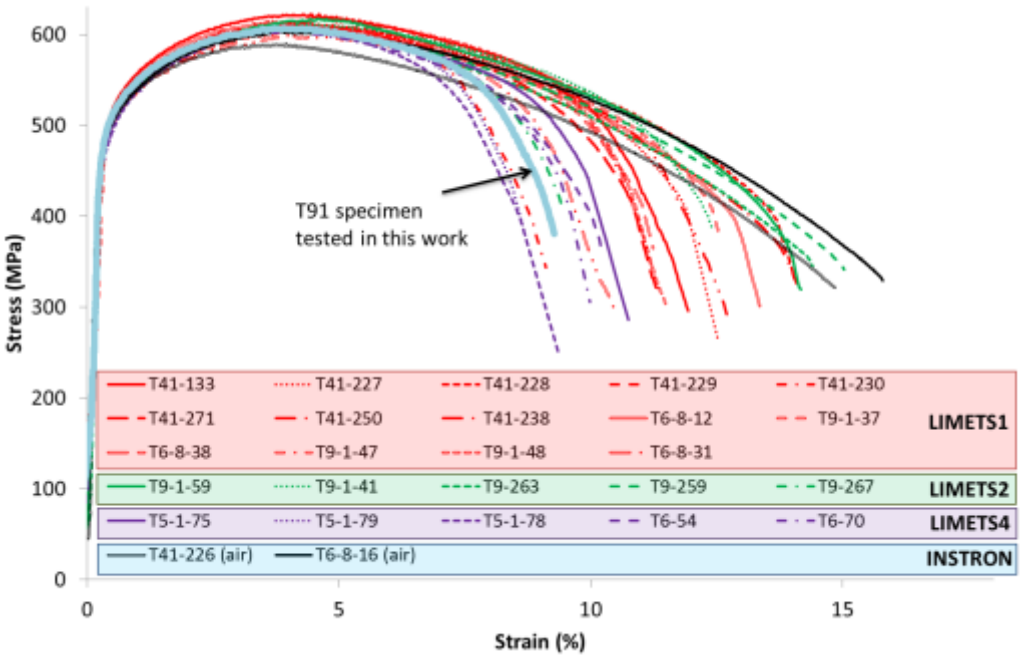

Figure 14. Comparison of engineering stress-strain curves of T91 steel tested in air and LBE at 350 °C with the test performed in this work

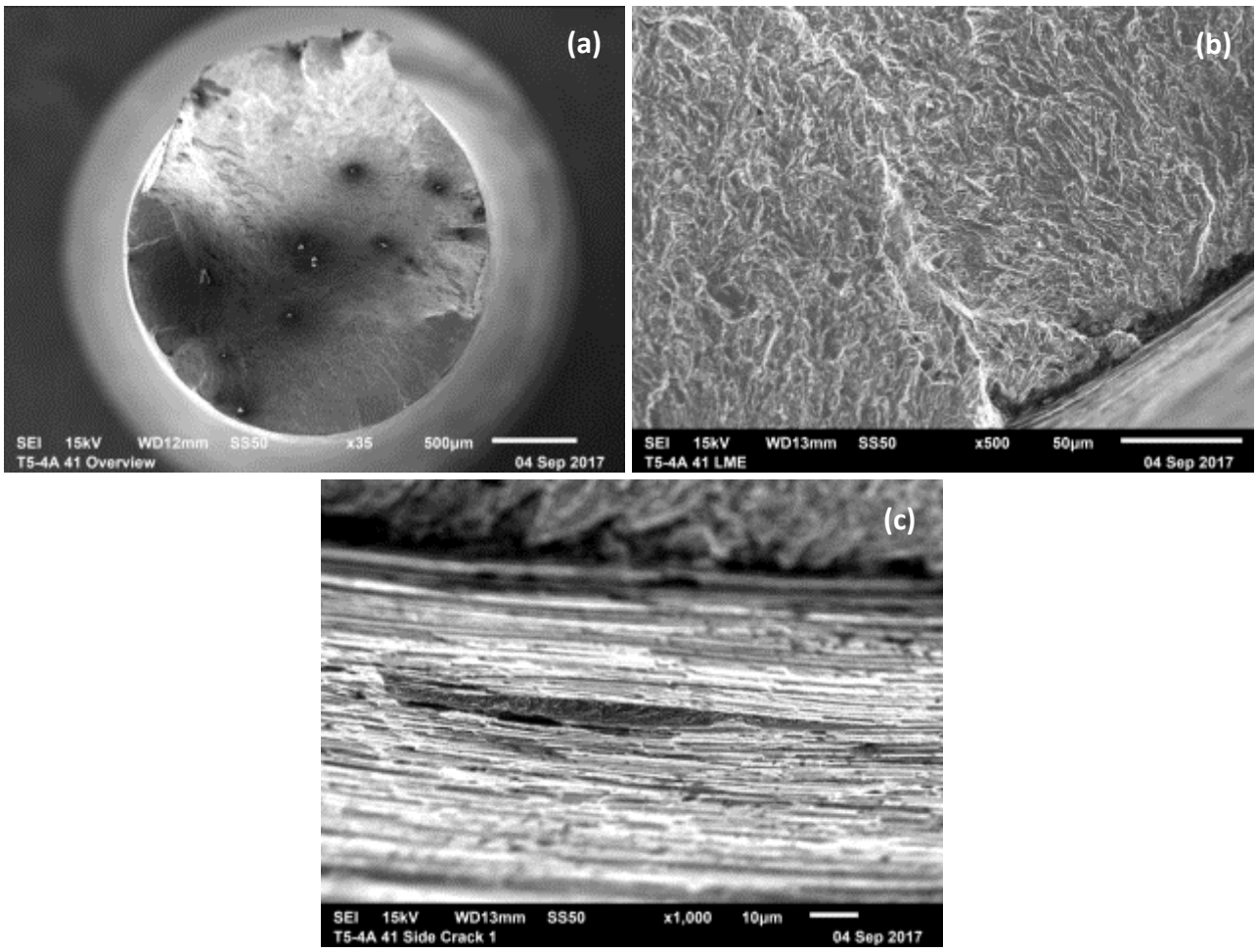

Figure 15. Fracture surfaces of T91 steel tested in LBE at 350 °C

9.3.5 SSRT tests of 14%Cr steel

To evaluate if indeed high chromium content of 14% have retarding effect on LME appearance in SSRT tests another 14%Cr steel fabricated in framework of FP7 GETMAT project was tested first in inert argon-hydrogen gas and in LBE. The obtained stress-strain curves are shown in Figure 16. The total elongation of the specimens tested in LBE was significantly less in comparison with the specimens tested in inert environment. Also the fractured surfaces shows very clear evidences of LME (Figure 17). Therefore the original hypothesis of retarding effect of high chromium content on LME appearance was not confirmed.

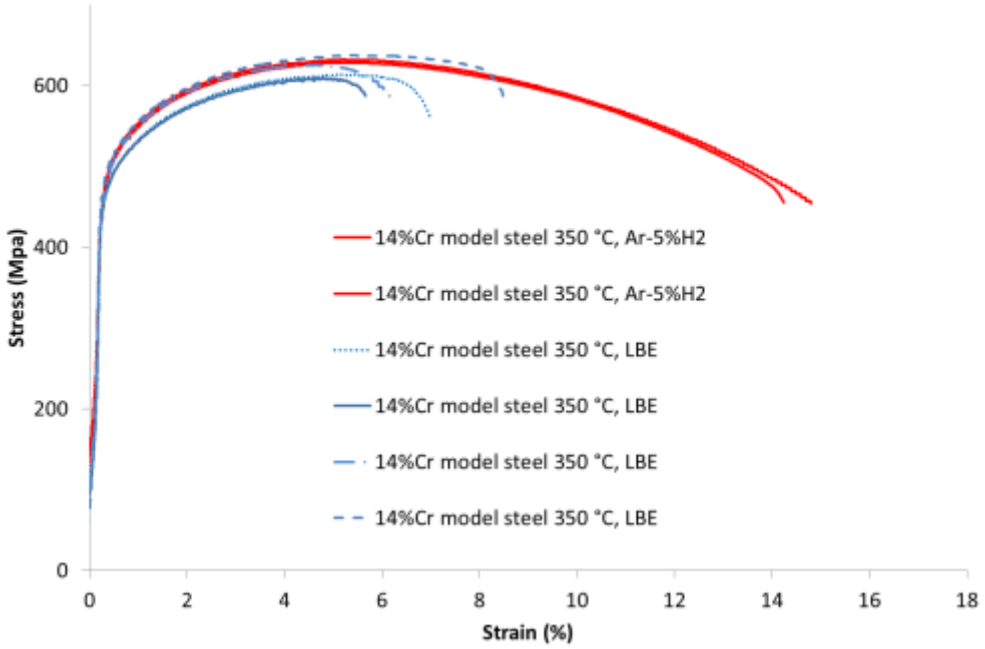

Figure 16. Engineering stress-strain curves of 14%Cr experimental steel at 350 °C

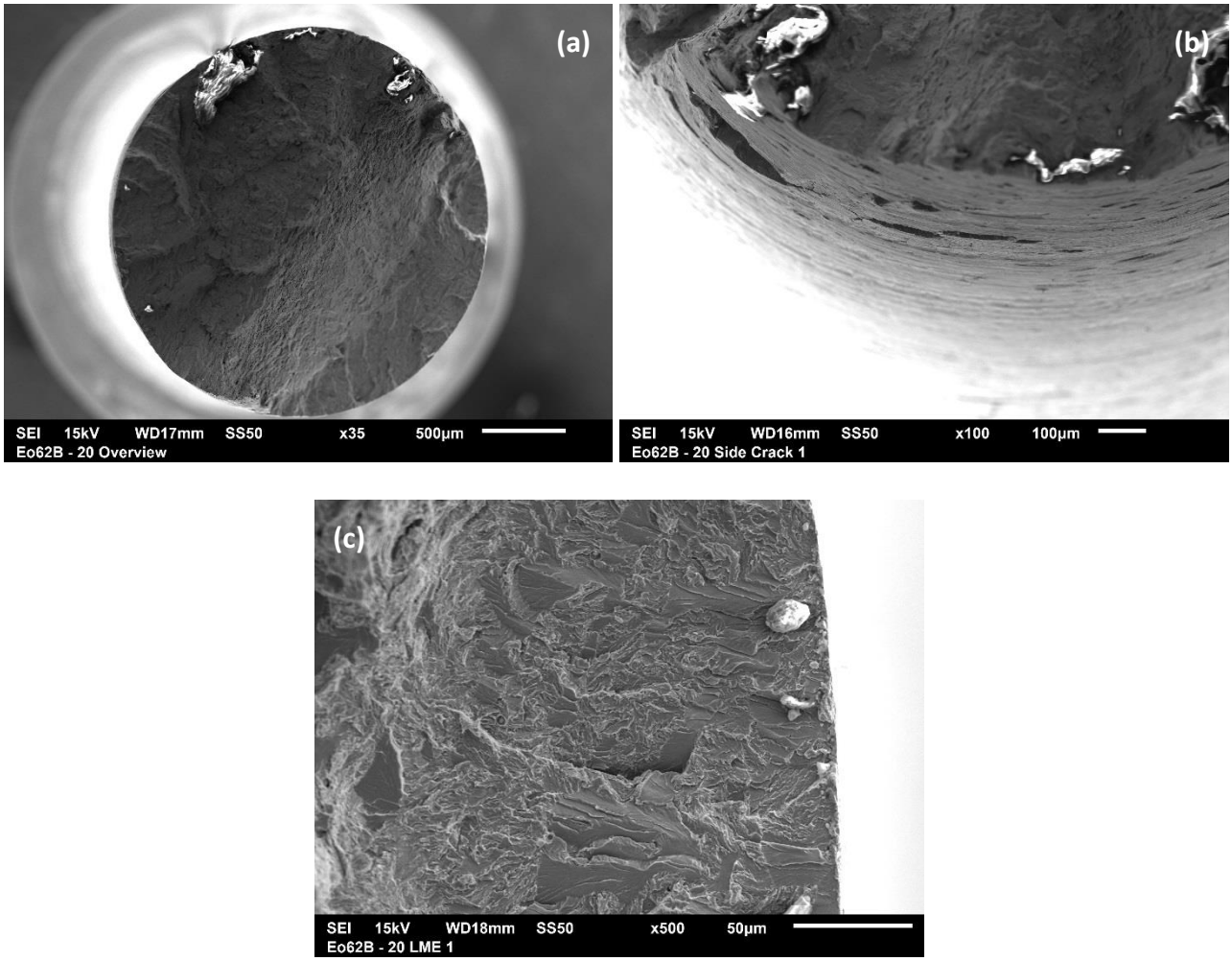

Figure 17. Fracture surfaces of 14%Cr experimental steel tested in LBE at 350 °C

Table 9.2 SSRT test results

Material	ID specimen	Test environment	T_{test} °C	orientation	Strain rate (s^{-1})	σ_y (MPa)	σ_u (Mpa)	ε_u (%)	ε_t (%)
ODS 9%Cr (KIT)	T12_2*	Air	300	L	$2.8\ 10^{-4}$	861	965	2.5	10.4
	T12_8*	Air	300	T	$2.8\ 10^{-4}$	828	959	2.4	8.7
ODS 9% Cr (KIT) GESA treated	KIT-II	LBE	300	-	$5\ 10^{-5}$	839	916	1.5	1.7
ODS 12%Cr (KOBELCO)	K11-3*	Air	300	L	$2.8\ 10^{-4}$	986	1030	3.0	9.0
	K11-6	LBE	300	L	$5\ 10^{-5}$	970	1020	2.9	5.1
	K11-7	LBE	300	L	$5\ 10^{-5}$	988	1030	2.6	3.9
	K11-11*	Air	300	T	$2.8\ 10^{-4}$	994	1024	1.7	5.3
	K11-14	LBE	300	T	$5\ 10^{-5}$	989	1020	1.4	3.0
	K11-15	LBE	300	T	$5\ 10^{-5}$	985	1014	2.0	2.9
ODS 12% (KOBELCO) GESA treated	KIT-III	LBE	300	-	$5\ 10^{-5}$	934	957	-	0.4
ODS 14%Cr (CEA)	1-1	LBE	450	L	$5\ 10^{-5}$	738.5	799	4.4	20.5
	1-2	LBE	350	L	$5\ 10^{-5}$	832	928	6.6	13.2
	2-1	LBE	300	L	$5\ 10^{-5}$	917	987	5.8	14.9
	2-2	LBE	300	L	$5\ 10^{-5}$	907	989	6.15	15.0
	3-1	LBE	350	L	$5\ 10^{-5}$	879	959	6.4	13.7
	B2-8-1F*	Air	300	L	$2.8\ 10^{-4}$	904	988	4.4	14.0
	B2-8-2B*	Air	300	L	$2.8\ 10^{-4}$	892	997	4.8	13.0
T91-DEMETRA (INDUSTEEL)	T5-A4	LBE	350	L	$5\ 10^{-5}$	507	607	3.6	9.0
14%Cr steel (OCAS)	E062B-14	Ar-5%H_2	350	L	$5\ 10^{-5}$	504	628	4.8	14.0
	E062B-15	LBE	350	L	$5\ 10^{-5}$	511	638	4.9	8.1
	E062B-16	LBE	350	L	$5\ 10^{-5}$	489	609	4.4	5.2
	E062B-19	Ar-5%H_2	350	T	$5\ 10^{-5}$	506	632	4.8	14.2
	E062B-20	LBE	350	T	$5\ 10^{-5}$	504	625	4.2	7.9
	E062B-21	LBE	350	T	$5\ 10^{-5}$	489	614	4.8	7.1

* Specimens tested in framework of FP7 GETMAT

9.4 Conclusions part 2

The following conclusions can be made on base of the obtained results:

- 9%Cr-, 12%Cr- and 14%Cr-ODS steels are susceptible to LME in LBE environment
- GESA surface treatment do not prevent appearance of LME in tensile tests, but probably even enhance it
- 14%Cr-ODS(CEA) demonstrated least susceptibility to LME, probably due to more effective LME crack arrest in columnar microstructure
- Chromium content is not the reason for LME retarding effect in 14%Cr ODS steel

9.5 References part 2

[1] R. Chaouadi, Crack Resistance Behavior of 12%Cr– and 14%Cr–ODS Steels at Elevated Temperatures, External report SCK•CEN-ER-190, FP7 GETMAT, 2011
[2] R. Chaouadi, Cr-steels to investigate the effect of chemical composition on irradiation sensitivity, External report SCK•CEN-ER-205, FP7 GETMAT, 2012
[3] Van den Bosch, J., Almazouzi A., Procurement and characterisation of T91 and 316L plates, Deliverable D4.2, FP6 EUROTANS, DM4-DEMETRA, 2005
[4] S. Gavrilov, M. Lambrecht, G. Coen, E. Stergar, J. Van den Bosch, PIE of ASTIR: Report on the full set of results of tests on irradiated and nonirradiated specimens, FP7 GETMAT deliverable D3.7, 2013
[5] S. Gavrilov, Y. Dai, E. Stergar, G.Coen, J. Joris, Slow Strain Rate Test round robin exercise, FP7 MATTER deliverable D2.3, 2014
[6] Müller, G et al. (2005), “Surface Alloying by Pulsed Intense Electron Beams”, Vacuum, Vol. 77, pp. 469-474.